

**DEVELOPMENT OF PHOTO-TRIGGERED CONTROLLED RELEASE
SYSTEMS AS PESTICIDE NANOFORMULATIONS**

by

Selin Öykü Gündođdu

Submitted to the Graduate School of Engineering and Natural Sciences

in partial fulfillment of

the requirements for the degree of

Master of Science

Sabanci University

Spring 2023

© Selin Öykü Gündođdu

All Rights Reserved

To my wonderful parents Gülsen and Şahin Gündoğdu

ABSTRACT

DEVELOPMENT OF PHOTO-TRIGGERED CONTROLLED RELEASED SYSTEMS AS PESTICIDE NANOFORMULATIONS

Selin Öykü Gündođdu

Master of Science Dissertation, July 2023

Supervisor: Asst. Prof. Hayriye Ünal

Keywords: Photothermal Nanocarriers, Halloysite Nanotubes, Polydopamine, Essential Oils, Abamectin, Lauric Acid, Sunlight-Triggered Controlled Release Systems, Pesticides

Conventional pesticide formulations frequently cause severe environmental impact, with only less than 1 % of applied pesticides successfully reaching their intended target and the majority being lost in the surrounding ecosystem. Controlled release systems have been a significant advance in agriculture as a solution to this problem. This study focuses on the development of a sunlight-triggered controlled release system and its utilization for the efficient delivery of natural essential oils as a model natural pesticide and abamectin as a model chemical pesticide. The design includes photothermal nanocarriers made of polydopamine functionalized halloysite nanotubes (HNT-PDAs) with light-to-heat conversion properties, and their functionalization with lauric acid (LA), which acts as a stopper that facilitates

the release of the loaded cargo only upon sunlight-triggered heating of the photothermal nanocarriers. The prepared release system was demonstrated to release essential oils and abamectin for at least 5 days when exposed to sunlight for 6 h every day. Aqueous dispersions of the LA/abm@HNT-PDA nanohybrids were studied as sprayable pesticide nanoformulations and were shown to present strong suspensibility, foliar retention, rainwater wash resistance, and significant pesticide activity on *Myzus persicae* aphids. The sunlight-triggered pesticide delivery systems developed in this study present an innovative, environmentally friendly design approach that provides an effective alternative for conventional pesticides.

ÖZET

PESTİSİT NANOFORMÜLASYONLARI OLARAK IŞIKLA TETİKLENEN KONTROLLÜ SALIMLI SİSTEMLERİN GELİŞTİRİLMESİ

Selin Öykü Gündoğdu

Yüksek Lisans Tezi, Temmuz 2023

Tez Danışmanı: Dr. Öğr. Üyesi Hayriye Ünal

Anahtar Kelimeler: Fototermal Nanotaşıyıcılar, Halloysite Nanotüpler, Polidopamin, Uçucu Yağlar, Abamectin, Laurik Asit, Güneş Işıyla Tetiklenen Kontrollü Salım Sistemleri, Pestisitler

Geleneksel böcek ilacı formülasyonları uygulanan böcek ilacının sadece %1'den azının hedeflenen bölgeye ulaşması ve çoğunluğunun çevredeki ekosisteme karışmalarına bağlı olarak genellikle ciddi çevresel etkilere neden olurlar. Kontrollü salım sistemleri, bu soruna bir çözüm oluşturarak tarım alanında önemli katkılar sunabilmektedir. Bu çalışma, güneş ışığı ile tetiklenen bir kontrollü salım sisteminin geliştirilmesine ve bu sistemin model doğal böcek ilacı olarak seçilen esansiyel yağlar ve model kimyasal böcek ilacı olarak seçilen abamectin için kullanımına odaklanmıştır. Tasarım, ışıktan ısıya dönüşüm özelliklerine sahip polidopamin ile fonksiyonelleştirilmiş halloysit nanotüplerinden

(HNT-PDAs) oluřan fototermal nanotařıyıcıları ve bu tařıyıcıların gneř ıřıęı ile tetiklenen ısıtılması sonucunda yklenmiř kargonun salımını kolaylařtıran bir tıkaç olarak iřlev gren laurik asit (LA) ile fonksiyonelleřtirilmesini ierir. Hazırlanan salım sisteminin, gneř ıřıęına her gn 6 saat maruz bırakıldıęında en az 5 gn boyunca esansiyel yaęlar ve abamektini salımı gerekleřtirdięi gsterilmiřtir. LA/abm@HNT-PDA nanohibritlerinin sulu dispersiyonlarının spreylenebilir bcek ilacı nanoformlasyonları olarak kullanımları incelenmiř ve gl sspanse edilebilme, yaprakta tutunma, yaęmura dayanıklılık ve *Myzus persicae* trne karřı nemli insektisit etkisine sahip oldukları gsterilmiřtir. Bu alıřmada geliřtirilen gneř ıřıęı ile tetiklenen pestisit salım sistemleri, geleneksel pestisitlere etkin bir alternatif saęlayan yeniliki ve evre dostu bir tasarım yaklařımı sunmaktadır.

ACKNOWLEDGEMENTS

I would like to start by sincerely thanking my advisor, Asst. Prof. Hayriye Unal, for her amazing support during the course of my master's degree. She has been an excellent guide for me as I explore many advanced concepts in science on this academic path. I am grateful to her for believing in me from the very beginning and for patiently addressing every question I had. I sincerely appreciate all the knowledge and experiences I have acquired thanks to her guidance. In addition, I want to say thank you for being a role model as a woman scientist. I'd like to thank my thesis jury members, Asst. Prof. Serap Hayat Soytaş and Asst. Prof. Senem Seven, for their participation in the thesis jury and their contributions to my thesis.

I experienced a wonderful opportunity to be a member of an excellent research group. I want to take this opportunity to express my sincere gratitude to my research team, Öykü Demirel (Öykütoşko), Sarp Kölgesiz (Sarpella), Sena Yüce (Senoşko), and honorary member of the group, Neslihan Şişman (Nesliko). You have become a second family to me here at Sabancı. You lifted me up every time I fell, you were there by my side in every moment of happiness or sadness, and whenever I stumbled, you tried your best to remove the obstacles in my path. I can't even count how many times we burst into fits of laughter together. Thanks to you, things that would have been much harder became easier and much more joyful for me. I will be forever grateful to you for being there beside me. I would also like to thank Mehmet Can Dursun (Memocan) and Mehmet Kahraman (Memo). I will cherish every moment I laughed, had fun, and even those times when I felt sad with you. Better late than never, I'm grateful that we met, and I'm grateful to have friendships like yours that I want to have in my life forever. I'd like to thank Dr. Buket Alkan Taş, Dr. Cüneyt Erdiñç Taş, and Baby Atlas. I thank them for always being supportive and continuously enlightening me as mentors whenever I sought their advice. I want to thank Gizem Beliktay, Karya Kölgesiz, Ekin Berksun, Farid Irani, Tuna Alp, and Yelda Yorulmaz for making SUNUM and FENS feel like a big family. Their support and encouragement have been very motivating throughout this time.

I would like to express my gratitude to my closest friends, İlayda Yılmaz, Merve Beliz Yılmaz, and Nergis Bilge, who have made my life more fun for the past 8 years. Thank you for always being there for me, even when there is distance between us, and for being just a phone call away. Life with you is like an endless festival. I would also like to thank İzzet Emre Turan and Mısra Karallı for their friendship and support, and for always being there by my side.

Last but not least, I would like to express my gratitude to my beloved parents, Gülsen and Şahin Gündoğdu, and my brother Ant Gündoğdu. Thank you for always being there for me, supporting me in every moment, and teaching me to see the good in every difficult situation. Thank you very much for guiding me to teach that being a good person is far more important than any worldly gain or success. If I am able to achieve anything today, it is because you have taught me to stand on my own feet and never give up. I love you all very, very much. Thank you very much for all.

Finally, I am thankful to TUBITAK for the scholarship and research funding. (Project no: 120Z723)

TABLE OF CONTENT

CHAPTER 1. INTRODUCTION	1
1.1 Controlled Release Systems	1
1.2 Application Areas of Controlled Release Systems	4
1.2.1 Cosmetics	4
1.2.2 Drug Delivery.....	5
1.2.3 Food.....	6
1.2.4 Agrochemicals	8
1.3 Different Designs of Stimuli-Triggered Controlled Release Systems	10
1.3.1 Temperature-Sensitive Controlled-Release Systems	10
1.3.2 pH-Responsive Controlled-Release Systems	11
1.3.3 Enzyme-Responsive Controlled-Release Systems.....	12
1.3.4 Photo-responsive Controlled-Release Systems	12
1.4 Thesis objective: The importance of controlled release systems for pesticide use	14
1.4.1 Controlled release systems of pesticides as an alternative approach ..	15
1.5 Dissertation Overview	16
CHAPTER 2. SUNLIGHT-TRIGGERED ESSENTIAL OIL RELEASE SYSTEMS AS NATURAL PESTICIDE NANOFORMULATIONS	18
2.1 Abstract	18
2.2 Introduction	20
2.3 Experimental.....	22
2.3.1 Chemicals	22
2.3.2 Preparation of the HNT-PDA nanohybrids	22
2.3.3 Characterization of the HNT-PDA nanohybrids	23
2.3.4 Preparation the EO@HNT-PDA and LA/EO@HNT-PDA nanohybrids....	23
2.3.5 Characterization of the EO@HNT-PDA and LA/EO@HNT-PDA nanohybrids.....	24
2.3.6 Release of EO from LA/EO@HNT-PDA nanohybrids	26
2.3.7 Antibacterial properties of the EO released from LA/EO@HNT-PDA Nanohybrids	27

2.3.8	Pesticide activity of the LA/EO@HNT-PDA and EO@HNT-PDA nanohybrids on <i>Myzus Persicae</i>	28
2.4	Results and Discussion.....	29
2.4.1	The design and preparation of LA/EO@HNT-PDA controlled release system	29
2.4.2	Release of EO from the LA/EO@HNT-PDA nanohybrids	35
2.4.3	Pesticide activity of the LA/EO@HNT-PDA nanohybrids	40
2.5	Conclusions	42
CHAPTER 3. SUNLIGHT-ACTIVATED ABAMECTIN RELEASE SYSTEMS AS CONTROLLED-RELEASE PESTICIDE NANOFORMULATIONS		
3.1	Abstract	43
3.2	Introduction	44
3.3	Experimental.....	46
3.3.1	Chemicals	46
3.3.2	Preparation of the HNT-PDA nanocarriers	46
3.3.3	Preparation and characterization of the abm@HNT-PDA and LA/abm@HNT-PDA nanohybrids	47
3.3.4	Abm Release Profiles of abm@HNT-PDA and LA/abm@HNT-PDA Nanohybrids	50
3.3.5	Killing activity of powder form of abm@HNT-PDA and LA/abm@HNT-PDA on <i>Myzus persicae</i>	51
3.3.6	Suspensibility of the LA/abm@HNT-PDA nanohybrids in water	51
3.3.7	Dispersion analysis of LA/abm@HNT-PDA nanohybrids in the water	52
3.3.8	Determination of leaching of abm into the soil.....	52
3.3.9	Retention of the LA/abm@HNT-PDA dispersion on the leaves.....	52
3.3.10	Determination of the foliar retention properties of the LA/abm@HNT-PDA PDA dispersions.....	53
3.3.11	Optical microscopy of eggplant leaf surfaces sprayed with aqueous LA/abm@HNT-PDA dispersions	54
3.3.12	Determination of LC ₅₀ values of LA/abm@HNT-PDA	54
3.4	Results and Discussion.....	56
3.4.1	Preparation of the sunlight-triggered abm release system.....	56
3.4.2	Characterization of the LA/abm@HNT-PDA release system.....	57

3.4.3	Sunlight-triggered abm release from the LA/abm@HNT-PDA release system.....	61
3.4.4	Sunlight-triggered pesticide activity of LA/abm@HNT-PDA release system.....	64
3.4.5	Aqueous formulations of LA/abm@HNT-PDA nanohybrids as pesticides.....	65
3.4.6	Foliar adhesion properties of LA/abm@HNT-PDA formulations.....	68
3.4.7	Pesticide activity of LA/abm@HNT-PDA nanoformulations	72
3.5	Conclusions	75
CHAPTER 4.	CONCLUSIONS.....	76
CHAPTER 5.	REFERENCES	78

LIST OF FIGURES

Figure 1. Schematic representation of a sunlight-triggered release system.....	2
Figure 2. Active packaging systems and sub-classifications ³⁵	7
Figure 3. Schematic illustration for the fabrication and mechanism of PRCRC ⁴⁰	9
Figure 4. Schematic illustration of fabrication procedure and mechanism of TCHP ³ ...	10
Figure 5. Effect of Nanoformulations as pesticide systems ⁶³	15
Figure 6. Schematic representation of experimental procedure of EO@HNT-PDA and LA/EO@HNT-PDA via Solvent-assisted impregnation method with vacuum treatment	24
Figure 7. The design of the sunlight triggered EO release system.	29
Figure 8. Time-temperature profiles of HNT and HNT-PDA nanohybrids under sunlight irradiation at 3 sun (300 mW/cm ²) and 1 sun (100 mW/cm ²) light density.	30
Figure 9. TGA of HNT-PDA nanocarriers loaded with cinnamon oil (a), peppermint oil (b), basil oil (c), and the mixture of all three EOs (d).....	31
Figure 10. DSC analysis of EO@HNT-PDA and LA/EO@HNT-PDA nanohybrids.	32
Figure 11. SEM images of EO@HNT-PDA (a, b), LA/EO@HNT-PDA (c, d) nanohybrids, neat HNT (e) and HNT-PDA nanohybrids (f).	33
Figure 12. TEM images of a) HNT, b) HNT-PDA, c) crv@HNT-PDA, and d) LA/crv@HNT-PDA nanohybrids.	34
Figure 13. Time-temperature profiles of LA/EO@HNT-PDA and EO@HNT-PDA nanohybrids under irradiation at 3 sun (300 mW/cm ²) and 1 sun (100 mW/cm ²).	35
Figure 14. Schematic representation of the experiment designed for the investigation of the release behavior of EOs from LA/EO@HNT-PDA nanohybrids.....	36
Figure 15. LA/EO@HNT-PDA nanohybrids after 2 and 5 cycles of 6 h sunlight irradiation/18h dark treatment.	37
Figure 16. a) EO release behavior of LA/EO@HNT-PDA nanohybrids at 3 sun (300 mW/cm ²) and at room temperature in the dark b) Release behavior of LA from the nanohybrids at 3 sun (300 mW/cm ²) and at room temperature in the dark	38
Figure 17. Schematic representation of Antibacterial activity analysis (a), nanohybrid containing agar plate incubated for 6 h in the dark, (b) nanohybrid containing agar plate exposed to sunlight (c), control sample in the dark (d), control sample exposed to sunlight (e).	39
Figure 18. Killing activity of the of EO@HNT-PDA and LA/EO@HNT-PDA nanohybrids on <i>Myzus persicae</i> under sunlight irradiation at 3 sun and in the dark. The nanohybrids were exposed to 6 h sunlight/18 h dark treatment, or to 24 h dark treatment for 10 days	41

Figure 19. Schematic representation of experimental procedure of abm@HNT-PDA and LA/abm@HNT-PDA preparation via solvent-assisted impregnation with vacuum treatment.	47
Figure 20. Design of the sunlight-triggered abm release system.....	56
Figure 21. a) TGA of HNT-PDA, LA, abm, abm@HNT-PDA and LA/abm@HNT-PDA. b) DSC of abm, abm@HNT-PDA and LA/abm@HNT-PDA.....	58
Figure 22. SEM images of LA/abm@HNT-PDA at a) 25k, b) 50k magnification and abm@HNT-PDA at c) 25k, d) 50k magnification.....	59
Figure 23. Time-temperature profiles of LA/abm@HNT-PDA and abm@HNT-PDA nano hybrids under irradiation at 1 sun and 3 sun light densities.....	60
Figure 24. UV-VIS absorption spectra of aqueous abm solution and aqueous dispersion of abm@HNT-PDA exposed to sunlight at 3 sun for 6 h and kept in the dark for 6 h. .	61
Figure 25. a) Schematic representation of the experimental design to monitor the release behavior of abm from nano hybrids, b) Abm release performance of LA/abm@HNT-PDA and abm@HNT-PDA nano hybrids which were i) irradiated with sunlight at 3 sun light density for 6 h followed by 18 h dark incubation, ii) kept in the dark for 10 days, c) Abm release performance of LA/abm@HNT-PDA nano hybrids for 30 days, during which the nano hybrids were irradiated with sunlight at 3 sun light density for 6 h followed by 18 h dark incubation for 30 days.	64
Figure 26. a) Mortality of <i>Myzus persicae</i> treated with LA/abm@HNT-PDA and abm@HNT-PDA nano hybrids, which are i) exposed to sunlight at 3 sun for 6 h followed by dark incubation for 18 h, ii) kept in the dark every day	65
Figure 27. Suspension test for LA/abm@HNT-PDA nano hybrids in water at different abm concentrations.	66
Figure 28. a) DLS analysis, b) photographs of the aqueous dispersion of LA/abm@HNT-PDA nano hybrids prepared at 4 mg/mL at different time periods.	67
Figure 29. FTIR of soil samples mixed with LA/abm@HNT-PDA nano hybrids and neat abm.....	68
Figure 30. Foliar retention values for water, abm dissolved in methanol, aqueous LA/abm@HNT-PDA dispersion and Agrimec.....	69
Figure 31. Contact angle values of eggplant leaves sprayed with aqueous dispersions of LA/abm@HNT-PDA nano hybrids at 0-18 mg/mL abm concentrations.....	70
Figure 32. a) Contact angle values of eggplant leaves sprayed with aqueous LA/abm@HNT-PDA dispersions and washed with water 1-5 times.	71
Figure 33. Optical microscopy images of eggplant leaf samples. a) neat leaf, b) leaf sprayed with 4 mg/mL aqueous LA/abm@HNT-PDA dispersion, c) leaf sprayed with 4 mg/mL aqueous LA/abm@HNT-PDA dispersion followed by washing with water.	72
Figure 34. a) <i>Myzus persicae</i> placed on eggplant leaf that was sprayed with the nano formulation and irradiated with sunlight for 6h, b) LC ₅₀ analysis of the aqueous LA/abm@HNT-PDA dispersions in the dark and under sunlight irradiation.	73

LIST OF TABLES

Table 1: Table of LC50 analysis for LA/abm@HNT-PDA dispersion, abm in methanol, and Agrimec for different conditions	78
--	----

LIST OF ABBREVIATIONS

HNT	:	Halloysite Nanotubes
PDA	:	Polydopamine
EO	:	Mixture of Essential Oils
LA	:	Lauric Acid
abm	:	Abamectin
<i>S. Aureus</i>	:	Staphylococcus aureus
DSC	:	Differential Scanning Calorimetry
TGA	:	Thermogravimetric Analysis
SEM	:	Scanning Electron Microscopy
TEM	:	Transmission Electron Microscopy
DLS	:	Dynamic Light Scattering
FTIR	:	Fourier-transform infrared spectroscopy
LC ₅₀	:	Lethal concentration for killing half of the population

CHAPTER 1.INTRODUCTION

1. NANOTECHNOLOGY-BASED CONTROLLED RELEASE SYSTEMS

1.1 Controlled Release Systems

Controlled release systems, in their most fundamental sense, determine when, how much, and where the active substance will be released based on external stimuli such as temperature, pH, magnetic field, or light. The release system only operates when these external factors are present and may result in minimal or no release otherwise. Nanoscale carrier systems that permit controlled release in response to specific stimuli have been the subject of substantial research in recent years. It is possible to create various host-guest complex combinations specific to the desired target region and associated response system. The carrier can be made active using a variety of techniques, such as the presence of a magnetic field¹, enzymes¹, pH², temperature³, or light⁴. Essentially, the host molecule has the ability to selectively open or close the gates of nanocapsules at specified times, permitting the release of the guest molecule.

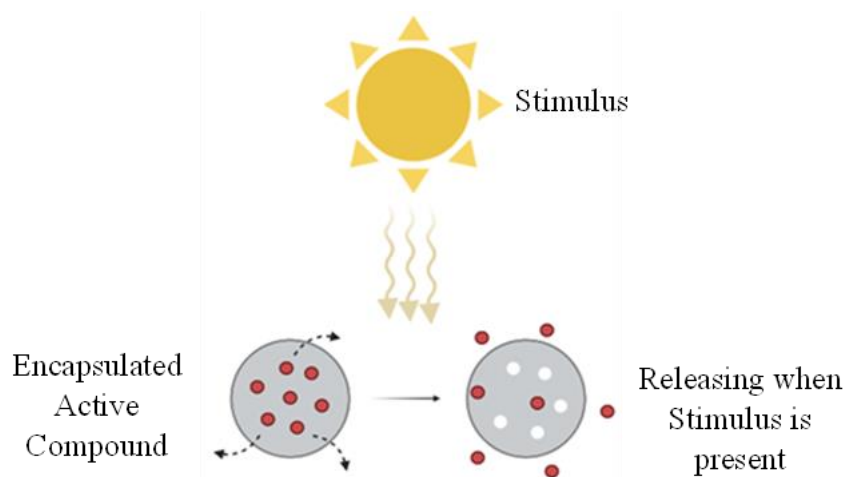


Figure 1. Schematic representation of a sunlight-triggered release system

The release of the active substance to the target point can be achieved using various carrier materials such as hydrogels, polymers, liposomes, or nanoparticles. Hydrogels are commonly used as carrier materials in the field of drug delivery, primarily due to their minimum tendency to absorb proteins in the body. Additionally, their high-water content and soft structure allow for easy compatibility with body tissues, resembling the characteristics of the human body. Synthetic biodegradable polymers are also among frequently used carriers. Controlled release systems mostly use poly(glycolic acid), poly (D,L-lactic acid), and poly(D,L-lactic-glycolic acid), among other synthetic biodegradable polymers. The pesticide release system using PLA as a carrier is one example of this^{5,6}. The lack of homogenous manufacturing is the main problem with pesticide systems made using PLA, according to the literature. To solve this problem, Liu et al. combined the emulsion approach with the PME technique to produce homogenous PLA-based carriers with adjustable diameters ranging from 0.6 μm , to 4.6 μm for pesticide-controlled release⁷. As drug delivery systems, liposomes offer a number of benefits including biocompatibility, high loading capacity, relatively lower toxicity, stability of integrating pharmaceuticals, and keeping the drugs from degrading in the physiological environment⁸. Liposomes in the stimuli-responsive controlled release systems entrapped the cargo molecule and deliver it to the desired target when the external stimuli are present⁹. A controlled release system with temperature sensitivity was developed by Qiu et al., using functionalized artificial bacterial flagella (ABFs)

combined with dipalmitoylphosphatidylcholine (DPPC), which is a type of temperature-sensitive liposome, to facilitate drug release¹⁰.

Researchers have shown significant interest in utilizing nanoparticles as effective carriers for drug and pesticide delivery in medicine and agriculture, respectively, in recent years. Nanoparticles such as silica, gold, chitosan, or silver are commonly used carriers to facilitate a delivery system. Among the numerous reasons for utilizing nanoparticles for controlled release systems, it can be highlighted that they are having high surface-to-volume ratio which enables the encapsulation of a higher amount of active compounds in them¹¹. One advantage they have in terms of their use in drug delivery systems, is their smaller size, which allows higher tissue penetration^{12,13}. Mesoporous silica nanoparticles (MSNs) are highly biocompatible and biochemically stable, and they play a vital role in the delivery of anticancer drugs¹⁴⁻¹⁶. The exterior surface of MSNs can be coated with a soluble material such as polyacrylic acid (PAA) to generate a stimulus-responsive system that permits drug release through its pores upon stimulation when the trigger is present in the environment, according to reports in the literature¹⁷. Chitosan nanoparticles are extensively used as carrier molecules in agricultural applications since they are regularly referenced in the literature as ecologically friendly and biodegradable materials. Encapsulating pesticides within chitosan have proven slow-release qualities and prevent the active component from deterioration¹⁸. With their hollow tubular nanostructure, halloysite nanotubes (HNTs) have drawn a lot of attention as ecologically acceptable and naturally occurring nanocarriers in controlled release systems¹⁹. They have a superior ability to be loaded with active components. HNTs are frequently utilized in a variety of fields, including food packaging²⁰⁻²² and cancer therapy²³⁻²⁵, as efficient slow and sustained release systems.

1.2 Application Areas of Controlled Release Systems

1.2.1 Cosmetics

The preservation of active compounds through encapsulation and their time-dependent release in cosmeceuticals have made controlled release systems a fascinating topic in recent years. Biopolymer-based delivery and release systems are predominantly utilized in the cosmetic field. This is due to their inherent non-reactivity upon contact with the human body and their ability to undergo breakdown, metabolism, and elimination through regular metabolic processes²⁶. Because many physiologically active chemicals are unstable to changes in temperature, pH, light, and oxidation, encapsulation is important to prevent unintended degradation and allow for the controlled release of the active ingredient for cosmetic products. As an example, skin permeability testing proved that retinoic acid that had been encapsulated with chitosan released at substantially slower and more controlled doses than free retinoic acid.²⁶

The body's connective tissue contains hyaluronic acid (HA), a naturally occurring glycosaminoglycan that is commonly used in cosmetics. According to research, controlled drug release from HA has a number of advantages, including preserving optimal drug concentrations, enhancing therapeutic effects, increasing treatment effectiveness by lowering drug dosage, reducing or eliminating toxicity, and attaining sustained release *in vivo*²⁷. Natural antioxidant vitamin E protects tissues from ultraviolet (UV) radiation, prevents photoaging, and has moisturizing properties. It is widely used as a major lipid-soluble antioxidant in cosmetic products because of its distinctive characteristics. Vitamin E must be microencapsulated during storage since it is relatively unstable and sensitive to high temperatures, oxygen, and light. Encapsulation protects the core chemical, minimizes its reactivity with outside influences, slows down the rate of transfer from the core to the environment, and allows for controlled release. In order to provide vitamin E for cosmetic applications, researchers have demonstrated the

production of microcapsules employing chitosan/sodium lauryl ether sulfate (SLES) complexes as wall materials via spray drying²⁸.

1.2.2 Drug Delivery

A controlled drug delivery system's goal is to deliver precisely controlled amounts of a therapeutic substance at the desired location for the required amount of time. This method offers important advantages over conventional dosage forms by increasing the treatment's efficacy while decreasing potential negative effects²⁹. It has been shown in the literature that a variety of carriers and drugs may be employed to achieve drug release. Jin et al. created a system that releases the anticancer medication 5-FU when it is exposed to light using micelle-drug conjugates. The idea was based on block copolymers with coumarin-functionalization that were used in biocompatible medication delivery systems. The study showed that under UV irradiation (254 nm), physiological conditions were reached for the controlled release of the anticancer agent 5-FU from the micelle-drug conjugates. However, the release of 5-FU from the micelle-drug conjugates was not seen in the absence of UV irradiation³⁰.

Due to their fewer side effects than chemotherapy and greater effectiveness, sustained drug delivery systems are a very desirable option for the treatment of cancer. In comparison to ultraviolet (UV) light, a recent study suggests that near-infrared (NIR) light may be a better photo-trigger because it harms living tissue less and penetrates deeper regions³¹. Using mesoporous silica-coated upconverting nanoparticles (UCNP@mSiO₂), Liu and colleagues created a novel technique for releasing the anticancer medication doxorubicin (DOX). These UCNP nanoparticles can absorb NIR light and produce high-energy photons. The release of DOX is controlled by including azobenzene groups on the mesoporous silica surface because these groups establish hydrogen bonds with the drug. The photosensitive azo molecules on the mesoporous silica absorb photons when exposed to NIR light, which causes the UCNPs to continuously rotate and invert and release the therapeutic anticancer drug DOX³².

Using a low molecular weight hydrogel, Liu and colleagues created a novel method for drug delivery³³. They suggest making use of a recently found photosensitive substance

made from 7-amino coumarin, which when exposed to UV light undergoes a photocleavage of the carbon and nitrogen linked to within the coumarin structure. When exposed to UV light, the drug is released in a controlled way via this process.

To construct a drug delivery system that reacts to visible light, researchers used a two-layered arrangement of TiO₂ nanotubes (TiNTs). A water-repellent coating on the nanotubes that comprises gold nanoparticles (AuNPs) is essential for facilitating the release of drugs when exposed to visible light. When placed under visible light, the photocatalytic action of the AuNPs renders it easier to break the water-repellent chain. Ampicillin (AMP) was introduced into the lower part of the TiO₂ nanotube arrangement to show this idea. Drug release was started using visible light, and antibacterial tests were then carried out. The drug is attached to the hydrophilic bottom layer using a silane grafting approach, and the researchers discovered that this strategy is most effective at controlling the release mechanism from the system³⁴.

1.2.3 Food

Food packaging materials containing controlled release systems are one of the examples of active packaging (AP), a novel type of packaging that contains bioactive materials. These packaging options release the active ingredients gradually throughout the course of storage, maintaining food quality and extending shelf life. The main challenge in creating active packaging systems lies in effectively slowing down the release rate of bioactive chemicals, thereby enabling their sustained and continuous action over time. Controlled-release active packaging (CRP), a cutting-edge technology that provides fine control over the release of active compounds during storage, has been developed as a solution to this problem³⁵. To create CRP systems, several methods and approaches have been proposed and investigated. Active packaging (AP) systems can be divided into two categories based on the manner in which they work: "releasing systems" and "absorbing systems." Preservatives that operate as active agents migrate to the surface of the food as part of releasing systems, thereby inhibiting deterioration and sustaining food quality. Packaging materials with antibacterial and antioxidant properties are examples of releasing systems³⁶. Contrarily, absorbing systems work by the active component absorbing unwanted elements from the food surface or the package's internal

atmosphere³⁷. The two most common categories of absorption systems are oxygen and ethylene scavengers.

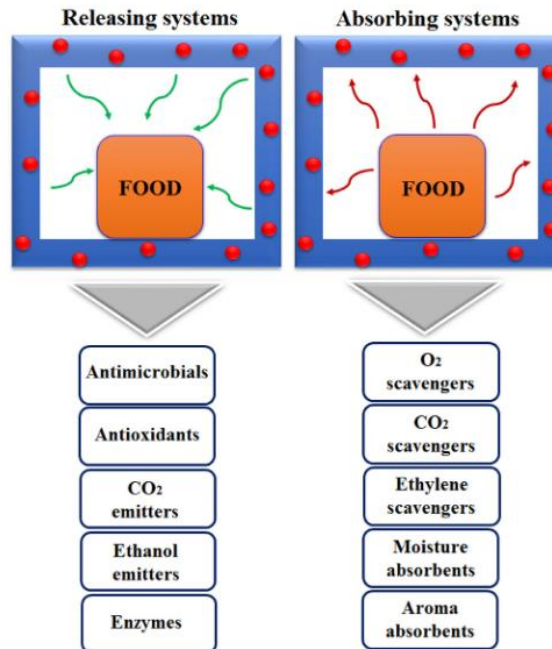


Figure 2. Active packaging systems and sub-classifications³⁵

Researchers have evaluated whether a sustained release systems obtained by the encapsulation of the ethylene production inhibitor cinnamaldehyde (CA) in halloysite nanotube (HNT) nanocarriers would increase the shelf life of fruits when incorporated into flexible packaging films²⁰. The ethylene hormone, which triggers the ripening process in climacteric plants, is essential for controlling how long fresh fruits will stay fresh. According to the study, ethylene production in bananas was effectively suppressed for more than 180 days by the gradual release of CA from HNT-CA nanohybrids. The HNT-CA nanohybrids were mixed with polypropylene (PP) using melt extrusion to create PP/HNT-CA nanocomposite films, which can be used in real-world applications. These films have appropriate mechanical characteristics, which made them ideal for use in flexible packaging.

The researchers also showed that changes in pH can be used to control the quantity of the active component released. A study on the controlled release of anthocyanins from a

gellan gum film was carried out by Wu et al., specifically at pH levels higher than 6. The research study explained the variations in the binding affinities between the active drug and the film at various pH levels as the cause of the triggered release. A mechanism created for controlled release at the same pH level can increase antibacterial activity because food degradation causes pH changes and bacteria thrive in neutral pH environments³⁸.

1.2.4 Agrochemicals

Pesticides are required to be used in massive quantities or in their purest form, without the addition of any other compounds, in traditional farming practices. The primary concern with utilizing traditional pesticides is that, depending on the application method and the weather, they may be lost in the soil. Studies have revealed that the majority of these compounds are not utilized entirely by the crops. However, a substantial amount is left unused as a result of diverse processes such as leaching, degradation into minerals, and conversion by organisms. In order to effectively control pests, treatments must be made repeatedly in conventional pesticide formulations. As a result of this, the residual chemicals disrupt not only human health but also the fragile environmental balance at various levels of the food chain³⁹. It became crucial to develop novel methods for enhancing pesticide efficiency as a consequence of this. The development of controlled-release pesticide systems addresses the need for prolonging the length and improving the efficiency of utilizing pesticides. To tackle this issue, Xiang et al. developed a controlled-release mechanism for the highly toxic insecticide chlorpyrifos (CPF). The pH-responsively controlled-release chlorpyrifos (PRCRC) system made use of several distinguished compounds. These included calcium alginate (CA), polydopamine (PDA), and attapulgit (ATP) as a carrier molecule. Through hydrogen bonding and electrostatic attraction, CPF was taken up by the nanonetwork-structured PDA-modified ATP (PA) to create the PRCRC. Then, PA was used as the framework to combine CPF-PA with CA to create porous CPF-PA-CA hydrogel spheres. This hydrogel system performed well in terms of controlled release and responded to pH changes, especially in alkaline solutions. The ability to manage insects was tested in order to demonstrate the aforementioned trait.

The CPF molecules were also well shielded from UV radiation deterioration by this design⁴⁰.

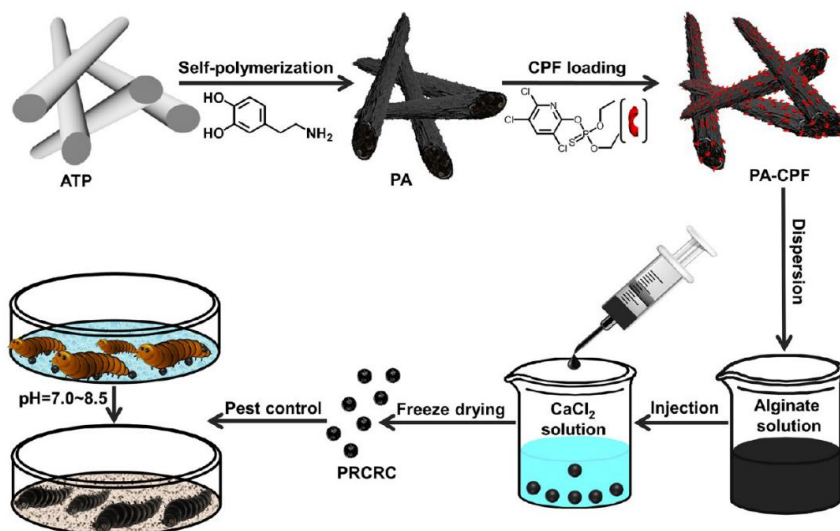


Figure 3. Schematic illustration for the fabrication and mechanism of PRCRC⁴⁰

Researchers have created site-specific controlled-release systems that respond to particular stimuli in order to improve the effectiveness of pesticide use. Xu et al. developed PDA@PNIPAm, a core-shell nanocomposite structure made of polydopamine and PNIPAm. As a photothermal agent, polydopamine absorbs light energy and transforms it into heat. It has a substantial surface loading capacity for chemically active groups. Both the photothermal agent and the insecticide are carried by PNIPAm. When exposed to near-infrared (NIR) light in this study, PDA placed in the polymer matrix absorbs light and causes the matrix to shrink. The imbedded insecticide, IMI, is then released as a result⁴¹

1.3 Different Designs of Stimuli-Triggered Controlled Release Systems

1.3.1 Temperature-Sensitive Controlled-Release Systems

There are multiple uses for temperature-responsive controlled release systems that use temperature as a stimulus. The controlled release systems designed to allow pesticide release caused by a temperature increase are one example of such systems. Chi et al. created core-shell-structured temperature-responsive controlled-release herbicide particles (TCHP). The TCHP formulation includes glyphosate (Gly) as a model herbicide. Amino silicone oil and poly (vinyl alcohol) are used as shell structures, and attapulgite (ATP) operates as an adsorbent for Gly. NH_4HCO_3 serves as a foaming agent to create CO_2 and NH_3 bubbles while forming micro- and nano-pores in the ASO-PVA shell under elevated temperatures which triggers the release of the herbicide. The technique presents a strategy that has the potential to minimize pesticide loss, improve use efficiency, and reduce environmental impact⁴².

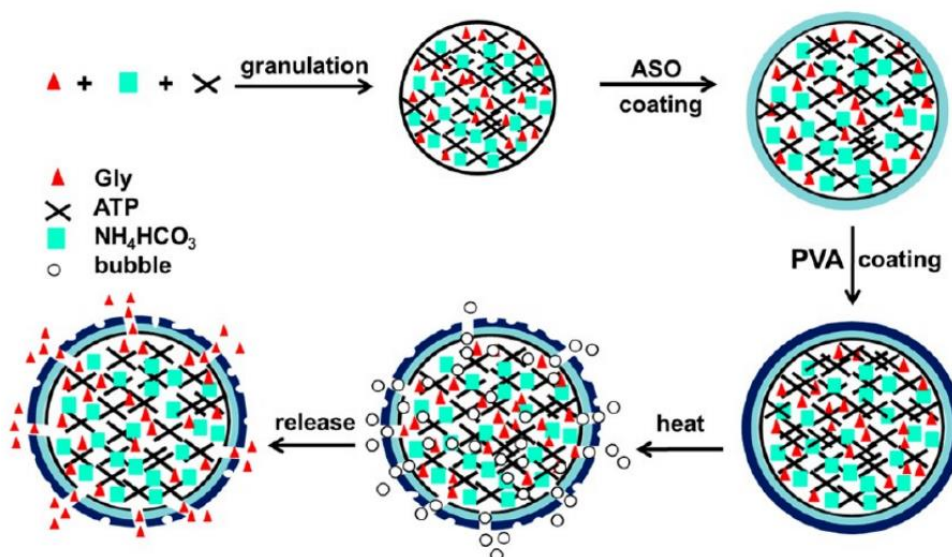


Figure 4. Schematic illustration of fabrication procedure and mechanism of TCHP³

In controlled release systems, it is common to employ materials that may undergo phase transitions at high temperatures as a carrier or triggering molecules^{43,44}. Poly(amino ester)-Poly(caprolactone)-Poly(ethylene glycol)-Poly(caprolactone)-Poly(amino ester) (PAE-PCL-PEG-PCL-PAE) is a pentablock copolymer that has been studied for its potential as a sustained injectable insulin delivery method. In order to generate an ionically connected compound with PAE, the hydrogel effectively contained insulin within its matrix. The hydrogel alternated between a gel and a liquid form depending on the temperature and pH level, which allowed control of the drug release⁴⁴.

1.3.2 pH-Responsive Controlled-Release Systems

pH-responsive materials such as polymers or nanocapsules have the ability to respond to pH as an external stimulus and accomplish both a targeted response and a controlled release of active substances. According to the response principle, changes in pH cause changes in a pH-responsive polymer's tendency to ionize. A change in the polymer's solubility results when the ionization capacity hits its isoelectric point⁴⁵. Imato et al. developed two kinds of weak polyelectrolytes, chitosan (CT) and poly(γ -glutamic acid) (γ -PGA), and established a novel method to produce biodegradable hollow nanocapsules. They first deposited LbL-assembled films on silica particles, then they removed the silica. Because of the swelling of the capsule membranes triggered by electrostatic repulsions between the ammonium groups of CT components at lower pH values, the hollow nanocapsules exhibited unique size growth. On the contrary, at pH values of 4.0, 7.0, and 10, no apparent alterations in capsule size were found. The release of compounds encapsulated in response to acidic pH levels was successfully accomplished by using CT-PGA nanocapsules.

Nanoparticle-based carrier molecules that are triggered by pH in release systems are extensively utilized. Sun et al. developed hybrid poly(2-(diethylamino)ethyl methacrylate)-coated mesoporous silica nanoparticles (MSN-PDEAEMA) utilizing the adaptable surface-initiated atom transfer radical polymerization (SI-ATRP). As a control switch to regulate the opening and closing of the nanopores, the pH-responsive PDEAEMA brushes are connected on the MSNs⁴⁶. When guest molecules were released experimentally at various pH levels, it was found that acidic aqueous solutions released

them rapidly whereas alkaline solutions released them slower. The release of molecules that have been encapsulated could be accurately switched on and off by constantly altering the pH of the solution. The authors believe that their nanosystem has potential for use in gene therapy and targeted drug delivery.

1.3.3 Enzyme-Responsive Controlled-Release Systems

Different controlled release systems utilizing enzymes as external stimuli have been reported in the literature^{1,47,48}. Drugs can be stabilized at physiological pH levels and released once they reach the designated pH trigger point by incorporating pH-responsive nanomaterials in the design of sensitive nano-systems for cancer therapy⁴⁹. Following a similar logic, Thornton et al. fabricated enzyme-responsive hydrogel particles for the regulated release of proteins. They used peptide actuators to modify the amino-functionalized poly (ethylene glycol acrylamide) (PEGA) hydrogel particles. In response to enzymatic triggers, these actuators made the particles enlarge and release the protein payload. The peptide actuator, which was connected to the polymer carrier presented an accurate controlled release mechanism.

1.3.4 Photo-responsive Controlled-Release Systems

Through exposure to various light sources, the release of active molecules trapped within a carrier material can be controlled through the employing of photo-stimuli. Numerous systems have been developed in the literature that use triggers like UV^{50,51}, NIR⁵², sunlight^{43,53}, etc. to cause the release of compounds that have been encapsulated via irradiation of the source. Drug delivery systems frequently use light-triggered controlled release systems. The potential of light as an external stimulus for regulating the spatial and temporal release of pharmaceuticals has been thoroughly investigated during the past decade. However, both in vitro and in vivo applications of the majority of these systems have been constrained. This is mainly because biological samples and living tissues are damaged by irradiation, which is utilized to activate the photosensitizer⁵⁴. There is a critical need to create an enclosed system that may be operated remotely utilizing a light

source in order to address these issues. One example of this is achieved by Liu et al.⁵⁴. They provided a novel and comprehensive method for releasing anticancer medications utilizing near-infrared (NIR) light. This method employs a structure known as UCNP@mSiO₂, which is composed of upconverting nanoparticles (UCNPs) coated with mesoporous silica. It has been proven to successfully control the amount of released anticancer medications by varying the NIR light exposure intensity and duration.

The urgent demand for more environmentally friendly pesticide formulations has recently generated a great deal of interest in the development of photo-activated controlled-release systems for pesticides. By developing an amphiphilic carboxymethyl chitosan compound (NBS-CMCS), Ye et al. pioneered a novel strategy⁵⁵. The major chains of CMCS were modified by joining hydrophobic photosensitive 2-nitrobenzyl succinate (NBS) to them. The conjugate was then used to create a shell cross-linking structure on a photo-responsive nanocarrier. A hydrophobic photosynthetic inhibitor called Diuron was encapsulated within this nanocarrier, and its controlled release was made possible by the nanocarrier's design. The research discovered that under dark environments, the micelles that had been cross-linked with glutaraldehyde (GA) had remarkable stability and confined size distribution. However, the average diameter of the micelles significantly increased after exposure to 365 nm UV radiation and consequently, the release of active compound is triggered. Using a similar approach, Liu et al. created a novel pesticide delivery system which utilized infrared light for intelligently control the release of imidacloprid (IMI).⁵⁶ Hollow carbon microspheres (HCMs) were employed in this system as IMI carriers. The light-controlled pesticide release system (HCMs/IMI/PEG/CD) was subsequently created by coating these HCMs with polyethylene glycol (PEG) and cyclodextrin (CD). The PEG/CD gel served as a gatekeeper to control the release of the pesticide, while the system used the HCMs as a reservoir for IMI. The gel network would collapse when the PEG/-CD gel reached the sol-gel transition temperature, causing the release of IMI owing to the strong heat-conversion capacity of HCMs in response to infrared light.

1.3.4.1. Photothermal Effect

The main step in photothermal conversion is the transformation of absorbed light energy into heat energy. Superior light absorption photothermal materials have the capacity to produce localized temperature increases when subjected to radiation.⁵⁷ Depending on the material, photothermal capacity depends on the spectrum of light that it absorbs. As an example, metallic nanoparticles have free electrons on their surface that can be activated by light at specific wavelengths, which is also referred to as localized surface plasmon resonance (LSPR). These nanoparticles demonstrate improved photothermal characteristics as a result of oscillating at the same frequency.⁵⁸

A semiconductor absorbs photons when they are exposed to light with energy equal to or greater than the bandgap between its conduction band and valence band. This energy is then transmitted to the crystal lattice, where it is converted into thermal energy and results in the photothermal effect.⁵⁹

In materials based on carbon and polymers, lattice vibrations play a role in a different mechanism for the photothermal effect through light absorption. When these materials are subjected to received light energy, electrons in the lower energy orbital can easily be stimulated and transfer to higher energy orbitals by light absorption.⁶⁰ This causes vibrations in the atomic lattices, which raise the temperature dramatically⁶¹.

1.4 Thesis objective: The importance of controlled release systems for pesticide use

One of the main issues with conventional pesticide systems is that a sizable amount of the active ingredient degrades without being efficiently used. Furthermore, most pesticide systems provided in solvent form use organic solvents which are mostly derived from petroleum or other non-renewable resources that have hazardous qualities. They may accumulate within soil, water, and the atmosphere, contaminating ecosystems and endangering the health of people, animals, and plants⁶². All of these elements put the

environment and people's health in danger, highlighting the demand for a pesticide system that can keep the active ingredient active for an extended amount of time. This would decrease soil and water contamination by allowing the same amount of pesticide to be utilized over an extended length of time.

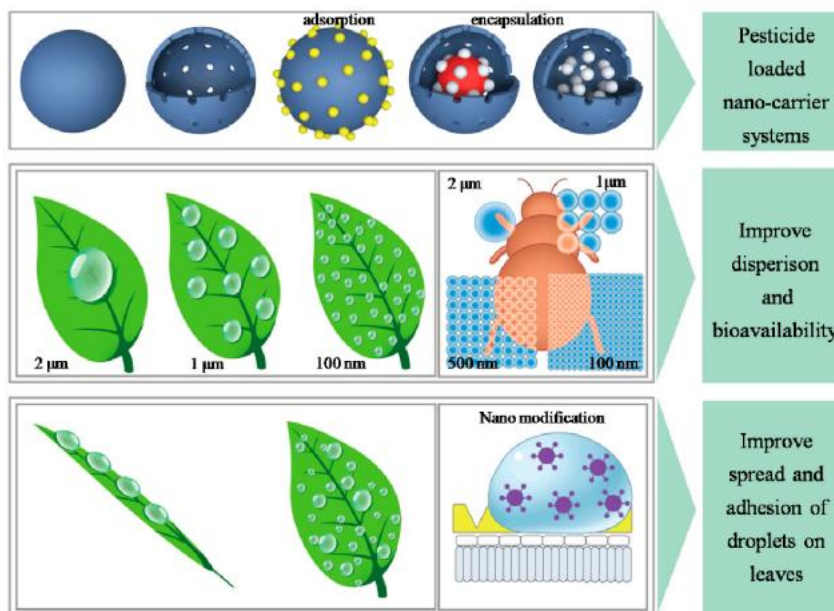


Figure 5. Effect of Nanoformulations as pesticide systems⁶³

1.4.1 Controlled release systems of pesticides as an alternative approach

Alternative pesticide delivery methods have been developed in the literature for all the reasons listed above. The main goal is to prevent pesticides from degrading after prolonged use and utilize more environmental-friendly compounds in formulations in order to mitigate the adverse effects of traditional pesticide use on the environment and human health. Consequently, the use of pesticide controlled-release systems and the development of smart delivery systems for agrochemicals are needed. Numerous release system types have been designed in the literature using various types of carriers, including hydrogels⁴⁰, polymers⁶⁴ and nanoparticles⁶⁵ as well as a range of stimuli, including pH⁴⁰, enzymes⁶⁶, and NIR⁶⁷ light. However, no studies have been conducted on a system that employs a constantly available trigger, like sunlight, utilizes water as the pesticide formulation's solvent, and is nearly entirely based on compounds derived from

biocompatible materials. Besides, there has been limited research in the design of HNT-based stimuli-responsive release mechanisms. This drawback results from the open-ended porous structure of HNTs, which causes the spontaneous release of cargo that has been encapsulated, although in a prolonged way. There are not many studies on the implementation of HNTs as natural carriers in pesticide delivery systems that incorporate external stimuli like sunlight. This inspired us to concentrate on this specialized subject and create a release system made entirely of substances that are organic. This thesis' major objective is to develop such a pesticide delivery technique and evaluate how effectively it works against pests.

1.5 Dissertation Overview

This thesis focuses on the design of a pesticide controlled-release system that is triggered by sunlight. Pesticide nanoformulations based on the designed sunlight-activated controlled release system are studied in terms of their pesticide activity. Two different pesticides, i) essential oils as a model natural pesticide, ii) abamectin as a model chemical pesticide have been incorporated into sunlight-activated controlled release systems and investigated in terms of their release properties, plant interactions and pesticide activity.

The first study involves sunlight-activated essential oil pesticide nanoformulations. Essential oils were loaded into photothermal nanocarriers prepared by the functionalization of HNTs. Encapsulated essential oils were further functionalized with a heat-activated stopper, lauric acid (LA) that will act as a stopper. The resulting controlled release system was investigated in terms of its morphological, photothermal and sunlight-activated release properties. Furthermore, the essential oil release system was tested in terms of its pesticide activity on *Myzus persicae* and demonstrated to present strong pesticide activity.

The second study involves sunlight-activated abamectin nanoformulations. The commonly used agrochemical abamectin (abm) was encapsulated within photothermal nanocarriers prepared by the polydopamine functionalized HNTs. LA was then utilized on the resulting nanohybrids and served as a release facilitator. The surface morphologies, sunlight-activated temperature increase profiles and sunlight-activated

abm release properties of the nanohybrids were studied. The aqueous dispersions of the LA/abm@HNT nanohybrids were further studied in terms of their suspensibility, soil infiltration, adhesion properties and pesticide activity on *Myzus persicae*.

Two different solutions to the problem of the degradation of pesticides and producing a solution without using an organic solvent have been provided by the design of sunlight-triggered controlled release systems.

CHAPTER 2. SUNLIGHT-TRIGGERED ESSENTIAL OIL RELEASE SYSTEMS AS NATURAL PESTICIDE NANOFORMULATIONS

2.1 Abstract

In this study, we have developed and investigated a controlled release system for the sunlight-triggered release of essential oils. Essential oils (EO) were encapsulated in photothermal nanocarriers composed of polydopamine-coated halloysite nanotubes (HNT-PDA), and further functionalized with lauric acid (LA) as stopper molecules, which prevent the release of the EO in the absence of the sunlight. HNT-PDA nanocarriers were synthesized by the oxidative polymerization of dopamine on HNTs and the resulting HNT-PDA nanohybrids were demonstrated to present temperature elevations when irradiated with sunlight. Via solvent-assisted impregnation the HNT-PDA nanocarriers were loaded with carvacrol, peppermint, basil, and cinnamon essential oils and their mixtures model natural pesticides, followed by impregnation of the LA stopper resulting in LA/EO@HNT-PDA nanohybrids. The produced nanohybrids were shown to retain their nanotubular structures by visualization by electron microscopy. Under irradiation from a solar simulator, LA/EO@HNT-PDA nanohybrids heated up to temperatures required for the LA stopper to melt and trigger the release. DSC analysis was employed to investigate the EO release from the nanohybrids in both the absence and presence of the sunlight-trigger. Over 5 days during which the nanohybrids were daily exposed to 6 h sunlight, LA/EO@HNT-PDA nanohybrids were shown to slowly release 50 % of the loaded EO, whereas the same nanohybrids did not present significant release when not exposed to sunlight. The released EO was demonstrated to retain its antibacterial activity against *Staphylococcus aureus*, thus confirming that the sunlight

irradiation did not decompose the loaded molecules. Furthermore, LA/EO@HNT-PDA nanohybrids that had been exposed to sunlight daily for 6 h presented significant killing activity on *Myzus persicae* aphids for at least 10 days. Overall, this study offers a novel design for a sunlight-triggered release system, that exhibits potential for applications involving controlled release in agriculture, especially as environmentally reliable and long-lasting alternatives for traditional pesticides.

2.2 Introduction

Due to the increasing use of synthetic pesticides, the amount of accumulated residues in the environment escalated, resulting in adverse effects on both the environment and human health⁶⁸. In parallel, the need for alternative, bio-degradable, and non-toxic pesticides has become highly significant. Essential oils, comprising volatile active constituents, are found in aromatic plants, wherein a primary component is present in higher concentrations compared to other constituents within the compound. There are some studies that exhibit the antimicrobial^{69,70}, antioxidant⁷¹, and insecticidal activities of essential oils⁷². Due to their significant volatility, essential oils exhibit a short degradation period when employed for pesticidal or insecticidal purposes. This is why further methods are needed to preserve their active ingredients for longer periods of time and to take advantage of their superior potential as natural, non-toxic pesticides.

EOs are encapsulated by various encapsulation techniques such as emulsification, spray drying, or vacuum to preserve their functionality for an extended time. Wang Et al.⁷³ designed a nano emulsion by emulsified LCEO (litsea cubeba essential oil) which has good stability at low temperatures. Another study shows the encapsulation of cumin Seed oil within the matrix consisting of chickpea protein isolate (CPI) and maltodextrin (MD) to maximize the oil encapsulation efficiency and oil retention⁷⁴. All of these are highly complex encapsulation methods that require additional chemicals. Due to their tubular structures, halloysites are excellent carriers for loading essential oils, and there are a number of systems where different essential oils have been loaded in the literature^{75,76}.

Although the antibacterial, antifungal, and antioxidant properties of essential oils have been highlighted in the literature, there are very few instances of essential oils being used as pesticides. This can be attributed to the highly volatile nature of essential oils, their low stability, and low water-solubility. More specifically, there are no examples of essential oils being used as pesticides in stimulus-triggered control-release systems. Due to this knowledge gap, we have investigated pesticide formulations of essential oils with

controlled release properties to explore and address this deficiency in the field. In this study, a novel, environmentally friendly system for controlling the release of essential oils from HNT nanocarriers was established. HNTs were functionalized with polydopamine (PDA) with great near-infrared (NIR) absorption, high light-to-heat conversion efficiency, and ability to stick to a variety of surfaces to result in photothermal HNT-PDA nanocarriers. These nanocarriers were employed to encapsulate a variety of essential oils, particularly peppermint, cinnamon, and basil oils, which were selected as representative natural pesticides. Lauric acid, a temperature-sensitive phase change material was further impregnated to the HNT-PDA nanocarriers, which was anticipated to act as a stopper that can be removed via its melting upon the sunlight-triggered heating of the HNT-PDA nanocarriers. The loading and sunlight-activated release characteristics of the HNT-based controlled EO release system and its potential as an efficient, and completely natural and environmentally safe pesticide release system was studied.

2.3 Experimental

2.3.1 Chemicals

HNTs were supplied by ESAN Eczacıbaşı in Istanbul, Turkey. Dopamine (3-hydroxytyramine hydrochloride) was provided from Acros Organics Inc (Geel, Belgium). Pure cinnamon, basil and peppermint oils were provided by Arifoğlu Marketing Distribution. Carvacrol was obtained from Tokyo Chemical Industry Co. LTD (Tokyo, Japan). Ultrapure Tris base (Tris(hydroxymethyl)aminomethane) was obtained from MP Biomedicals, LLC (Irvine, CA, USA). Lauric acid was obtained from Merck (Darmstadt, Germany). Agar powder and Tryptic soy broth (TSB) were supplied from Medimark (Italy). Extra pure methanol (99.8%) was obtained from Tekkim Ltd. (Bursa, Turkey). Using the Milli-Q Plus system, pure water was produced. All compounds were utilized without any further purification.

2.3.2 Preparation of the HNT-PDA nanohybrids

Prior work provided a detailed description of the HNT-PDA nanohybrids' synthesis⁷⁷. In brief, pure HNTs were dispersed in deionized water at a concentration of 10 mg/mL using ultrasonication (QSonica, Q700, Newtown, CT, USA) at 50 % amplitude with 5 s pulse on and 2 s pulse off in an ice bath for 20 min. Dopamine was added to the HNT dispersion at 8 mg/mL concentration. Tris base was added to the dispersion to bring the pH down to 8.5 while it was continually stirred for 24 h at 30 °C. The leftover dopamine was removed from the dispersion by centrifuging it at 11 000 rpm and washing it six times with deionized water. Powdered HNT-PDA nanohybrids were dried for 24 h at 70 °C.

2.3.3 Characterization of the HNT-PDA nanohybrids

Thermogravimetric analysis (TGA) was carried out on prepared HNT-PDAs using a Shimadzu Corp. DTG-60H (TGA/DTA) instrument. The sample was heated at a rate of 10 °C/min up to 1000 °C in a controlled nitrogen atmosphere. The samples were dried within the instrument's chamber for 20 min at 100 °C in order to remove any remaining moisture content before the testing process started.

A solar simulator was used to simulate exposure to sunlight in order to create the time-temperature profiles of HNT-PDA nanocarriers. Oriel LCS-100 solar simulator was used to irradiate 0.1 g of powder for 15 min at a light density of 100 mW/cm² and 300 mW/cm². In order to record temperatures, a FLIR 6XT2 2.1L thermal camera was used. The photothermal powder samples were exposed to irradiation three times to produce time-temperature profiles; data were collected from three different locations on the samples and mean and standard error values were reported.

2.3.4 Preparation the EO@HNT-PDA and LA/EO@HNT-PDA nanohybrids

HNT-PDAs were impregnated with essential oils using the solvent assisted impregnation method with the vacuum process to create LA/EO@HNT-PDA and EO@HNT-PDA nanohybrids⁷⁶. Cinnamon, basil, peppermint essential oils, their combinations (0.1 g of each essential oil) and carvacrol were utilized separately as EOs. HNT-PDAs were dried for 24 h at 100 °C in a vacuum oven before being impregnated. 10 mL of methanol was used to dissolve 0.3 g of the essential oil, and after introducing 0.7 g of HNT-PDA, the mixture was placed in an ultrasonic bath for 20 min. The resultant nanohybrids were denoted as EO@HNT-PDA. The mixture was then combined with 0.5 g of LA and sonicated for 5 min. The pressure was subsequently reduced to 0.3 kPa and the methanol was removed from the system and the mixture was transferred to a water bath at 70 °C.

The synthesized LA/EO@HNT-PDA and EO@HNT-PDA nanohybrids were dried for 24 h at room temperature, and the resulting powder samples were kept at 4 °C in closed glass vials. Theoretically, the weight ratios of lauric acid and essential oils in the nanohybrids were 20 % and 33 %, respectively.

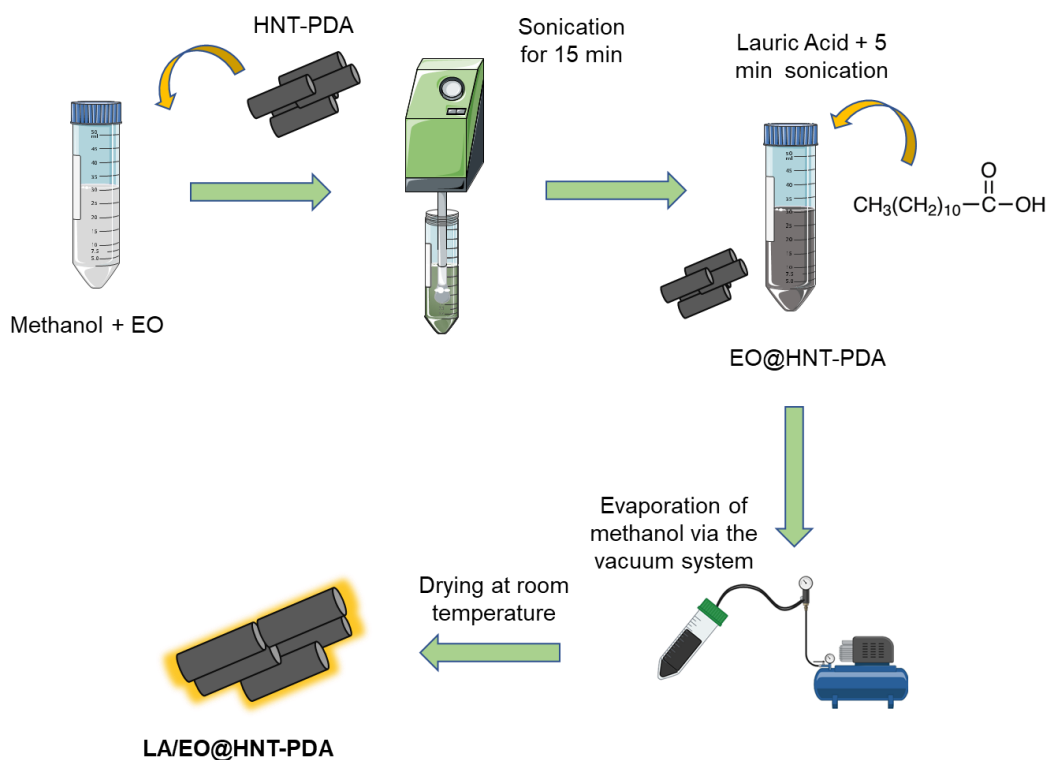


Figure 6. Schematic representation of experimental procedure of EO@HNT-PDA and LA/EO@HNT-PDA via Solvent-assisted impregnation method with vacuum treatment

2.3.5 Characterization of the EO@HNT-PDA and LA/EO@HNT-PDA nanohybrids

The amount of essential oils impregnated in HNT-PDA nanohybrids was determined by thermogravimetric analysis (TGA) (Shimadzu Corp. DTG-60H (TGA/DTA)). The samples were heated to 1000 °C at a rate of 10 °C/min with nitrogen flow. The wt. % of

EO in each LA/EO@HNT-PDA nanohybrid was calculated utilizing the same approach. Since each EO has a distinct decomposition temperature, the calculation of the encapsulation amount for each nanohybrid was performed by considering different temperature ranges. The formula below provides the calculation utilized for each of essential oil types encapsulated in nanohybrids and functionalized with lauric acid:

$$E_{EO}\% = [(WL\%_{20-250\text{ }^{\circ}\text{C}, \text{nanohybrid}} \times A)] + [(WL\%_{250-T_1\text{ }^{\circ}\text{C}, \text{nanohybrid}}) - (WL\%_{250-T_1\text{ }^{\circ}\text{C}, \text{HNT-PDA}})]$$

$E_{EO}\%$ denotes the wt. % of EO encapsulated. LA decomposition is completed at 250 °C, ‘A’ is the percentage of the specified pure EO that decomposes at 250°C. The temperature at which the specified pure EO is entirely decomposed is denoted by T_1 . The aim of the second part of the equation is to eliminate HNT-PDAs from the total encapsulation amount in the same temperature range that the specified EO totally decomposes.

The formula below provides the calculation utilized for each of EOs encapsulated in nanohybrids:

$$E_{EO}\% = (WL\%_{20-T_1\text{ }^{\circ}\text{C}, \text{nanohybrid}}) - (WL\%_{20-T_1\text{ }^{\circ}\text{C}, \text{HNT-PDA}})$$

The temperature at which the specified pure essential oil is entirely decomposed is denoted by T_1 . Similar to the equation designed for LA-functionalized nanohybrids above, the aim of the second part of the equation is to eliminate HNT-PDAs from the total encapsulation amount in the same temperature range that the specified essential oils totally decompose.

The produced LA/EO@HNT-PDA and EO@HNT-PDA nanohybrids were visualized with a Zeiss LEO Supra 35VP scanning electron microscope (SEM). Images were captured using a secondary electron detector at 6 kV after the samples were coated with Au-Pd.

LA/EO@HNT-PDA and EO@HNT-PDA nanohybrid samples in powder form were placed on carbon-coated grids for examination using transmission electron microscopy (TEM). A JEOL JEM ARM200CF operating at 200 kV was used for the TEM analysis.

To obtain time-temperature profiles for LA/EO@HNT-PDA and EO@HNT-PDA nanohybrids, exposure to sunlight was simulated using a solar simulator. 0.1 g of powder was exposed to 300 mW/cm² of irradiation for 15 min using the Oriel LCS-100 solar simulator and temperature measurements were observed using a FLIR 6XT2 2.1L thermal camera. Photothermal powder samples were irradiated three times to generate time-temperature profiles; data were obtained from three distinct sites on the samples and mean and standard error values were reported.

Differential scanning calorimetry (DSC) (Thermal Analysis MDSC TAQ2000) with a heating rate of 10 °C/min between 0 and 300 °C in nitrogen atmosphere was used for analyzing the thermal characteristics of the produced nanohybrids.

2.3.6 Release of EO from LA/EO@HNT-PDA nanohybrids

By analyzing the essential oil vaporization enthalpy of the nanohybrid at each time point, the DSC analysis was utilized to determine the EO release from the nanohybrids in powder form. The nanohybrid to be investigated was spread out on a plate without a cover and left at room temperature to determine its release profile in the absence of sunlight. Three samples were obtained from different regions of the plate at predetermined time intervals, placed in DSC crucibles, and DSC measurements were carried out. To determine the sunlight release profile of the nanohybrids, the powdered nanohybrid was spread on a plate and placed under a solar simulator (Oriel LCS-100) at a light intensity of 3 sun (300 mW/cm²) and 1 sun (100 mW/cm²). Three cycles of 6 h of sunlight-irradiation followed by 18 h of dark-incubation were performed. Three samples were obtained from various areas of the plate at predetermined time intervals, placed in DSC crucibles, and DSC measurements were made. The enthalpy values were computed using the TA universal analysis software, and the start and end points of the transition peaks were identified using the tangent method⁷⁸. Equation below was used to determine the percent EO release at the time point by averaging the three Enthalpy of vaporization values.

$$\% R_{EO} = 100 - \left(\frac{\Delta H_t}{\Delta H_0} \times 100 \right)$$

where "% R_{EO}" denotes the amount of EO that has been released from the nanohybrid, " ΔH_0 " denotes the enthalpy of EO evaporation in the nanohybrid at initial time frame, and " ΔH_t " is the enthalpy of EO evaporation in the nanohybrid at the moment of measurement. All tests were performed at 23.5 °C and around 53.8% relative humidity.

2.3.7 Antibacterial properties of the EO released from LA/EO@HNT-PDA

Nanohybrids

Staphylococcus aureus (*S. aureus*) (ATCC 29213) were grown in 3 mL of TSB growth medium by an overnight incubation at 37 °C. 100 μ L (10⁹ cfu/mL) of grown bacteria were spread uniformly on the agar plates by using a sterile swab. A sterile filter paper cut to a circular shape of 2 cm diameter was placed on the center of the plate, 0.2 g of LA/EO@HNT-PDA was placed on the filter paper and the plate was fit with a glass cover. Black cardboard with a round hole the same size as the filter paper in the middle was placed on top of the plates, so that the sunlight contacts the LA/EO@HNT-PDA powder sample on the filter paper only. The plate containing the LA/EO@HNT-PDA and the control plate that contained the filter paper only were irradiated with light from a solar simulator (Oriel, LCS-100) at 1 sun (100 mW/cm²) for 6 h. Another plate that contained the LA/EO@HNT-PDA powder was not exposed to light and kept in the dark for 6 h. Following the 6 h sunlight/dark period, filter papers with the samples were gently removed from the surface of the plate with a sterile tweezer and all plates were incubated overnight at 37 °C.

2.3.8 Pesticide activity of the LA/EO@HNT-PDA and EO@HNT-PDA nanohybrids on *Myzus Persicae*

Myzus persicae was grown in a climate-controlled environment on eggplant seedlings with an 8 h light and 16 h dark photoperiod at 25 °C. The eggplant leaves (*Solanum melongena*) were consumed by the aphids. The prepared nanohybrids were developed under a variety of conditions to evaluate their success in killing aphids. Identical quantities of the LA/EO@HNT-PDA and EO@HNT-PDA nanohybrids were daily exposed to sunlight for 6 h for 10 days. The light exposure was stopped right away after each 6-h interval, and 10 aphids were put onto the surfaces that had been treated with sunlight. The mortality rate was calculated by counting the number of dead aphids. For ten days, this experimental process was conducted. The nanohybrids that were kept in the dark underwent a similar experiment. The LA/EO@HNT-PDA and EO@HNT-PDA nanohybrids, which were not exposed to light over the duration of the entire experiment, had 10 aphids placed on nanohybrids after the 6-h irradiation each day. The mortality rate was then determined by counting the number of dead aphids.

2.4 Results and Discussion

2.4.1 The design and preparation of LA/EO@HNT-PDA controlled release system

The design of the sunlight-triggered EO release system is based on HNTs that are functionalized with PDA to impart light-to-heat conversion properties. The light-induced heating attributes of the HNT-PDA nanocarriers were expected to be utilized to remotely heat the EO-loaded and LA-functionalized HNT-PDA nanocarriers to the temperature needed to trigger the phase change transition of LA. The LA, which serves as a stopper for volatile EOs, was designed to undertake a phase change, allowing the release of the EO encapsulated in the HNT-PDAs when irradiated with sunlight (Figure 7).

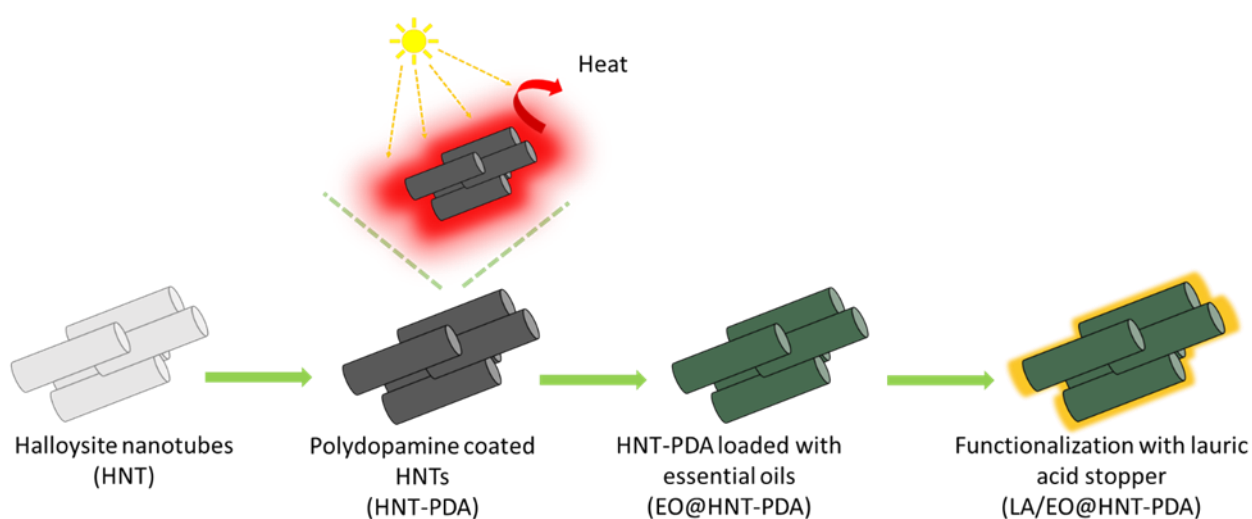


Figure 7. The design of the sunlight triggered EO release system.

Dopamine was oxidatively polymerized on HNT carriers to create HNT-PDA nanohybrids, which later served as photothermal carriers for the encapsulation of essential oils⁷⁷. When exposed to sunlight for 60 min at a light density of 1 sun and 3 sun, respectively, it was found that the HNT-PDA nanocarriers were heated to 46 °C and 101

°C (Figure 8), confirming that produced HNT-PDA nano hybrids were imparted photothermal character after PDA coating. Neat HNTs did not exhibit significant temperature elevations under the same conditions. The PDA coating on the HNTs introduced photothermal capabilities and facilitated their implementation as organic, non-toxic, low-cost nanocarriers that can provide light-to-heat conversion ability.

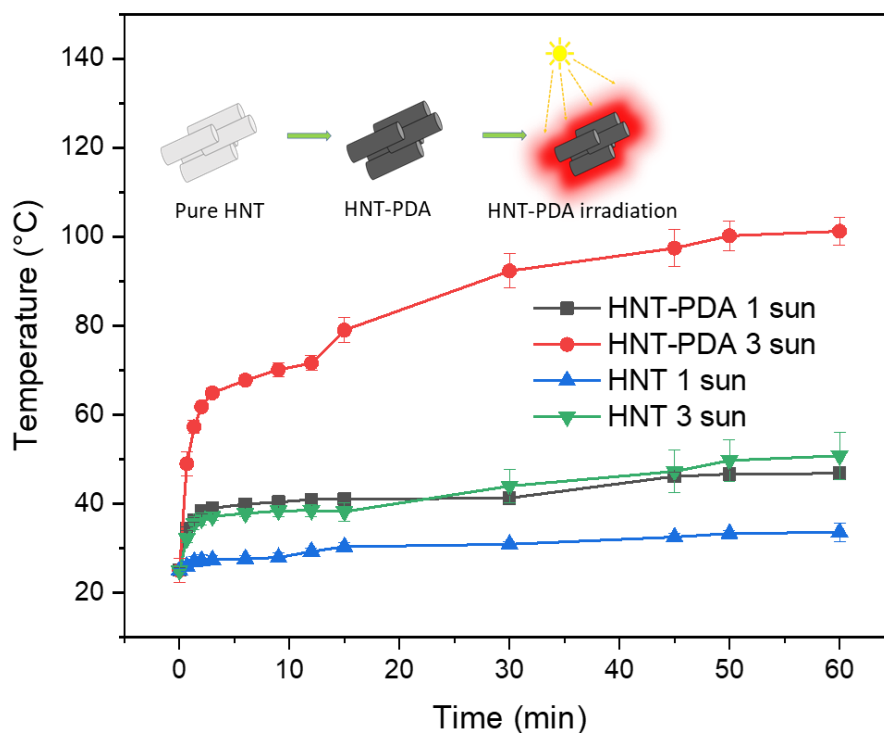


Figure 8. Time-temperature profiles of HNT and HNT-PDA nano hybrids under sunlight irradiation at 3 sun (300 mW/cm^2) and 1 sun (100 mW/cm^2) light density.

As a model natural pesticide, a blend of peppermint, cinnamon, and basil oils (EO) were loaded onto HNT-PDA nanoparticles using solvent-assisted impregnation. Using the same approach, the resulting EO@HNT-PDA nanoparticles were loaded with LA to produce LA/EO@HNT-PDA nano hybrids with theoretical weight ratios of 20 % and 33 % for EO and LA, respectively. The experimental loading ratios of three EOs, namely cinnamon oil, peppermint oil, and basil oil, as well as the mixture of them, were calculated using TGA by contrasting the weight loss ratios of the neat and loaded essential oils. The loading percentages of cinnamon oil, peppermint oil, and basil oil that were

present in the non-lauric acid functionalized HNT-PDA nanohybrids were 34%, 29%, and 24%, respectively, as shown in Figure 9a, 9b, and 9c. These values did not vary considerably from the expected loading ratio of 30 %. The loading ratios of cinnamon oil, peppermint oil, and basil oil in the LA-functionalized HNT-PDA nanohybrids were 26.6 %, 27.2 %, and 14.3 %, respectively, illustrating the successful loading of both components into the nanohybrids. The loading ratio of the EO mixture was shown to be 23.9% for LA-functionalized nanohybrids and 31.9 % for non-LA-functionalized nanohybrids (Figure 9d). The encapsulation of LA in the HNT pores and some loss during the solvent-assisted impregnation procedure may have caused the the small deviations from the theoretical loading ratios.

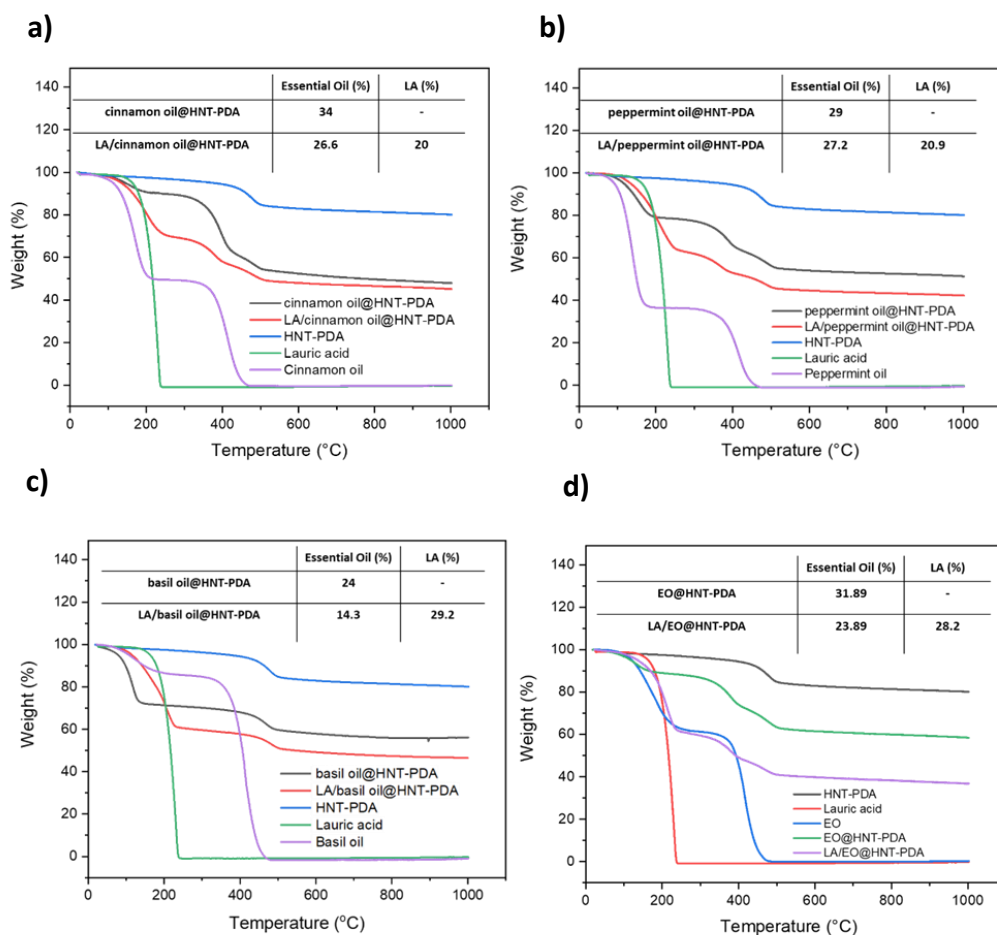


Figure 9. TGA of HNT-PDA nanocarriers loaded with cinnamon oil (a), peppermint oil (b), basil oil (c), and the mixture of all three EOs (d).

The LA EO@HNT-PDA release system was further characterized with DSC. Figure 10 illustrates how, following the functionalization with LA, the evaporation transition temperature of the EO mixture, which was approximately 85 °C in the EO@HNT-PDA nano hybrids, shifted to around 260 °C. LA seems to act as a protective layer around the EO@HNT-PDA nano hybrids, preventing the evaporation of the EO as seen in the shift of their transition temperature to higher temperatures.

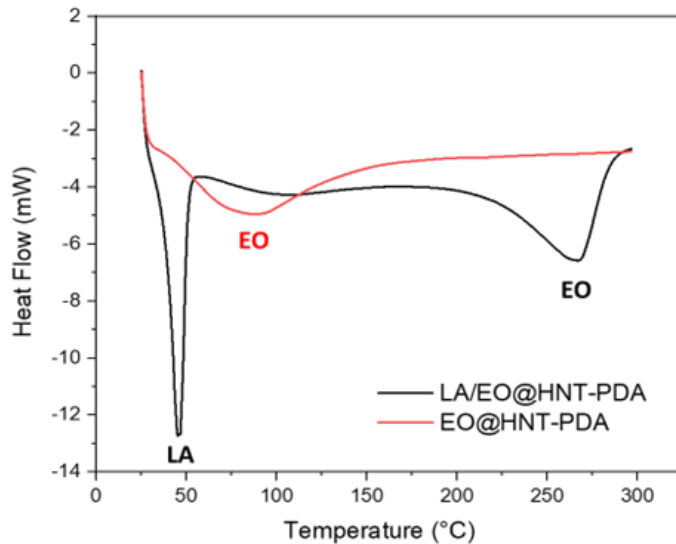


Figure 10. DSC analysis of EO@HNT-PDA and LA/EO@HNT-PDA nano hybrids.

According to the SEM analysis of the EO@HNT-PDA and LA/EO@HNT-PDA nano hybrids, the HNT-PDA nanocarriers maintained their nanotubular structure following encapsulation of EO and LA functionalization and the LA contributed to an even coating on the EO@HNT-PDA nanocarrier surface (Figure 11).

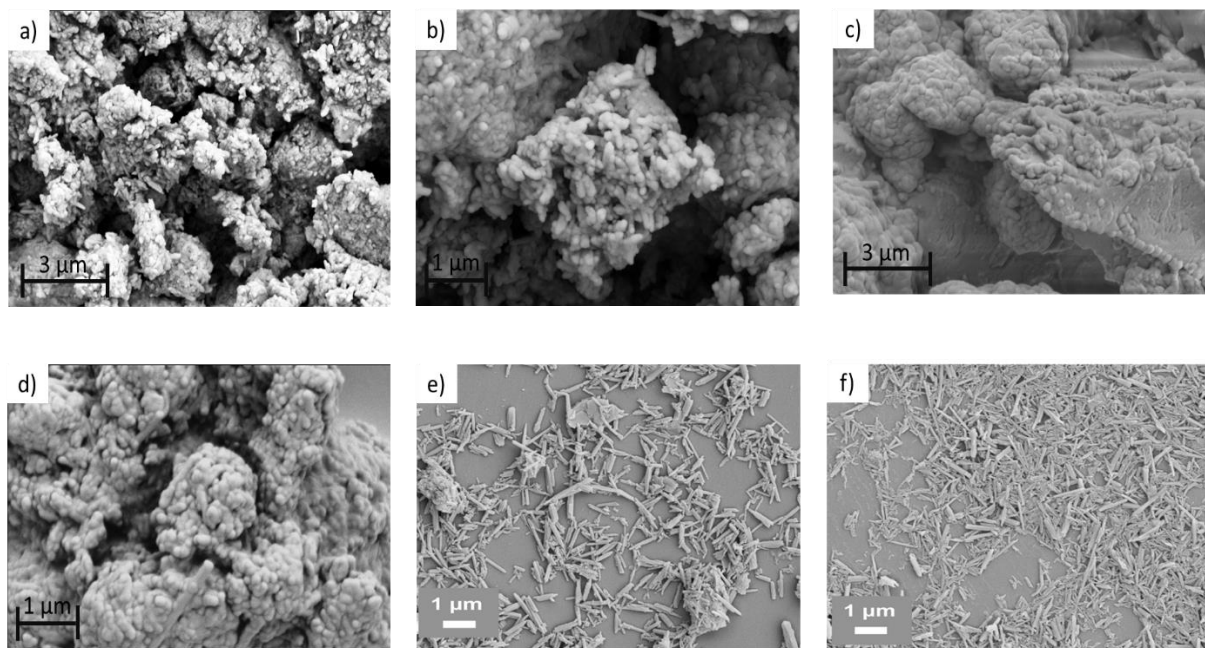


Figure 11. SEM images of EO@HNT-PDA (a, b), LA/EO@HNT-PDA (c, d) nanohybrids, neat HNT (e) and HNT-PDA nanohybrids (f).

TEM analysis was employed to visualize the surface morphologies of the LA/crv@HNT-PDA nanohybrids, prepared by encapsulation of carvacrol (crv), the active component of thyme oil, in comparison to neat HNTs and HNT-PDA nanocarriers. Figure 12 displays the TEM images that reflect each nanohybrid. The neat HNTs, HNT-PDA nanohybrids, and HNT-PDA nanohybrids impregnated with crv presented a nanotubular structure with an open-ended lumen and a smooth surface. The LA/crv@HNT-PDA nanohybrids, however, demonstrated that the LA molecules were sufficiently adsorbed on the crv@HNT-PDA nanohybrids by capillary and surface tension forces and could act as a stopper to prevent the release of the encapsulated active substance. The transparent area inside the HNT also went away, and the open ends of the HNT appeared to have become closed when the nanocarriers were functionalized with LA.

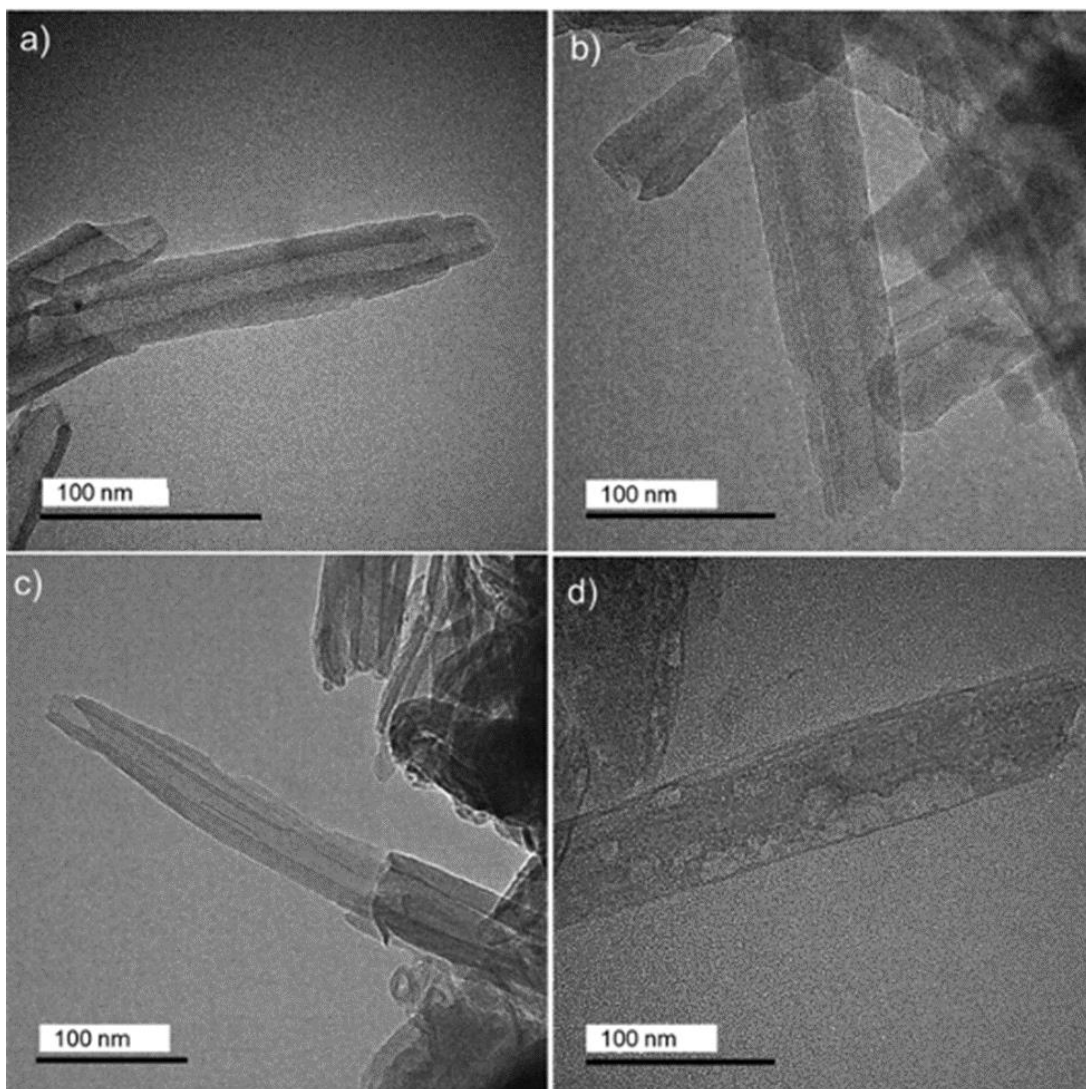


Figure 12. TEM images of a) HNT, b) HNT-PDA, c) crv@HNT-PDA, and d) LA/crv@HNT-PDA nanohybrids.

Whether the LA/EO@HNT-PDA nanohybrids can experience light-activated heating upon sunlight irradiation and reach temperatures that can trigger the release mechanism was investigated. The time-temperature profiles of nanohybrids were generated by monitoring the temperature increases following irradiation from a solar simulator. According to the findings illustrated in Figure 13, when the EO@HNT-PDA and LA/EO@HNT-PDA nanohybrids were exposed to sunlight with a light density of 1 sun (100 mW/cm^2), a temperature increase of about $60 \text{ }^\circ\text{C}$ occurred, and the nanohybrids reached $110 \text{ }^\circ\text{C}$ when the light density went up to 3 sun (300 mW/cm^2). This result has

demonstrated that the sunlight-activated heating of the LA/EO@HNT-PDA nanohybrid could easily trigger the melting of the LA, as anticipated.

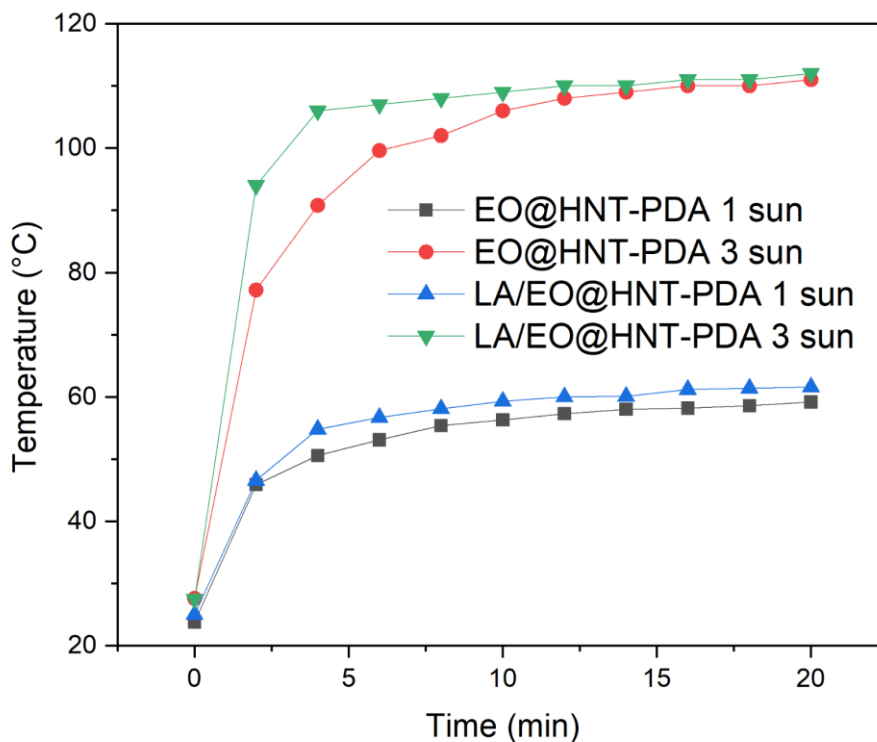


Figure 13. Time-temperature profiles of LA/EO@HNT-PDA and EO@HNT-PDA nanohybrids under irradiation at 3 sun (300 mW/cm^2) and 1 sun (100 mW/cm^2).

2.4.2 Release of EO from the LA/EO@HNT-PDA nanohybrids

The sunlight-activated release of EO from the LA/EO@HNT-PDA nanohybrids was analyzed using DSC. Due to the volatile nature of the EO, its release from the nanohybrids in powder form exposed to light over time was expected to be monitored directly from the enthalpy values of the sample obtained with DSC. Figure 14 demonstrates the experimental design for monitoring the release of sunlight-exposed LA/EO@HNT-PDA powder. LA/EO@HNT-PDA powder was exposed to sunlight for a period of 6 h followed by dark incubation for 18 h every day, for 5 consecutive days.

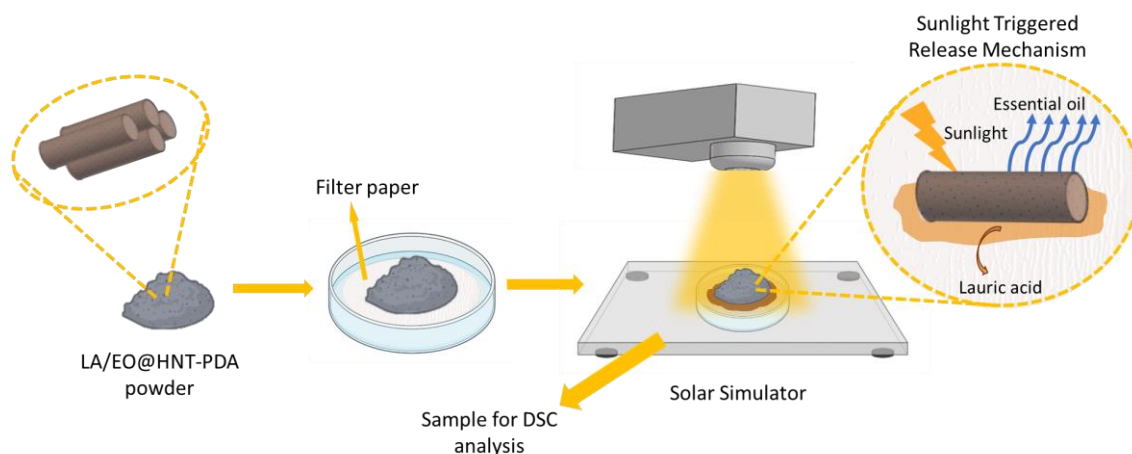


Figure 14. Schematic representation of the experiment designed for the investigation of the release behavior of EOs from LA/EO@HNT-PDA nanohybrids.

Due to the volatile nature of essential oils, nanohybrids exposed to light over time lose their active component concentration. Figure 15 demonstrates the DSC curves of the LA/EO@HNT-PDA samples that were exposed to 6 h sunlight for 2 and 5 days, respectively, as an example of how the EO release was monitored. The enthalpy of evaporation of the EO decreased when the nanohybrids were exposed to sunlight for 3 more days. A shift of the evaporation transition to higher temperatures was also visible on the nanohybrids irradiated for 5 days relative to the nanohybrids irradiated for 2 days. Apparently, the EO molecules absorbed on the outer surface of the HNT-PDA carriers were released first and the EO molecules impregnated in the lumen were released later, resulting in a higher evaporation temperature for the nanohybrids exposed to sunlight for longer time periods.

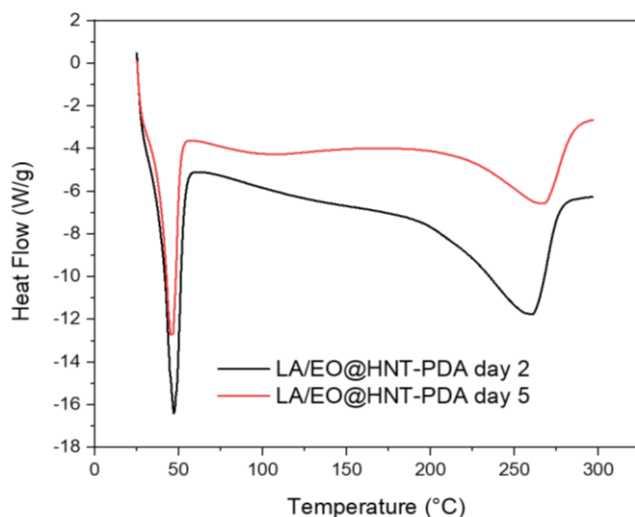


Figure 15. LA/EO@HNT-PDA nanohybrids after 2 and 5 cycles of 6 h sunlight irradiation/18h dark treatment.

Figure 16a shows the release behavior of the LA/EO@HNT-PDA nanohybrids over 5 days of daily sunlight irradiation. The samples were daily exposed to sunlight for 6 h followed by 18 h dark incubation. Another set of samples were kept in the dark for 24 h for the same duration. After 6 h each day, samples were taken for DSC analysis for both sunlight-activated and dark-incubated samples. Nanohybrids that were not exposed to sunlight presented only a 26 % release of the EO by the end of the 5th day. On the other hand, the same nanohybrids presented 55 % release of EO when were subjected to sunlight at 3 sun during the same period of time. As expected, the sunlight-activated heating of the HNT-PDA nanocarrier facilitated the release of the EO. It is clear from Figure 16b that LA was not released from the environment after it reached its melting transition. At the end of the fifth day, samples exposed daily to sunlight exhibited only 10 % release of the LA. This outcome suggests that a sizeable amount of the LA was still present on the surface of the nanohybrids and was still functioning as a stopper.

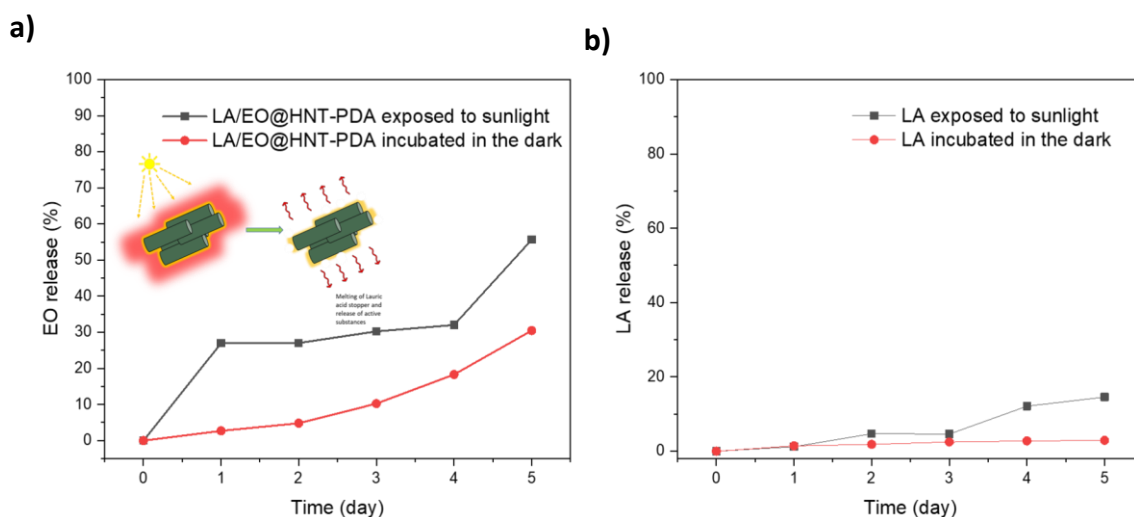


Figure 16. a) EO release behavior of LA/EO@HNT-PDA nanohybrids at 3 sun (300 mW/cm^2) and at room temperature in the dark b) Release behavior of LA from the nanohybrids at 3 sun (300 mW/cm^2) and at room temperature in the dark

The antibacterial activity of the crv released from the LA/crv@HNT-PDA was investigated to determine whether the released active substance retained its functionality, or it was negatively affected by the sunlight irradiation. Neat crv is known to have strong antibacterial effect against both gram-positive and gram-negative bacteria. Crv encapsulated in HNTs maintains its antibacterial effects when released gradually at ambient temperature, according to a prior study⁷⁹. The goal of the present study was to investigate whether crv released from the LA/crv@HNT-PDA nanohybrid still had antibacterial activity despite being heated by sunlight by designing an experiment as shown in Figure 17a. LA/crv@HNT-PDA powder placed on a Petri dish inoculated with *S. aureus* was exposed to sunlight for 6 h in order to release the crv from the nanohybrids. After that, the LA/crv@HNT-PDA nanohybrids were removed from the plate, and the plate was incubated to observe whether the released carvacrol altered the growth of the bacteria (Figure 17b). On the LA/crv@HNT-PDA powder-containing plate held in the dark for 6 h, a 3.1 cm inhibition zone was seen; however, total bacterial death was achieved, and no growth was seen on the plate exposed to sunlight for the same period of time (Figure 17c). The control plate without any nanohybrids, when exposed to sunlight, demonstrated growth inhibition of 1.4 cm only in the area of direct sunlight but did not present any growth inhibition at the rest of the plate. This result illustrated that sunlight

did not kill the bacteria on its own but the carvacrol released from the LA/crv@HNT-PDA powder killed the bacteria (Figure 17d and Figure 17e). These findings point out that the active substance released by the sunlight-activation was not decomposed and retained its inherent properties without being adversely affected by the temperature increase it was exposed to.

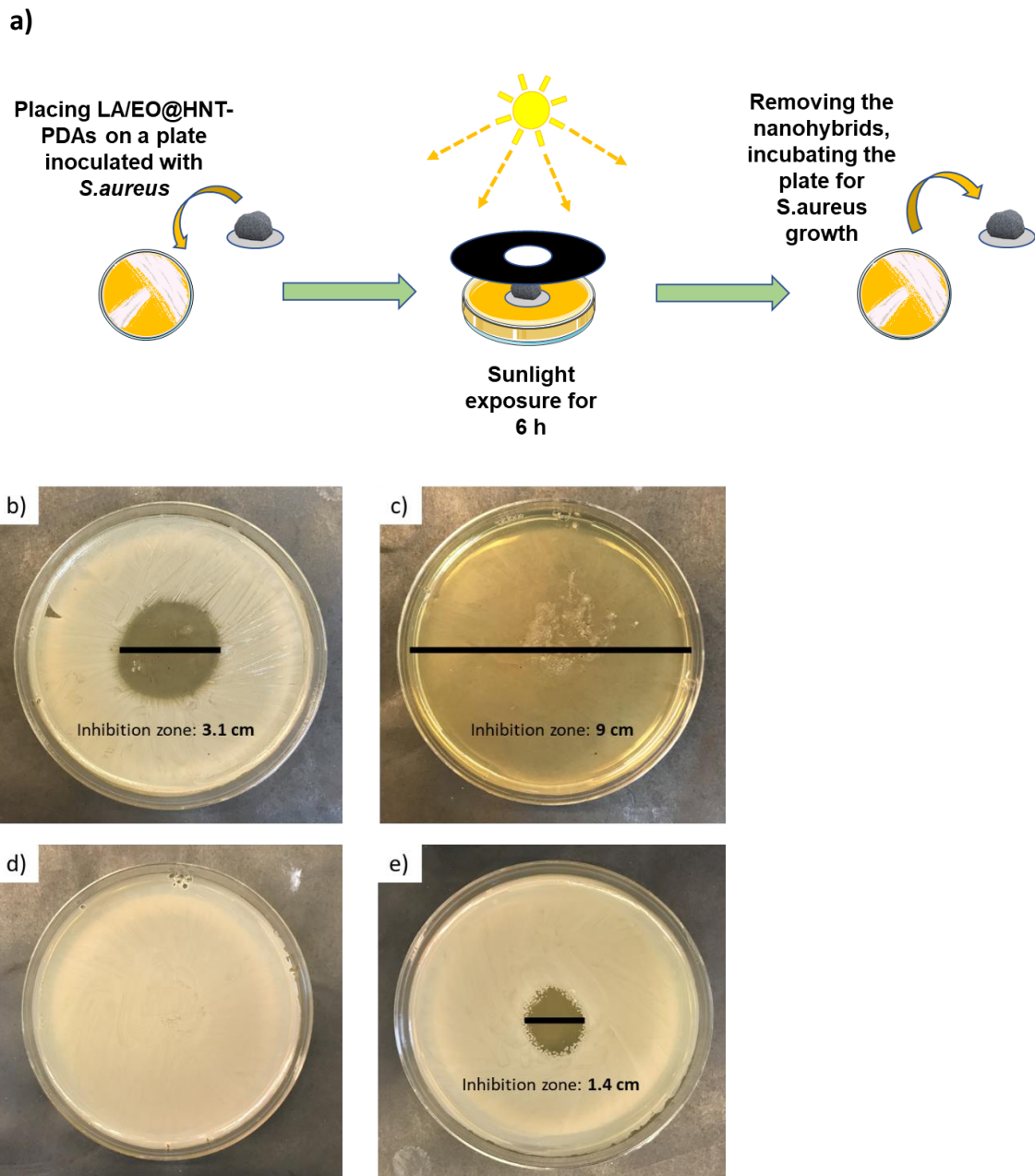


Figure 17. Schematic representation of Antibacterial activity analysis (a), nano hybrid containing agar plate incubated for 6 h in the dark, (b) nano hybrid containing agar plate

exposed to sunlight (c), control sample in the dark (d), control sample exposed to sunlight (e).

2.4.3 Pesticide activity of the LA/EO@HNT-PDA nanohybrids

The prepared LA/EO@HNT-PDA and EO@HNT-PDA nanohybrids have been examined in terms of their pesticide activity on *Myzus persicae* aphids in both their light-activated and dark-incubated powder forms. LA/EO@HNT-PDA and EO@HNT-PDA nanohybrids in powder form were either exposed to a 6 h sunlight or dark treatment, at the end of which live aphids were placed on the powders. This cycle was repeated 10 times and the mortality of the aphids was determined at the end of each cycle. Figure 18 illustrates that while EO@HNT-PDA nanohybrids treated with sunlight resulted in a very low mortality of the aphids only in the first and second cycles, LA/EO@HNT-PDA nanohybrids exposed to sunlight resulted in a 90% death in the aphid population at the first cycle and continued their killing effect even after 10 cycles. This result demonstrated that there was EO release from the LA/EO@HNT-PDA nanohybrids over at least 10 cycles of 6 h sunlight irradiation and the release of the EO could be easily controlled by the sunlight stimulus. The LA/EO@HNT-PDA and the EO@HNT-PDA samples, which was kept in the dark for 10 cycles, exhibited no mortality on the aphids, indicating that the non-exposed sample's restricted essential oil release was not adequate to kill the aphids.

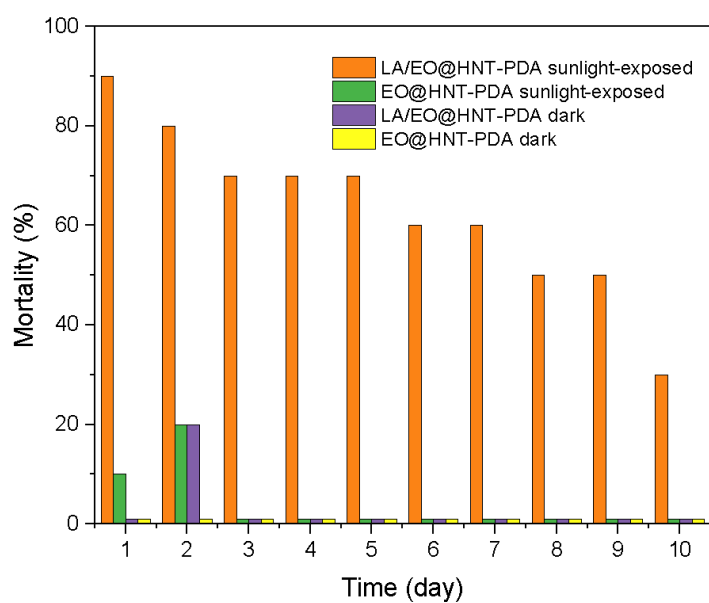


Figure 18. Killing activity of the of EO@HNT-PDA and LA/EO@HNT-PDA nanohybrids on *Myzus persicae* under sunlight irradiation at 3 sun and in the dark. The nanohybrids were exposed to 6 h sunlight/18 h dark treatment, or to 24 h dark treatment for 10 days.

2.5 Conclusions

There are numerous adverse effects on the ecosystem and human health as a result of the increased use of synthetic pesticides that build up in the environment. In the present work, EOs were embedded in a controlled-release system composed of naturally occurring HNTs that had been modified with PDA. The HNT-PDAs were utilized to encapsulate a mixture of peppermint, cinnamon, and basil essential oils, and the system's controlled-release abilities were examined in response to sunlight as an external stimulus. LA, a phase change material, was incorporated into the system to act as a stopper that prevents the release of EO in the absence of sunlight. When exposed to sunlight, LA can melt and release the cargo molecule, but in a dark environment, it can effectively entrap the active ingredient. The results indicated that the LA/EO@HNT-PDA nanohybrids exhibited controlled EO release over at least 5 days during which the samples were irradiated daily with sunlight for 6 h. The study additionally examined the extent to which the controlled release was performed by investigating the pesticide activity of the developed nanohybrids on the *Myzus persicae* aphids and the nanohybrids were shown to present strong killing activity even after 10 cycles on which they were exposed to sunlight. The sunlight-activated release system for the controlled release of EOs developed in this study has a strong potential as a promising replacement for synthetic pesticides.

CHAPTER 3. SUNLIGHT-ACTIVATED ABAMECTIN RELEASE SYSTEMS AS CONTROLLED-RELEASE PESTICIDE NANOFORMULATIONS

3.1 Abstract

Controlled release systems play a significant role in agriculture due to their ability to deliver various substances to plants and soil in a targeted and controlled manner. In this study, polydopamine functionalized halloysite nanotube (HNT-PDA) nanocarriers were utilized for the first time to encapsulate abamectin (abm) as a model agrochemical to accomplish sunlight-triggered release. Lauric acid (LA), a phase change material, was employed to functionalize the nanocarriers with an agent that facilitates the release mechanism when sunlight is present. The temperature of the system raised when the photothermal nanocarriers were exposed to solar irradiation, resulting in a phase transition of the LA, which triggers the release of abm from the nanocarriers to the surrounding environment. The release studies showed that abm was released gradually over a time period of 30 days, when nanohybrids were exposed daily to sunlight for 6 h and there was no abm release when the nanohybrids were kept in the dark. The released abm was shown to remain stable and kill *Myzus persicae* aphids at a rate over 70 % during at least 10 days, at which the nanohybrids were exposed to sunlight for 6 h every day. Aqueous dispersions of the LA/abm@HNT-PDA nanohybrids were prepared and studied in terms of their potential as aqueous sprayable pesticide nanoformulations. Aqueous dispersions of LA/abm@HNT-PDA nanohybrids presented over 30 % suspensibility and strong foliar retention even at environmental conditions simulating the rainfall. The LA/abm@HNT-PDA dispersion's LC₅₀ value was determined to be 9 mg/mL on *Myzus persicae*. Overall, the proposed sunlight-activated controlled release system based on photothermal, lauric acid-functionalized HNT-PDA nanocarriers holds a great potential as controlled release pesticide nanoformulations.

3.2 Introduction

Pesticides are essential for crop protection and enhancing agricultural productivity⁸⁰. However, their indiscriminate use can cause negative drawbacks to both human health and the environment⁸¹. Conventional pesticide formulations may lead to adverse ecological problems including the majority of the applied pesticides being lost to the environment and only less than 1% being effectively utilized at the intended target⁸². As an alternative approach, the delivery of the pesticides can be accomplished by the stimuli-responsive controlled-release systems which prolong the lifetime of the active ingredients in the pesticide and reduce the degradation time associated with external factors such as rainwater leaching or photodegradation⁸³⁻⁸⁶. The literature has reported different external factors for remotely triggered-controlled release systems of pesticide delivery. Xiang et al. designed a pH-responsive attapulgite-based hydrogel pesticide release system and characterized its release behavior in aqueous solutions with varying pH levels⁸⁷. Kaziem et al. developed an enzyme-responsive insecticide delivery system based on surface-functionalized hollow mesoporous silica loaded with insecticide and capped with α -CD, which is designed to release the pesticide cargo upon hydrolysis triggered by the presence of α -amylase⁸⁸. Even though all those designs have their own novelty, they all require an external stimulus which may be an additional cost or challenging to apply. The lack of an effortless, practical, and accessible stimulus that allows farmers to reach without being trained, causes majority of these controlled release systems not to be implemented in agriculture.

Sunlight-irradiation as photothermal stimulus stands out among the various external triggers due to its continuous availability, zero cost, and non-toxic nature and offers a powerful alternative as a trigger for agrochemical delivery systems. The most practical way to exploit sunlight as a controlled release trigger is to utilize photothermal materials that can convert sunlight to heat, and design release systems that are triggered by temperature elevations. A limited number of studies have demonstrated light-driven controlled release systems where the pesticide is released by light via photothermal

effects^{41,89,90}. However, a sunlight-triggered pesticide delivery system that is composed of natural, low-cost components, is easy to manufacture and easy to apply on the field and yet presents strong pesticide activity has not been reported.

Halloysite nanotubes (HNTs) with hollow tubular structures are naturally occurring inorganic clay nanoparticles, making them suitable for use as environmentally friendly nanocarriers^{91–95}. HNTs were commonly utilized as scavenging agents in food packaging applications⁹⁶, as drug delivery vehicles for cancer therapy⁹⁷, or as fillers for improving the mechanical properties of composites⁹⁸. Due to their open-ended and positively charged Al_2O_3 inner lumen and negatively charged SiO_2 outer surface porous structure, HNTs have been commonly used nanocarriers for the encapsulation of varied active substances such as pigments⁹⁹, essential oils^{92,100–102}, dyes¹⁰³, or drugs^{104,105}. However, utilization of HNTs as environmentally friendly nanocarriers of pesticides has not been demonstrated.

In this work, we designed a novel HNT-based sunlight-triggered controlled pesticide release system that allows pesticides to be released only under the sunlight and keeps the pesticide when no stimuli are present in the environment. The release system is composed of a photothermal nanocarrier that is loaded with pesticide molecules and a heat-activable release facilitator that helps the release of the pesticide upon sunlight-activation of the photothermal nanocarrier. While HNTs functionalized with polydopamine⁷⁷, a promising photothermal agent due to its robust NIR adsorption via excellent efficiency in light-to-heat conversion¹⁰⁶, have been utilized as the photothermal nanocarrier; lauric acid (LA), a temperature-sensitive phase change material was utilized as a release-facilitator. LA was expected to present a melting transition when the photothermal HNT-PDA nanocarriers are heated under sunlight irradiation and lead to the release of the loaded pesticide. We have previously demonstrated that a similar design allows sunlight-activated the release of a volatile molecule, carvacrol⁷⁶. Here, we demonstrate the utilization of the HNT-based sunlight-triggered release system for abamectin (abm), a non-volatile, widely used commercial pesticide¹⁰⁷, which can be easily degraded when directly exposed to sunlight¹¹² and the use of this release system in the form of aqueous sprayable nanoformulations presenting strong adhesion properties and strong pesticide activity on aphids.

3.3 Experimental

3.3.1 Chemicals

HNTs were supplied by ESAN Eczacıbaşı. Dopamine (3-hydroxytyramine hydrochloride) was purchased from Acros Organics Inc (Geel, Belgium). Ultrapure Tris base (Tris(hydroxymethyl) aminomethane) was acquired from MP Biomedicals, LLC (Irvine CA, USA). Abm was purchased from Sigma Aldrich, (US). Agrimec was obtained from Syngenta (Turkey). LA was purchased from Merck (Darmstadt, Germany). Extra pure methanol (99.8%) was obtained from Tekkim Ltd. (Bursa, Turkey). Pure water was obtained using a Milli-Q Plus system. All chemicals were utilized without any further purification.

3.3.2 Preparation of the HNT–PDA nanocarriers

As previously reported, oxidative polymerization of the dopamine monomer in the presence of HNTs was used to create HNT-PDA nanocarriers¹⁰⁸. In an ice bath, HNTs were dispersed in purified water (10 mg/mL) with ultrasonication (Qsonica, Q700) for 30 min at 40 % amplitude with 3 s pulse on and 2 s pulse off. Then, dopamine monomer was added to the dispersion to obtain an 8 mg/mL concentration of HNT-PDAs. A Tris-base powder was used to bring the pH to 8.5. For 24 h, the produced mixture was stirred at 30 °C. By centrifugation at 11000 rpm for 10 min HNT-PDAs were isolated from the reaction mixture. Afterwards, the obtained sample was rinsed 6 times with water to remove any residue of Tris-base and unreacted dopamine. In a vacuum oven, the prepared HNT-PDAs were dried for a 24 h period at 80 °C.

3.3.3 Preparation and characterization of the abm@HNT-PDA and LA/abm@HNT-PDA nanohybrids

Based on a previously published methodology^{20,109}, HNT-PDAs were impregnated with abm using a solvent-assisted impregnation approach followed by vacuum treatment to produce LA/abm@HNT-PDA and abm@HNT-PDA nanohybrids as shown in Figure 18. The HNT-PDAs were dried for 24 h at 100 °C in a vacuum oven before impregnation. A solution consisting of 0.4 g of abamectin, and 40 mL of methanol was prepared, and 0.6 g of HNT-PDAs were added. The resulting mixture was subsequently subjected to an ultrasonic treatment for 20 min. Additionally, the mixture was then added 0.5 g of lauric acid (LA) for LA-functionalized LA/abm@HNT-PDA nanohybrids, then sonicated for 5 min afterward.

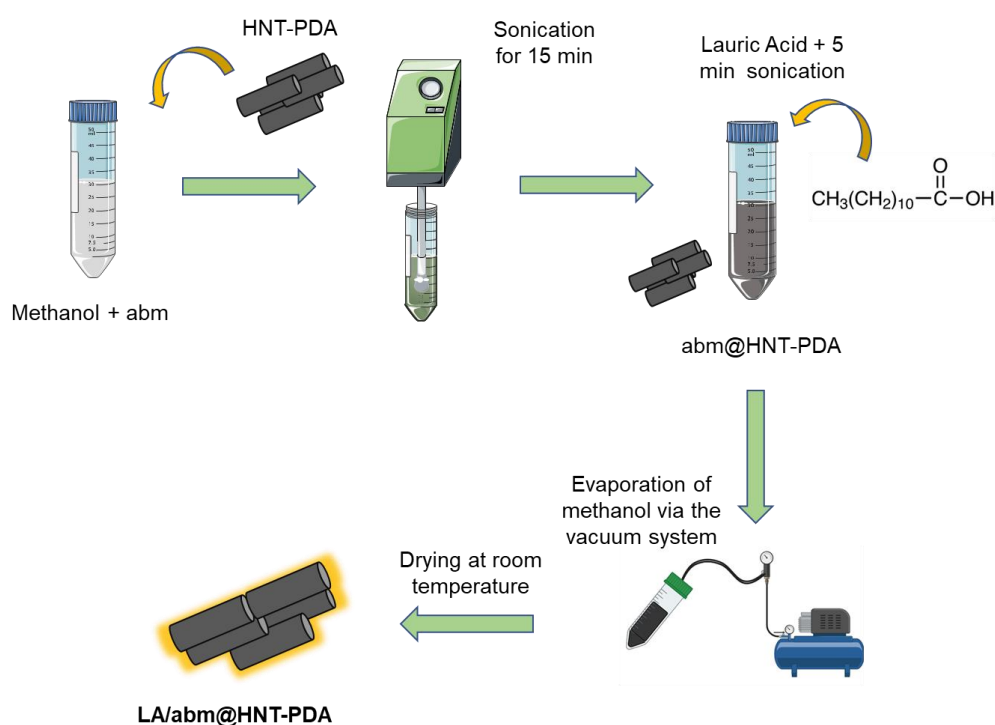


Figure 19. Schematic representation of experimental procedure of abm@HNT-PDA and LA/abm@HNT-PDA preparation via solvent-assisted impregnation with vacuum treatment.

TGA (Shimadzu Corp. DTG-60H (TGA/DTA) was utilized to determine the amounts of loaded abm and LA. With a scan range of 30-1000 °C and a heating rate of 10 °C/min, TGA was performed in nitrogen flow. Equation below was used to determine the precise weight ratios of abm and LA in the LA/abm@HNT-PDA nanohybrids:

$$\%WR_{abm} = [(\%WL_{T=20-240\text{ }^{\circ}\text{C, LA/abm@HNT-PDA}} \times 0.28) + (\%WL_{T=240-450\text{ }^{\circ}\text{C, LA/abm@HNT-PDA}} - \%WL_{240-450\text{ }^{\circ}\text{C, HNT-PDA}})]$$

where $\%WR_{abm}$ denotes the encapsulated abm content in the nanohybrids and $\%WL_{LA/abm@HNT-PDA}$ denotes the weight loss of LA/abm@HNT-PDA between 240 °C (the temperature at which all LA was decomposed) and 450 °C (the temperature at which all abm was decomposed). The coefficient of 0.28 represents the weight loss ratio of abamectin in the total weight loss of a nanohybrid material containing both lauric acid and abamectin at 240 °C. The calculation is derived based on the comparison of degradation behaviors between pure lauric acid and pure abamectin. When pure lauric acid degrades at 240 °C, it undergoes complete degradation, which is considered 100%. On the other hand, pure abamectin degrades at the same temperature to a degree of 40%. If it is defined as complete degradation of the material as 100%, the weight loss of lauric acid would be 100 units (represented as 100%). The weight loss of abamectin would be 40 units (represented as 40%). Therefore, the total weight loss would be 140 units. Considering the nanohybrid material containing both lauric acid and abamectin, at 240 °C, the weight loss ratio of abamectin in the total weight loss can be calculated as 40 units (abamectin weight loss) divided by 140 units (total weight loss), resulting in a ratio of 0.28 or 28%.

The equation below was used to determine the precise weight ratio of abm in the abm@HNT-PDA nanohybrids:

$$\%WR_{abm} = \%WL_{20-450\text{ }^{\circ}\text{C, abm@HNT-PDA}} - \%WL_{20-450\text{ }^{\circ}\text{C, HNT-PDA}}$$

where %WR_{abm} denotes the encapsulated abm content in the nanohybrids, %WL_{abm@HNT-PDA} denotes the weight loss of abm@HNT-PDA between 20 °C, and 450 °C, (the temperature at which all abm was decomposed).

Differential scanning calorimetry (DSC) (Thermal Analysis MDSC TAQ2000) instrument was utilized for investigating the thermal properties of the developed abm@HNT-PDA and LA/abm@HNT-PDA nanohybrids, and abm. With a heating rate of 10 °C/min and a temperature range of 25 to 300 °C, the experiments were carried out in a nitrogen atmosphere.

Using a secondary electron detector with a 5 kV acceleration voltage, scanning electron microscopy (SEM) images of abm@HNT-PDA and LA/abm@HNT-PDA nanohybrids were acquired. To avoid generating a charging when exposed to the electron beam during SEM analysis, a thin layer of Au/Pd was sputter deposited onto samples.

The abm-encapsulated nanohybrids' time-temperature profiles were constructed to investigate their photothermal characteristics. Temperatures were measured using a FLIR E6xt thermal camera while 0.5 g of abm@HNT-PDA and LA/abm@HNT-PDA powders were placed individually in Teflon holders under the solar simulator (Oriel LCS100) at 3 sun (300 mW/cm²) and 1 sun (100 mW/cm²) light densities.

Using an Agilent Carry 5000 UV-VIS-NIR Spectrophotometer between the spectral range from 200 to 800 nm, the absorbance spectra of abm in the dark and abm@HNT-PDA in the dark, abm exposed to sunlight at 3 sun (300 mW/cm²), and HNT-PDA/abm exposed to sunlight at 3 sun (300 mW/cm²) were recorded. 0.5 g abm@HNT-PDA was exposed to sunlight at 3 sun light density for 6 h, and then mixed with 30 mL of methanol with the aim of releasing and dissolving the abm in methanol. The abm@HNT-PDA and methanol mixture was then centrifuged to precipitate the HNT-PDA nanocarriers, and the supernatant was then gathered for UV-Vis examination with a VARIAN 5000 UV-vis-NIR spectrophotometer, recording absorbance values between 200 and 800 nm. As the dark-stored control sample, 0.5 g of abm@HNT-PDA was incubated in the dark for 6 h followed by mixing with 30 mL of methanol, centrifugation and UV-Vis analysis of the supernatant. For the stability analysis of neat abm, 0.2 g of neat abm was dissolved in 30 mL methanol and UV-Vis spectrum was acquired before and after being exposed to sunlight at 3 sun light density for 6 h.

3.3.4 Abm Release Profiles of abm@HNT-PDA and LA/abm@HNT-PDA

Nanohybrids

The release of abamectin from the nanohybrids in the powder form was evaluated by TGA analysis. For the release experiments, 0.4 g of abm@HNT-PDA and LA/abm@HNT-PDA nanohybrid powders were weighed precisely and placed on plates lined with filter paper. The filter paper acted as an environment simulating a leaf that would absorb the released substance. Two sets of samples were prepared, of which one was incubated in the dark, and the other one was irradiated with sunlight at 3 sun light density for 6h followed by 18 h dark incubation. All samples were wetted by adding 2 mL of deionized water at the end of 1 and 2 h incubation. The procedure was repeated for 30 days. Each day, three samples were taken from different parts at the end of 6 h incubation, inserted into TGA crucibles, and analyzed.

The release of abamectin from the nanohybrids in the powder form was evaluated by TGA where abm content in the abm@HNT-PDA and LA/abm@HNT-PDA was calculated for each day based on Equation below. Three measurements were taken for each sample and the average encapsulated-abm is determined. The % abm release was calculated with:

$$\%R_{abm} = 100 - (\%WR_{abm,T} / \%WR_{abm,T0}) \times 100$$

where $\%R_{abm}$ denotes the percentage of released abm, $\%WR_{abm,T0}$ denotes the weight ratio of initially encapsulated abm in nanohybrids and $\%WR_{abm,T}$ denotes the encapsulated abamectin in nanohybrids in the specified time.

3.3.5. Killing activity of powder form of abm@HNT-PDA and LA/abm@HNT-PDA nanohybrids on *Myzus persicae*

The pesticide activity of LA/abm@HNT-PDA and abm@HNT-PDA nanohybrids in powder forms on *Myzus persicae* aphids were examined. In a climate-controlled setting with an 8 h light and 16 h dark photoperiod at 25 °C, *Myzus persicae* pests was grown. The aphids consumed the leaves of the eggplant (*Solanum melongena*). 0.5 g of the nanohybrid to be tested in the powder form was placed on filter paper. The nanohybrid samples were daily exposed to 6 h sunlight at 3 sun light density for 10 consecutive days. The samples were wetted with 2 mL of deionized water every hour during the sunlight irradiation. Subsequently, the powders were removed from under the light source, and immediately 10 aphids were placed on them using a sterile swab. After 15 min, the number of dead aphids was counted, and the percentage of mortality was calculated. The same procedure was applied to samples of 0.5 g LA/abm@HNT-PDA and 0.5 g abm@HNT-PDA nanohybrids that were not exposed to light.

3.3.6. Suspensibility of the LA/abm@HNT-PDA nanohybrids in water

The suspensibility of LA/abm@HNT-PDA nanohybrids at 18 mg/mL, 9 mg/mL and 1 mg/mL concentrations in deionized water was investigated. Dispersions prepared at three different concentrations were subjected to bath sonication for 15 min. The dispersions were then kept aside for 15 min, afterwards, 500 µL of each were collected from the center using a micropipette and centrifuged to precipitate the substance. The precipitated nanohybrids in the Eppendorf tube were weighed after the supernatant was removed to determine the suspensibility ratios with the following formula:

$$\text{Suspensibility \%} = \frac{\text{Experimental wt\% of abm in suspended nanohybrids}}{\text{Theoretical wt\% of abm in suspended nanohybrids}}$$

3.3.7. Dispersion analysis of LA/abm@HNT-PDA nanohybrids in the water

Aqueous dispersions of LA/abm@HNT-PDA were prepared at 4 mg/mL concentration and subjected to ultrasonication using a QSonica, Q700, Newtown, CT, USA, at 60% amplitude, with a 5 s pulse on and a 2 s pulse off for 30 min. Then, dynamic light scattering (DLS) measurements of aqueous dispersions were carried out using a Malvern Zetasizer Nano ZS (Malvern Instruments Ltd., U.K.) at 15-, 30-, 45- and 60-min time periods to determine the size distribution and agglomeration state of nanohybrids.

3.3.8. Determination of leaching of abm into the soil

5 g of soil was mixed with 30 mL of 5 mg/mL aqueous LA/abm@HNT-PDA dispersion and incubated in the dark for 24 h. Following the incubation, the liquids were removed by vacuum filtration via a Buchner funnel and the soil mixture was dried overnight at room temperature. The FTIR spectrum of the dried sample was obtained using Thermo Scientific Nicolet Is10 FTIR spectrophotometer. As the control sample, 0.04 g neat abm powder was mixed with 5 g soil. The FTIR spectrum of the soil and abm mixture was obtained.

3.3.9. Retention of the LA/abm@HNT-PDA dispersion on the leaves

A method reported in the literature was used for the leaf retention calculation¹¹⁰. Aqueous LA/abm@HNT-PDA nanohybrid dispersions, Agrimec, and abm dissolved in methanol were prepared at varying abm concentrations. 15 mL of sample in a beaker was placed on sensitive balance. Leaves that had been cut into 2 × 2 cm squares, with a surface area of $S=4\text{ cm}^2$ were immersed into the liquid to be tested for its retention for 15 s, were removed and held up inside the weighing chamber until there were no droplets left on the

surface. The decrease in the weight of the liquid (W) was recorded, and the retention was reported as $1000 \times W/S$ (mg/cm²).

3.3.10. Determination of the foliar retention properties of the LA/abm@HNT-PDA PDA dispersions

Aqueous dispersions of LA/abm@HNT-PDA were prepared at concentrations at 18, 9, 4.5, 2.25, 1.15, and 0.6 mg/mL abm concentrations and bath-sonicated for 15 min. The air pressure was set to 15–35 psi when the airbrush for spray coating (Magicbrush Airbrush Kit Ab-101a) was assembled in a chemical hood. The chamber of the airbrush was filled with the prepared LA/abm@HNT-PDA dispersion. The airbrush nozzle was held 10 cm in front of a set of eggplant leaves that had been cut into 2×2 cm squares which were positioned 30° from the surface axis, and each leaf sample was manually sprayed for 10 s with 10 mL of the dispersion. The spray-coated leaves were dried at room temperature.

The sessile-drop contact angle method was performed on both the pristine leaf samples and the leaf samples coated with spray-applied nanohybrids. This was accomplished using the optical tensiometer-equipped Theta Lite Contact Angle Measurement System. The optical tensiometer, which was equipped with a high-resolution digital camera, was used to measure the contact angles after 10 μ L of pure water was carefully dropped on the surface at room temperature. Each sample had a minimum of three measurements made, and the average contact angle values were recorded.

Contact angle measurements were also taken after sprayed leaf samples were washed with water to simulate rainfall after the spray application of LA/abm@HNT-PDA nanohybrid dispersion at 9 mg/mL abm concentration. Each wash cycle involved spraying 1 mL of water with an airbrush. In between each wash cycle, leaf samples were dried at room temperature for 15 min. After the samples had dried, contact angle measurements were then taken from at least three spots of the samples.

3.3.11. Optical microscopy of eggplant leaf surfaces sprayed with aqueous

LA/abm@HNT-PDA dispersions

The attachment of the nanohybrids on the eggplant leaf surfaces was characterized by optical microscopy. The Zeiss Axiocam ERc 5s microscope was used throughout the investigation to capture all the images, and 3 repetitions of the experiment were performed. LA/abm@HNT-PDA, prepared at 4 mg/mL concentration was bath-sonicated for 15 min, then spray-coated onto leaves that had been cut into 2 × 2 cm squares. Optical microscopy images were taken at 5x magnification after waiting for 30 min at room temperature for drying. 10 mL of water was gently dispensed onto leaves that were sprayed with LA/abm@HNT-PDA dispersion with an airbrush to replicate rainy conditions. Optical microscopy images were once more taken at 5x magnification after an additional 30 min of drying time for the leaves.

3.3.12. Determination of LC₅₀ values of LA/abm@HNT-PDA

The minimum concentration of the LA/abm@HNT-PDA dispersion required to kill 50 % of the *Myzus persicae* population was determined by spraying aqueous LA/abm@HNT-PDA nanohybrid dispersion, Agrimec diluted in cyclohexanol, and abm dissolved in methanol, at abm concentrations varying between 0.6 and 18 mg/mL abm, onto eggplant leaves cut to 2 x 2 cm squares. The airbrush nozzle was held 10 cm in front of a set of leaves which were positioned 30° from the surface axis, and the leaves were manually sprayed with formulations for 10 s with the pesticide to be tested. The samples were exposed to sunlight at 3 sun for 1 h. Immediately following the sunlight irradiation, 10 *Myzus persicae* aphids were placed on the leaves using a sterile swab. The dead aphids were counted after a 15 min, and the lowest dose leading to a 50 % death rate in the overall population was calculated for each formulation dose. Similarly, another set of formulations sprayed on the leaf surface was prepared and 10 *Myzus persicae* aphids were placed on the leaves. The dead aphids were counted after a 15 min, and the lowest dose

leading to a 50% death rate in the overall population was calculated for each formulation dose.

3.4 Results and Discussion

3.4.1 Preparation of the sunlight-triggered abm release system

HNTs modified with PDA were employed as photothermal nanocarriers of the sunlight-activated abm release system to enable light-to-heat conversion. The objective was to remotely increase the temperature of the abm-loaded and LA-functionalized HNT-PDA nanocarriers and trigger the phase transition of LA by using the advantage of the heat produced by the HNT-PDA nanocarriers when exposed to light. Through the LA phase transition, which serves as a release facilitator for abm release, the system enables the abm to be released from the HNT-PDAs (Figure 20).

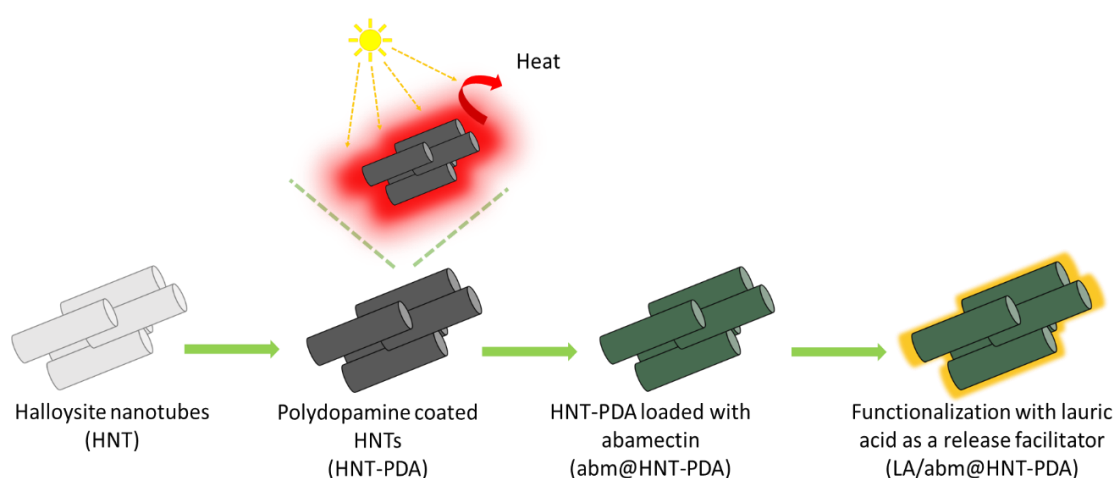


Figure 20. Design of the sunlight-triggered abm release system.

Abm was loaded onto the HNT-PDA nanoparticles, via solvent-assisted impregnation. The resulting abm@HNT-PDA nanoparticles were further loaded with LA using the same method resulting in LA/abm@HNT-PDA nanohybrids at a theoretical weight ratio of 26.6% and 33.3% for abm and LA, respectively. The abm-loaded and LA-functionalized HNT-PDA nanocarriers were expected to be remotely heated to the

temperatures required for the phase change transition of LA via the light-induced heating of the HNT-PDA nanocarriers. The LA release facilitator was aimed to go through a phase change, allowing the abm encapsulated in the HNT-PDAs to be released. Ultimately, sunlight was the required element for the triggered release of abm.

3.4.2 Characterization of the LA/abm@HNT-PDA release system

TGA was employed to calculate the experimental loading ratio of abm and the LA in the nanohybrids, by using the relative weight loss ratios of neat and loaded abm and LA. Figure 21a demonstrates that the abm loading was 33.2 % in the sample in abm@HNT-PDA nanohybrids, which was theoretically loaded with abm at 40 wt. %. In the LA/abm@HNT-PDA nanohybrids, which theoretically contained 26.6 wt. % abm and 33.3 wt. % LA, the abm and LA loading ratios were 23.5% and 31%, respectively, demonstrating that both components were successfully loaded into the nanohybrids. The slight variations from the theoretical loading ratios might have been caused by the encapsulation of the LA in the pores of the HNTs and some abm loss during the solvent-assisted impregnation.

DSC was further utilized to characterize the thermal properties of the LA/abm@HNT-PDA nanohybrids. Figure 21b shows that the nanohybrid presents the melting transition of the LA around 50 °C, which was expected to facilitate the release of abm when the HNT-PDA nanocarriers are heated. Furthermore, the melting transition of abm at around 200 °C was shifted to a higher temperature. This finding indicates that some of the abm molecules entrapped in the HNT-PDA nanocarriers melted at higher temperatures when the LA was present, confirming that the LA acted as a coating on the abm loaded HNT-PDA.

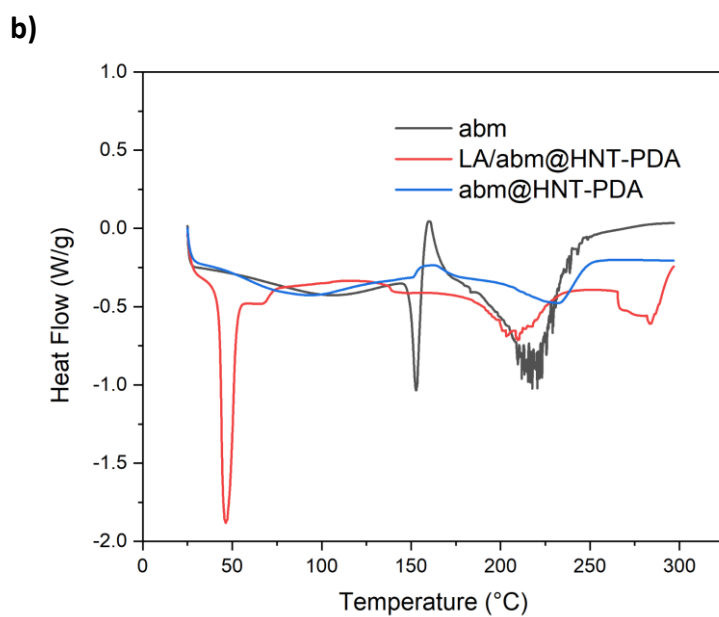
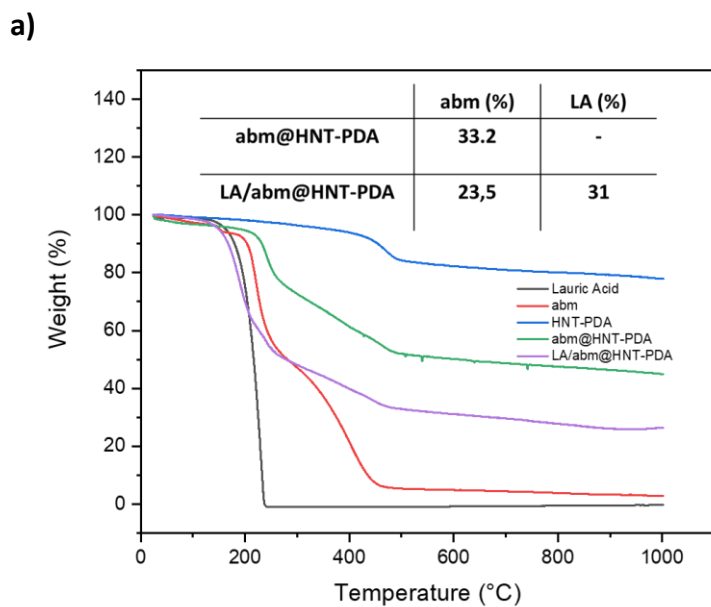


Figure 21. a) TGA of HNT-PDA, LA, abm, abm@HNT-PDA and LA/abm@HNT-PDA. b) DSC of abm, abm@HNT-PDA and LA/abm@HNT-PDA.

The SEM analysis of the abm@HNT-PDA and LA/abm@HNT-PDA nanohybrids has demonstrated that the HNT-PDA nanocarriers retained their nanotubular structure upon

abm loading and the LA functionalization resulted in an evenly distributed coating over the surface of the abm loaded HNT-PDA nanocarriers (Figure 22).

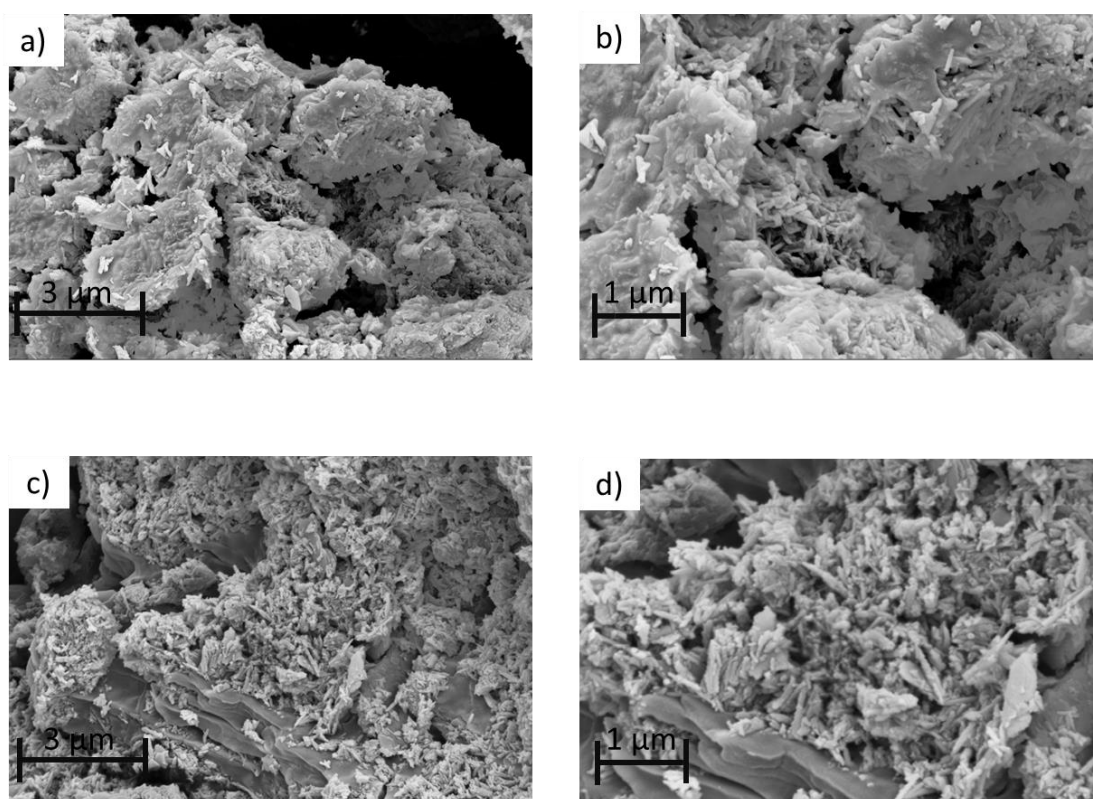


Figure 22. SEM images of LA/abm@HNT-PDA at a) 25k, b) 50k magnification and abm@HNT-PDA at c) 25k, d) 50k magnification.

The ability of LA/abm@HNT-PDA nanohybrids to undergo light-activated heating and achieve temperatures that may initiate the release mechanism when exposed to sunlight was examined. By observing the temperature increases upon irradiation from a solar simulator, the time-temperature profiles of nanohybrids were constructed. According to the results presented in Figure 23, when abm@HNT-PDA and LA/abm@HNT-PDA nanohybrids were exposed to sunlight with a light density of 1 sun (100 mW/cm^2) they reached $50 \text{ }^\circ\text{C}$. The temperatures were further elevated for both the LA/abm@HNT-PDA and abm@HNT-PDA nanohybrids when the light density was raised to 3 sun (300 mW/cm^2) and the nanohybrids were heated to $120 \text{ }^\circ\text{C}$. These findings demonstrated that the functionalization of the abm loaded HNT-PDA nanohybrids with LA did not affect their photothermal capacity and the LA/abm@HNT-PDA nanohybrids can be heated up to desired temperatures in a controlled manner when exposed to sunlight at different light

densities. Furthermore, it was demonstrated that the release system can be heated above the temperatures required for the melting transition of the LA release facilitator under sunlight irradiation.

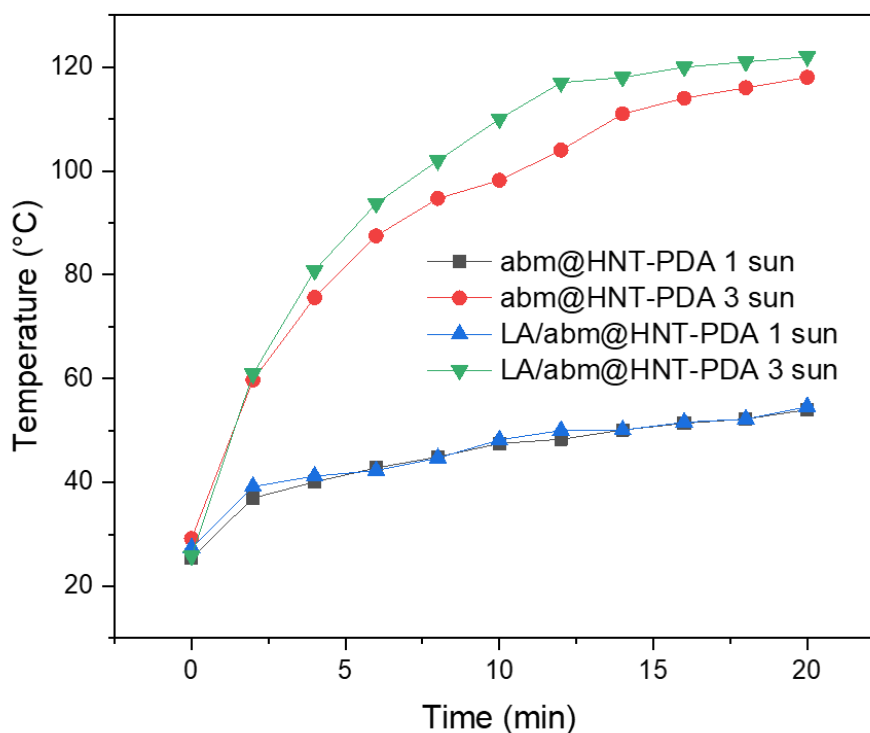


Figure 23. Time-temperature profiles of LA/abm@HNT-PDA and abm@HNT-PDA nanohybrids under irradiation at 1 sun and 3 sun light densities.

Abm is known to be prone to degradation when exposed directly to solar irradiation, which results in a short half-life and low utilization rate¹¹². As a result, numerous kinds of encapsulation strategies have been designed in order to enable abm to retain its effectiveness for an extended period of time^{113–115}. These approaches aim to prolong the stability as well as the efficacy of abm. By monitoring variations in absorbance values, the photostability of abm encapsulated within HNT-PDA nanocarriers was investigated. The absorbance spectra of the two abm@HNT-PDA aqueous dispersion samples, one exposed to sunlight for 6 h and the other kept in the dark were found to overlap (Figure 24). However, the absorbance of the two non-encapsulated abm solution samples, one

exposed to sunlight and the other kept in the dark, exhibited significant differences. After exposure to sunlight, a substantial drop in the characteristic absorbance peak of non-encapsulated abm between 200 and 300 nm was observed. This finding illustrates explicitly that photostability of abm is preserved by its encapsulation within HNT-PDA.

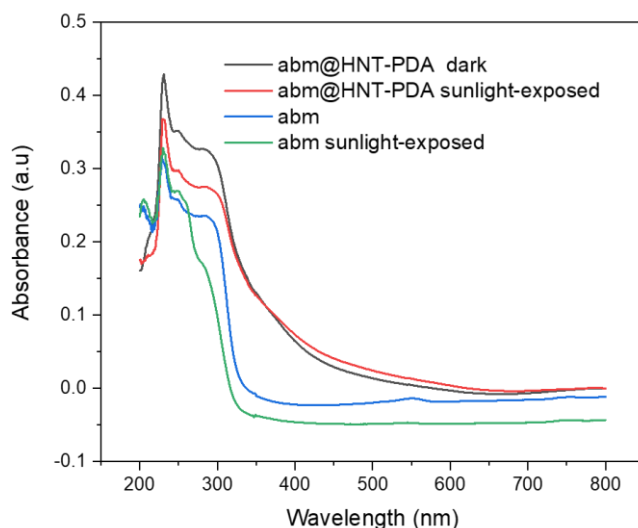


Figure 24. UV-VIS absorption spectra of aqueous abm solution and aqueous dispersion of abm@HNT-PDA exposed to sunlight at 3 sun for 6 h and kept in the dark for 6 h.

3.4.3 Sunlight-triggered abm release from the LA/abm@HNT-PDA release system

Figure 25a displays the experimental design for investigating the release behavior of sunlight-exposed LA/abm@HNT-PDA and abm@HNT-PDA samples. The nanohybrid samples were continuously wetted on a filter paper simulating a moist plant surface that would retain the released abm and irradiated with sunlight for 6 h followed by 18h dark incubation for 10 consecutive days. As controls, another set of each nanohybrid samples was kept in the dark without any sunlight activation for the same duration. At the end of each day samples were collected for TGA. Figure 25b demonstrates that the LA/abm@HNT-PDA nanohybrids have released 39.5 % of the encapsulated abm over

the course of the 10-day period when they were irradiated with sunlight for 6 h each day. When they were not exposed to the sunlight, however, the abm release was only 9.7%, confirming that the abm release was triggered with sunlight irradiation. Under the same conditions, abm@HNT-PDA nanohybrids, which were not functionalized with LA did not present a significant abm release when irradiated with sunlight for 6 h every day, demonstrating that the LA acted as a release facilitator, which melts upon sunlight-activated heating of the HNT-PDA nanocarrier and eases the release of abm. The abm@HNT-PDA and LA/abm@HNT-PDA nanohybrids kept in the dark exhibited almost no release at the end of the 10-day period, as predicted. At the end of the first day, a burst release appeared in the samples that had been exposed to sunlight. This was attributed to the release of abm absorbed on the outer surface of HNT-PDA nanocarriers as opposed to abm entrapped in the lumen, which were released more slowly. All of these findings support the idea that abm is being released in response to sunlight exposure and the phase transition of the LA. The fact that the release efficiency was reduced in samples without the LA confirmed the role of LA as a release facilitator in the proposed sunlight-triggered controlled release system.

The same release experiment was extended to 30 days to investigate the activity of the LA/abm@HNT-PDA sunlight-triggered release system over a long period of time. The release clearly continued at the end of 20 and 30 days, as can be seen in Figure 25c. This result demonstrated that the LA/abm@HNT-PDA controlled release system provides abm release for an extensive period of time making it useful as an effective pesticide delivery system.

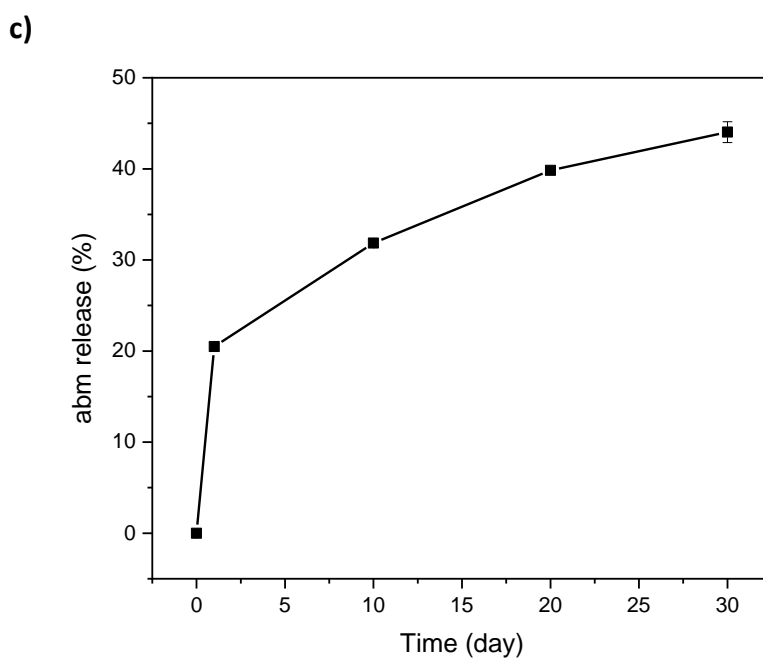
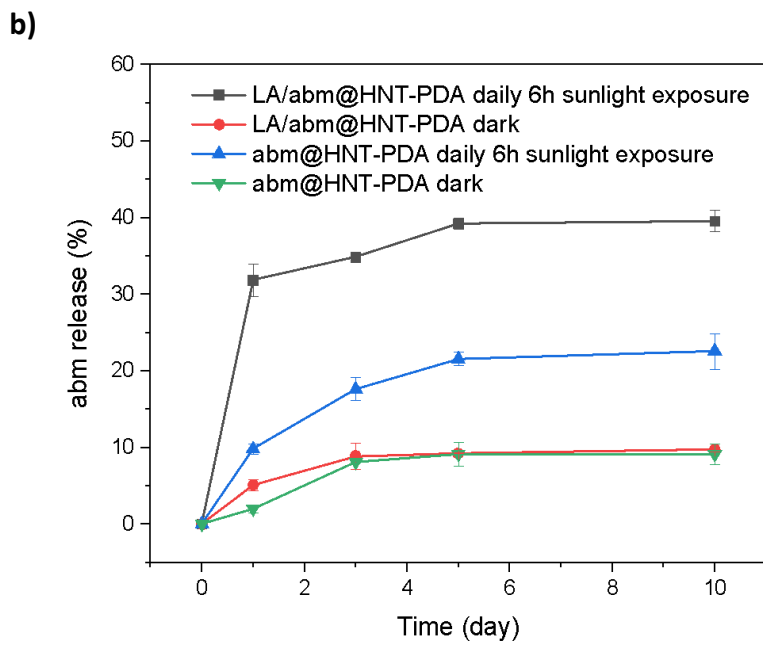
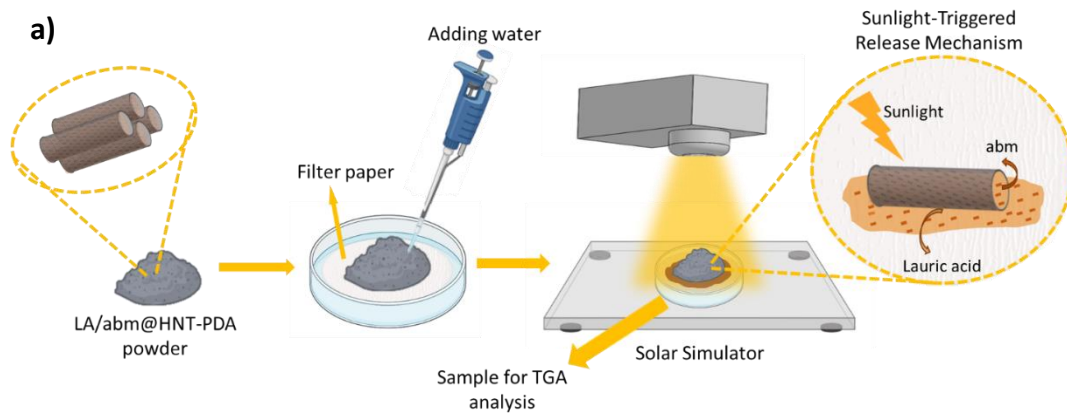


Figure 25. a) Schematic representation of the experimental design to monitor the release behavior of abm from nanohybrids, b) Abm release performance of LA/abm@HNT-PDA and abm@HNT-PDA nanohybrids which were i) irradiated with sunlight at 3 sun light density for 6 h followed by 18 h dark incubation, ii) kept in the dark for 10 days, c) Abm release performance of LA/abm@HNT-PDA nanohybrids for 30 days, during which the nanohybrids were irradiated with sunlight at 3 sun light density for 6 h followed by 18 h dark incubation for 30 days.

3.4.4 Sunlight-triggered pesticide activity of LA/abm@HNT-PDA release system

The effect of sunlight-triggered abm release from the LA/abm@HNT-PDA nanohybrids on the viability of *Myzus persicae* aphids was examined. Over the course of a period of 10 days, the LA/abm@HNT-PDA nanohybrids were irradiated with sunlight for 6 h each day, at the end of which aphids were placed on the sunlight-irradiated powder samples. The viability of the aphids was recorded, and new aphids were placed on the powder after it was irradiated again next day. The LA/abm@HNT-PDA nanohybrids presented 100 % killing activity on the first day when irradiated with sunlight and significantly retained their insecticidal activity over a period of 10 days (Figure 26). Even after being exposed to sunlight for 10 days, the aphids treated with the nanohybrids presented 70 % mortality, confirming that the LA/abm@HNT-PDA controlled release system presents sunlight-activated release of abm and effective pesticide activity over at least 10 days. Under the same conditions, the abm@HNT-PDA nanohybrids, which were not functionalized with the LA did not present any insecticidal activity, confirming that no significant release of abm occurred even under sunlight when LA was not present. After 10 days being incubated in the dark, neither the LA/abm@HNT-PDA nor the abm@HNT-PDA nanohybrid powders had an impact on the killing of aphids. All these findings illustrated that LA functions effectively as a release facilitator in the abm release mechanism, and that the controlled release mechanism only allows abm to be released from the nanohybrids when sunlight is available, which leads to killing of the pests. Abm is not

being released from the nanotubes in the absence of sunlight or in an environment where LA does not undergo phase transition, and consequently, its insecticidal ability is absent.

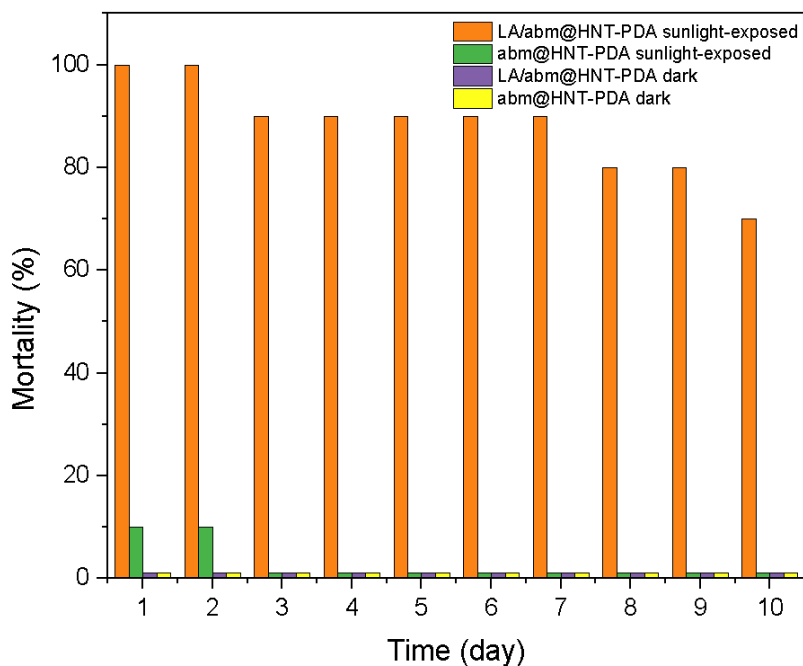


Figure 26. a) Mortality of *Myzus persicae* treated with LA/abm@HNT-PDA and abm@HNT-PDA nanohybrids, which are i) exposed to sunlight at 3 sun for 6 h followed by dark incubation for 18 h, ii) kept in the dark every day

3.4.5 Aqueous formulations of LA/abm@HNT-PDA nanohybrids as pesticides

To evaluate the potential of the sunlight-triggered release system in agricultural applications, their aqueous dispersions were studied as sprayable nanoformulations. LA/abm@HNT-PDA nanohybrids were dispersed in water at different abm concentrations and were examined using suspensibility analysis. As shown in Figure 27, the LA/abm@HNT-PDA nanohybrids were easily suspended in water with a suspensibility of above 30 %. Apparently, the PDA functionalization of the HNT nanocarriers imparted hydrophilic character, which allowed the HNT-PDA nanocarriers

to be suspended in water by simple bath sonication. The nanoformulation with the lowest concentration, 1 mg/mL LA/abm@HNT-PDA, showed the highest suspensibility at 42 %, while the 9 mg/mL LA/abm@HNT-PDA formulation had a suspensibility of 37%, followed by the formulation with the highest concentration, 18 mg/mL LA/abm@HNT-PDA, with a suspensibility of 32%. As expected, the agglomeration of the HNT-PDA nanocarriers has increased at higher concentrations and nanoformulations with lower concentrations presented a greater ability to be dispersed in water. The fact that the LA/abm@HNT-PDA can be easily suspended in water, without the need of any organic solvent, demonstrated their potential as environmentally friendly sprayable pesticide formulations.

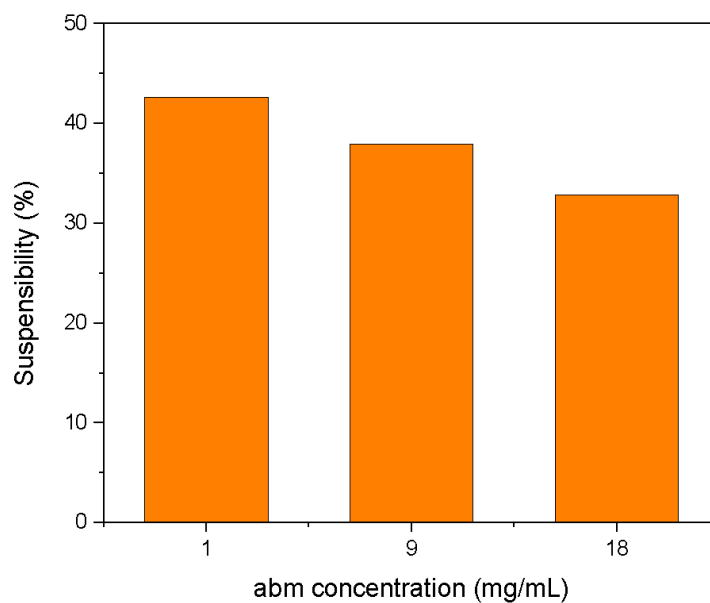


Figure 27. Suspension test for LA/abm@HNT-PDA nanohybrids in water at different abm concentrations.

The dispersion stability of the LA/abm@HNT-PDA nanohybrids were qualitatively evaluated using DLS analysis (Figure 28). The size distributions of an aqueous dispersion of LA/abm@HNT-PDA nanohybrids at 4 mg/mL were analyzed at different time periods. While agglomeration of particles started to occur by time as seen by the new peak at

higher hydrodynamic diameters, the size distribution of LA/abm@HNT-PDA dispersion did not significantly change over the period of 1 h. This result demonstrated that the LA/abm@HNT-PDA nanoparticles were mainly stable during the course of 1 h, which will allow spray-application of the developed sunlight-triggered release system in the field.

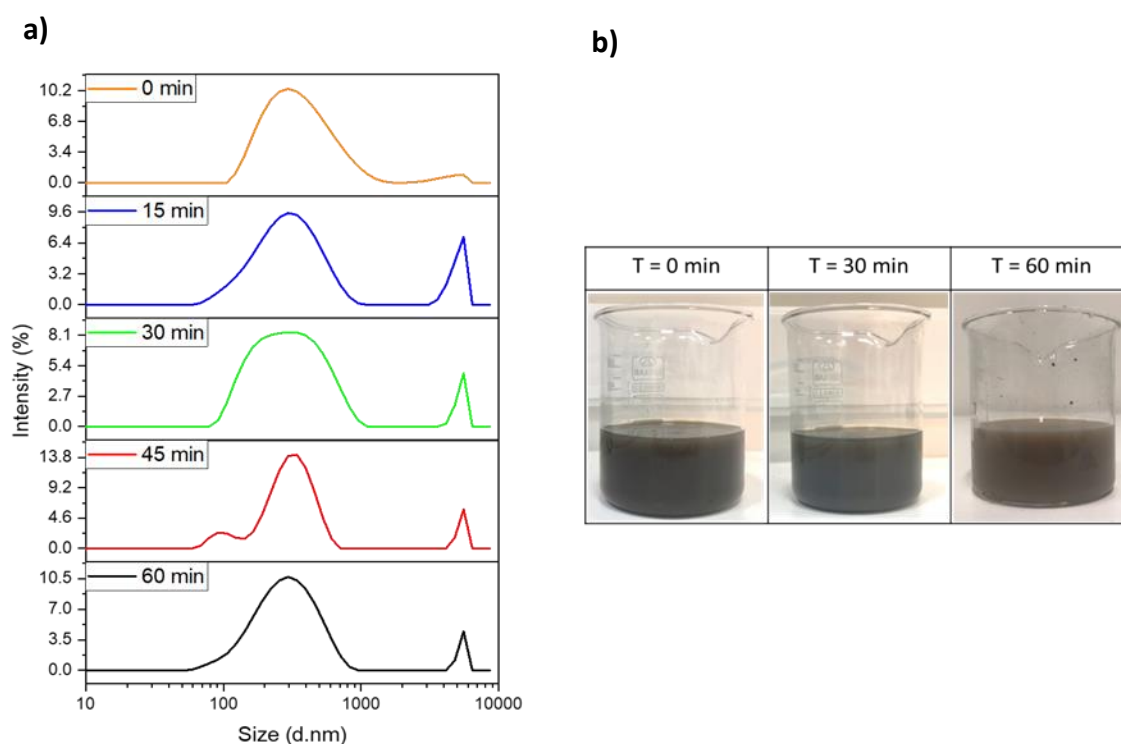


Figure 28. a) DLS analysis, b) photographs of the aqueous dispersion of LA/abm@HNT-PDA nanohybrids prepared at 4 mg/mL at different time periods.

To investigate the effect of the LA/abm@HNT-PDA controlled release system on the environmental pollution caused by the leaching of pesticides to soil, the soil leaching of abm from the LA/abm@HNT-PDA was evaluated. The aqueous dispersion of LA/abm@HNT-PDA nanohybrids at 5 mg/mL abm concentration was mixed with soil sample and incubated for 6 h followed by the removal of the liquids by vacuum filtration. The dried soil mixture was then analyzed with FTIR for the presence of abm (Figure 29). While the FTIR spectrum of the positive control sample, that was prepared by mixing soil and neat abm powder presented the abm-specific peak at 1735 cm^{-1} due to $\text{C}=\text{O}$

stretching, the FTIR spectrum did not reveal any abm-related peaks when the soil sample was mixed with the LA/abm@HNT-PDA dispersion. This finding indicated that the abm did not leach to the soil when encapsulated in the HNT-PDA nanocarriers reducing its load on the environment.

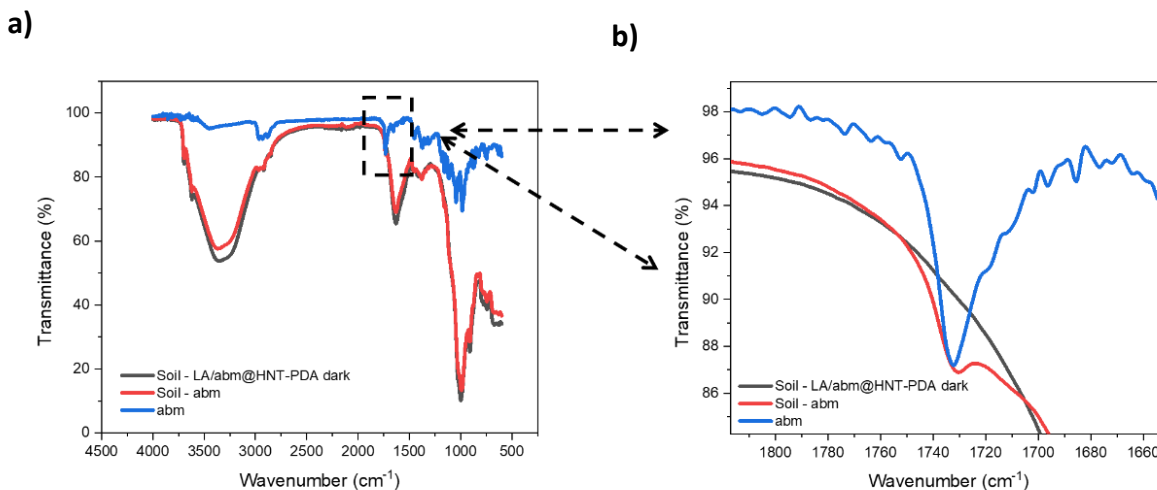


Figure 29. FTIR of soil samples mixed with LA/abm@HNT-PDA nanohybrids and neat abm.

3.4.6 Foliar adhesion properties of LA/abm@HNT-PDA formulations

Strong affinity of the pesticide formulations to the crop's leaves leading to efficient deposition of the pesticides on the plants is essential to minimize the pesticide loss. The capacity of the aqueous LA/abm@HNT-PDA dispersion to adhere to plant leaves was determined by retention tests where eggplant leaves were immersed in the dispersions followed by monitoring the weight increase of the leaves. The retention rate of the LA/abm@HNT-PDA formulation was determined relative to control samples including abm dissolved in methanol, water and Agrimec, a commercial abm formulation in cyclohexanol. Figure 30 shows that the aqueous LA/abm@HNT-PDA dispersion presented a higher retention rate than abm dissolved in methanol, demonstrating that the encapsulation in the HNT-PDA nanocarriers allowed abm to better adhere to the leaf compared to its neat form. Apparently, the highly adhesive properties of the HNT-PDA nanocarriers caused by the polydopamine functionalization played a role in the strong attachment and resulted in a release system with strong foliar retention properties. The

fact that the aqueous LA/abm@HNT-PDA dispersion presented the same retention as the cyclohexanol-containing Agrimec demonstrated that the developed pesticide formulation presents a strong environmentally friendly, non-toxic alternative to commercially available pesticide formulations.

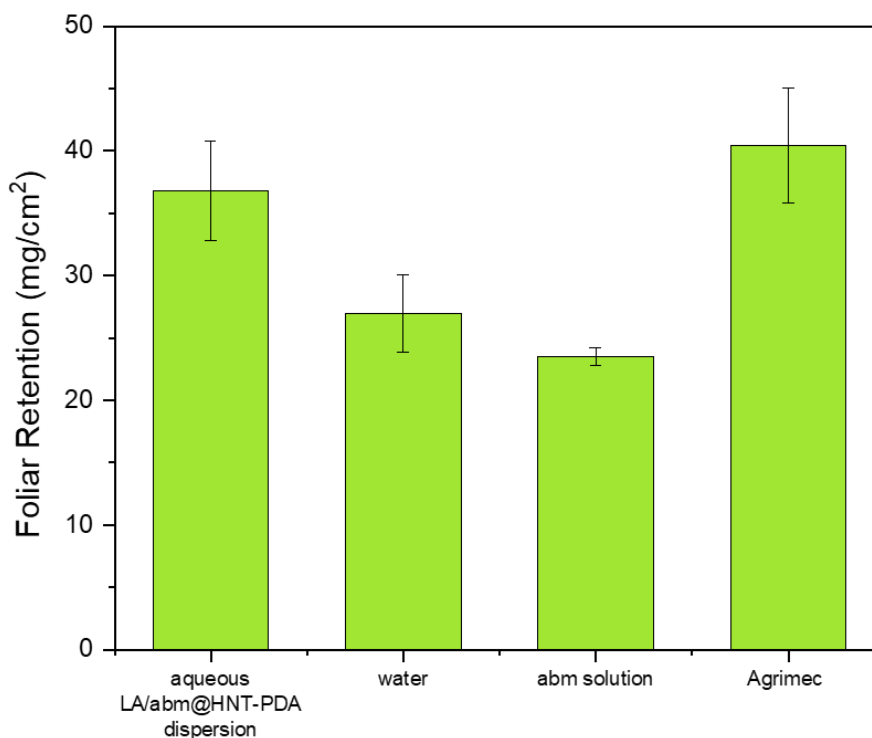


Figure 30. Foliar retention values for water, abm dissolved in methanol, aqueous LA/abm@HNT-PDA dispersion and Agrimec.

The foliar adhesion characteristics of the aqueous LA/abm@HNT-PDA nanoformulations were further examined using water contact angle measurements. Contact angle values of eggplant leaves sprayed with aqueous LA/abm@HNT-PDA dispersions at varied concentrations were determined. Figure 31 demonstrates that the water contact angle values of the leaf samples decreased as the concentration of the LA/abm@HNT-PDA dispersion sprayed on the leaf was increased, illustrating that the hydrophilic PDA layer on the HNT-PDA nanocarriers enhanced the hydrophilic nature of the nanohybrids. This finding further confirmed that the developed pesticide

nanoformulation presents strong adhesion when applied to leaf surfaces, allowing efficient use in real-life conditions for agricultural purposes.

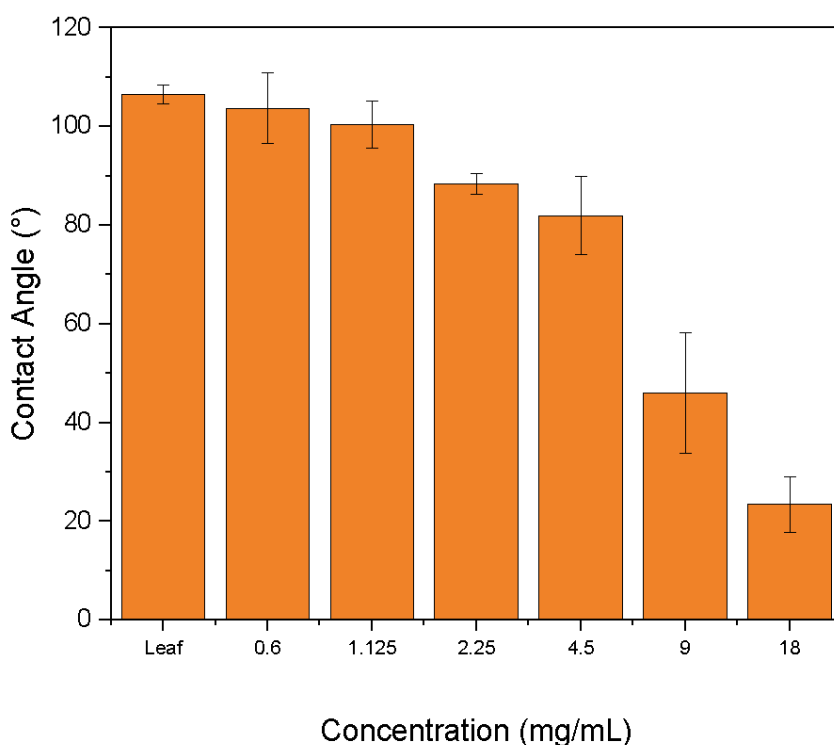


Figure 31. Contact angle values of eggplant leaves sprayed with aqueous dispersions of LA/abm@HNT-PDA nano hybrids at 0-18 mg/mL abm concentrations

To evaluate the resistance of the sunlight-triggered pesticide formulation to rainwater washing, contact angle values of the eggplant leaves sprayed with the 9 mg/mL LA/abm@HNT-PDA dispersion were determined after 1-5 washing cycles. There was only a slight upward trend in the contact angle values as the number of washes of the sprayed leaves increased, which was caused by the removal of the LA/abm@HNT-PDA nano hybrids from the leaf surface (Figure 32). However, even after 5 cycles of washes, the contact angle values of the sprayed leaf sample remained considerably lower than the contact angle of the neat leaf sample, indicating that a significant amount of the LA/abm@HNT-PDA nano hybrids remained attached to the leaf. This result confirmed

the strong retention of the developed pesticide nanoformulation on the leaf surface and also demonstrated their strong resistance to rainwater washing.

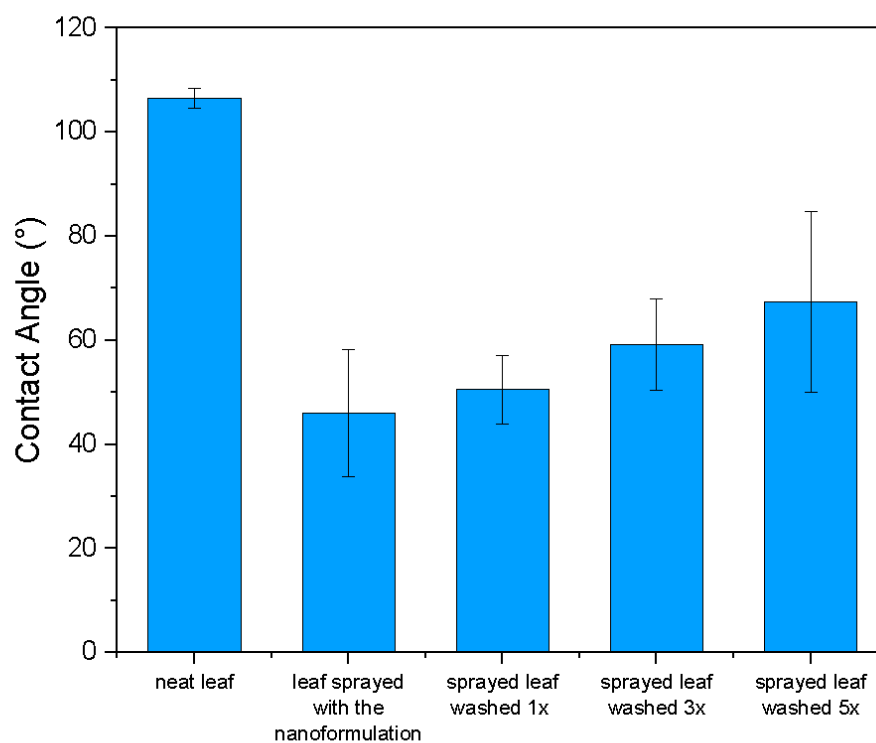


Figure 32. a) Contact angle values of eggplant leaves sprayed with aqueous LA/abm@HNT-PDA dispersions and washed with water 1-5 times.

The foliar adhesion of the aqueous LA/abm@HNT-PDA nanohybrid dispersions was also visualized with optical microscopy. The presence of the LA/abm@HNT-PDA nanohybrids was easily apparent in regions of the leaves sprayed with the nanoformulation as orange-brown spots (Figure 33b). When the leaf samples sprayed with the nanohybrid dispersions were subjected to a further 10 mL water spray to mimic rainy conditions and examine the effect of washing, optical images again presented regions appearing orange-brown (Figure 33c). This finding supports the results of the contact angle measurements, proving that the PDA functionalization enables the nanohybrids to attach to the leaf surface even after washing.

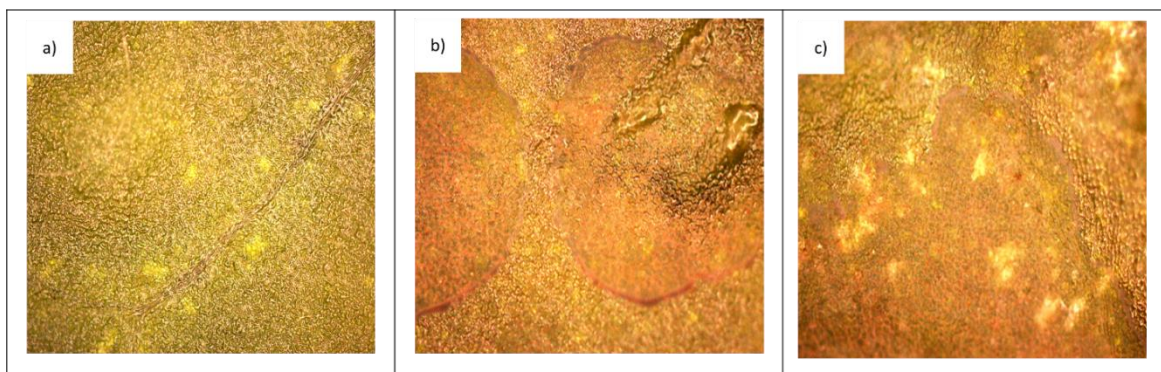


Figure 33. Optical microscopy images of eggplant leaf samples. a) neat leaf, b) leaf sprayed with 4 mg/mL aqueous LA/abm@HNT-PDA dispersion, c) leaf sprayed with 4 mg/mL aqueous LA/abm@HNT-PDA dispersion followed by washing with water.

3.4.7 Pesticide activity of LA/abm@HNT-PDA nanoformulations

The pesticide activity of the LA/abm@HNT-PDA nanoformulations was determined on *Myzus persicae* aphids by determining their LC_{50} values. The lowest dose that results in the death of 50 % of a population is referred to as the LC_{50} value. Using an airbrush, the aqueous LA/abm@HNT-PDA nanohybrid dispersions prepared at various concentrations were sprayed on eggplant leaf surfaces. Following daily 6h sunlight irradiation of the sprayed leaf samples, aphids were placed on the leaves and the mortality of the aphids on each sample was determined (Figure 34a). As the control set of samples, leaf samples sprayed with nanohybrid dispersions at different concentrations were stored in the dark. The dark-stored leaves sprayed with the LA/abm@HNT-PDA dispersion did not demonstrate any mortality at any concentration. However, aphids on the leaf samples sprayed with LA/abm@HNT-PDA nanohybrid dispersions at 9 and 18 mg/mL concentration exhibited a mortality rate of 50 % or greater when the sprayed leaves were exposed to sunlight (Figure 34b). Thus, the LC_{50} value for the aqueous LA/abm@HNT-PDA was identified to be 9 mg/mL. These findings revealed the development of a release system that is only active in the presence of sunlight

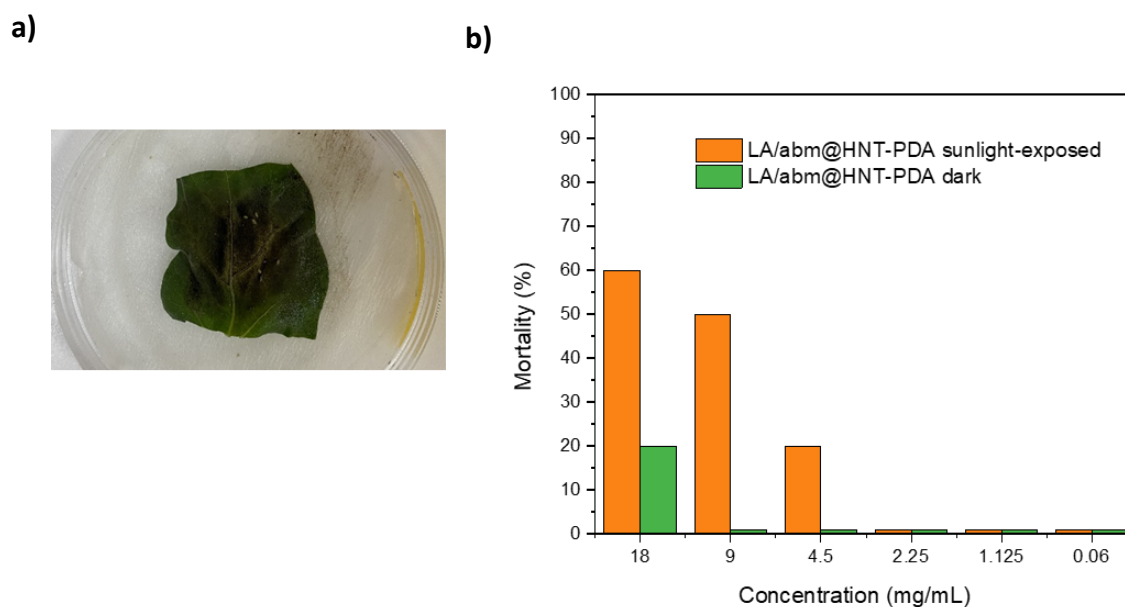


Figure 34. a) *Myzus persicae* placed on eggplant leaf that was sprayed with the nanoformulation and irradiated with sunlight for 6h, b) LC₅₀ analysis of the aqueous LA/abm@HNT-PDA dispersions in the dark and under sunlight irradiation.

The pesticide activity of the aqueous LA/abm@HNT-PDA dispersions was compared with neat abm dissolved in methanol and also to Agrimec, a commercial abm formulation, by comparing the LC₅₀ values of each pesticide (Table 1). Whereas leaf samples sprayed with abm dissolved in methanol and held in the dark exhibited considerable mortality and the LC₅₀ value was determined to be 9 mg/mL, leaves exposed to sunlight displayed no mortality. This outcome was attributed to the methanol evaporating as a result of sunlight irradiation at 3 sun and the fact that remaining undissolved abm did not present an pesticide activity. The results for the Agrimec-sprayed samples revealed that the LC₅₀ value for Agrimec was 9 mg/mL under sunlight irradiation of the leaves, whereas it was determined to be 0.6 mg/mL when the sprayed-leaf samples were not exposed to sunlight. The decreased pesticide activity of the Agrimec under sunlight was also related to the evaporation of the solvent, the cyclohexanol, which also indicated that the solvent had an impact on the killing effect. The fact that the aqueous nanohybrid formulation developed in this study presented the same LC₅₀ value as a commercially available cyclohexanol-based pesticide demonstrates its significant advantages in terms its solventless,

environmentally friendly nature with sunlight-triggered, long-term effective pesticide activity.

Table 1. LC₅₀ values for aqueous LA/abm@HNT-PDA dispersion, abm dissolved in methanol, and Agrimec under sunlight and in the dark, determined against *Myzus persicae*.

Abm concentration in the dispersion (mg/mL)	LA/abm@HNT-PDA sunlight-exposed (%)	LA/abm@HNT-PDA dark (%)	Abm sunlight-exposed (%)	Abm dark (%)	Agrimec sunlight-exposed (%)	Agrimec dark (%)
18	60	20	0	70	90	80
9	50	0	0	50	60	80
4.5	20	0	0	40	30	80
2.25	0	0	0	40	0	70
1.125	0	0	0	30	0	70
0.6	0	0	0	30	0	70

3.5 Conclusions

This study introduced a sunlight-triggered release system for abm, a commonly used agrochemical in agriculture, based on its encapsulation in photothermal HNT-PDA nanocarriers and functionalization with LA as release facilitator. The developed release system, that is composed of environmentally friendly, non-toxic components allows the release of the entrapped abm molecules when exposed to sunlight upon the light-to-heat conversion of the HNT-PDA nanocarriers, whereas the release is not triggered in the absence of the sunlight. The encapsulated abm within HNT-PDA remained stable despite the fact that abm was degraded when exposed to sunlight irradiation, proving that nanotubes acted as ideal carriers for the prolonged preservation of abm. With the prepared release system, abm was shown to be released in a controlled manner over at least 30 days when the samples were irradiated daily with sunlight for 6 h and presented long-term killing activity on *Myzus persicae*. Aqueous dispersions of LA/abm@HNT-PDA nanohybrids were studied as pesticide formulations and studied in terms of their suspensibility, foliar retention and rainwater resistance. An LC₅₀ value of 9 mg/mL was determined after assessing the efficiency of the aqueous nanoformulations on *Myzus persicae* aphids. Presenting comparable LC₅₀ values to commercial solvent-based abm formulations, the developed abm release system provides strong potential as environmentally friendly, solventless pesticide formulation with unique sunlight-triggered release mechanism that prevents abm from degrading in the presence of light and allows its time-dependent release.

CHAPTER 4. CONCLUSIONS

Pesticides can only be used in enormous amounts or in their pure form, without any additional components, in traditional agricultural applications. Yet, because of multiple mechanisms including leaching, the decomposition into minerals, and conversion by organisms, a significant portion of these pesticides stay ineffective. Controlled-release pesticide systems have been generated in response to the requirement to extend the duration and improve the effectiveness of the application of pesticides. The development of a pesticide-controlled-release system that can be initiated by sunlight is the primary focus of this thesis.

In Chapter 2, natural halloysite nanotubes (HNTs) that have been modified with polydopamine (PDA) are used for encapsulating essential oils in a controlled-release system. This system examines the essential oils' capacity for controlled release in response to environmental stimulus. HNT-PDA comprises a combination of peppermint, cinnamon, and basil essential oils. The procedure contains lauric acid (LA), a phase transition substance, as a stopper for essential oils. While LA successfully keeps the active substance in a dark environment, it melts in sunlight and releases the cargo molecule. The findings demonstrate that those exposed to 3 sun irradiation of the LA/EO@HNT-PDA nanohybrids display the maximum release behavior, whereas those exposed to 1 sun and held in the dark showed comparable amounts of an essential oil release. The study indicates that the powder form of the LA/EO@HNT-PDA system demonstrates higher aphid-killing functions by evaluating the efficiency of the controlled-release behavior on the aphid species *Myzus persicae*.

In Chapter 3, it is introduced that the encapsulation of Abamectin and its controlled release mechanism using HNT-PDA nanocarriers and functionalization with Lauric acid as release facilitator. Thanks to this approach, system can allow releasing the entrapped

Abamectin molecule to the desired target when exposed to sunlight by creating a light-to-heat conversion, whereas release is slightly triggered by external stimuli in the absence of the light by offering an environmentally friendly design. Abamectin degrades when exposed to sunlight irradiation; nevertheless, the encapsulated Abamectin within HNT-PDA remained robust, demonstrating that HNTs are suitable carriers for the sustained preservation of Abamectin. In order to determine the quantities of abamectin released from HNT-PDA, thermogravimetric analysis was used to compare samples with and without Lauric acid, exposed to light and stored in the dark. The sample with the highest release rate was discovered to be the LA/abm@HNT-PDA sample, which also contained the release facilitator and was exposed to light. After preparing dispersions of the nano pesticides in various concentrations, the qualities of the nano pesticides' capacity to stick on leaves were evaluated by contact angle measurements. The results suggested that PDA's hydrophilic properties contribute to the high leaf adhesion levels of the prepared pesticides, which were preserved even after washing. After evaluating the efficiency of the nanopesticides in aqueous dispersions at different concentration levels against *Myzus persicae* aphids, an LC₅₀ value of 9 mg/mL was found. Additionally, the killing power of powdered LA/abm@HNT-PDA was assessed on *Myzus persicae* aphids, demonstrating 70% of the population was still dead after 10 days. This method of production has led to a potential development in the market for ecologically friendly pesticides.

CHAPTER 5. REFERENCES

- (1) Thornton, P. D.; Mart, R. J.; Ulijn, R. V. Enzyme-Responsive Polymer Hydrogel Particles for Controlled Release. *Advanced Materials* 2007, 19 (9), 1252–1256. <https://doi.org/10.1002/adma.200601784>.
- (2) Ulbrich, K.; Etrych, T.; Chytil, P.; Jelínková, M.; Říhová, B. HPMa Copolymers with PH-Controlled Release of Doxorubicin: In Vitro Cytotoxicity and in Vivo Antitumor Activity. In *Journal of Controlled Release*; Elsevier, 2003; Vol. 87, pp 33–47. [https://doi.org/10.1016/S0168-3659\(02\)00348-6](https://doi.org/10.1016/S0168-3659(02)00348-6).
- (3) Chi, Y.; Zhang, G.; Xiang, Y.; Cai, D.; Wu, Z. Fabrication of a Temperature-Controlled-Release Herbicide Using a Nanocomposite. *ACS Sustain Chem Eng* 2017, 5 (6), 4969–4975. <https://doi.org/10.1021/acssuschemeng.7b00348>.
- (4) Hossion, A. M. L.; Bio, M.; Nkepan, G.; Awuah, S. G.; You, Y. Visible Light Controlled Release of Anticancer Drug through Double Activation of Prodrug. *ACS Med Chem Lett* 2013, 4 (1), 124–127. <https://doi.org/10.1021/ml3003617>.
- (5) Wang, Y.; Li, C.; Wang, Y.; Zhang, Y.; Li, X. Compound Pesticide Controlled Release System Based on the Mixture of Poly(Butylene Succinate) and PLA. *J Microencapsul* 2018, 35 (5), 494–503. <https://doi.org/10.1080/02652048.2018.1538265>.
- (6) Rychter, P.; Lewicka, K.; Rogacz, D. Environmental Usefulness of PLA/PEG Blends for Controlled-Release Systems of Soil-Applied Herbicides. *J Appl Polym Sci* 2019, 136 (33). <https://doi.org/10.1002/app.47856>.
- (7) Liu, B.; Wang, Y.; Yang, F.; Wang, X.; Shen, H.; Cui, H.; Wu, D. Construction of a Controlled-Release Delivery System for Pesticides Using Biodegradable PLA-Based

- Microcapsules. *Colloids Surf B Biointerfaces* 2016, *144*, 38–45.
<https://doi.org/10.1016/j.colsurfb.2016.03.084>.
- (8) Abri Aghdam, M.; Bagheri, R.; Mosafer, J.; Baradaran, B.; Hashemzaei, M.; Baghbanzadeh, A.; de la Guardia, M.; Mokhtarzadeh, A. Recent Advances on Thermosensitive and PH-Sensitive Liposomes Employed in Controlled Release. *Journal of Controlled Release*. Elsevier B.V. December 10, 2019, pp 1–22.
<https://doi.org/10.1016/j.jconrel.2019.09.018>.
- (9) Zhang, S.; Zhao, Y. Controlled Release from Cleavable Polymerized Liposomes upon Redox and PH Stimulation. *Bioconjug Chem* 2011, *22* (4), 523–528.
<https://doi.org/10.1021/bc1003197>.
- (10) Qiu, F.; Mhanna, R.; Zhang, L.; Ding, Y.; Fujita, S.; Nelson, B. J. Artificial Bacterial Flagella Functionalized with Temperature-Sensitive Liposomes for Controlled Release. *Sens Actuators B Chem* 2014, *196*, 676–681. <https://doi.org/10.1016/j.snb.2014.01.099>.
- (11) Kamaly, N.; Yameen, B.; Wu, J.; Farokhzad, O. C. Degradable Controlled-Release Polymers and Polymeric Nanoparticles: Mechanisms of Controlling Drug Release. *Chemical Reviews*. American Chemical Society February 24, 2016, pp 2602–2663.
<https://doi.org/10.1021/acs.chemrev.5b00346>.
- (12) Desai, P.; Patlolla, R. R.; Singh, M. Interaction of Nanoparticles and Cell-Penetrating Peptides with Skin for Transdermal Drug Delivery. *Molecular Membrane Biology*. October 2010, pp 247–259. <https://doi.org/10.3109/09687688.2010.522203>.
- (13) Prow, T. W.; Grice, J. E.; Lin, L. L.; Faye, R.; Butler, M.; Becker, W.; Wurm, E. M. T.; Yoong, C.; Robertson, T. A.; Soyer, H. P.; Roberts, M. S. Nanoparticles and Microparticles for Skin Drug Delivery. *Advanced Drug Delivery Reviews*. May 30, 2011, pp 470–491. <https://doi.org/10.1016/j.addr.2011.01.012>.
- (14) Wang, Y.; Zhao, Q.; Han, N.; Bai, L.; Li, J.; Liu, J.; Che, E.; Hu, L.; Zhang, Q.; Jiang, T.; Wang, S. Mesoporous Silica Nanoparticles in Drug Delivery and Biomedical Applications. *Nanomedicine: Nanotechnology, Biology, and Medicine*. Elsevier Inc. February 1, 2015, pp 313–327. <https://doi.org/10.1016/j.nano.2014.09.014>.

- (15) Lu, J.; Liong, M.; Li, Z.; Zink, J. I.; Tamanoi, F. Biocompatibility, Biodistribution, and Drug-Delivery Efficiency of Mesoporous Silica Nanoparticles for Cancer Therapy in Animals. *Small* 2010, 6 (16), 1794–1805. <https://doi.org/10.1002/sml.201000538>.
- (16) Meng, H.; Xue, M.; Xia, T.; Zhao, Y. L.; Tamanoi, F.; Stoddart, J. F.; Zink, J. I.; Nel, A. E. Autonomous in Vitro Anticancer Drug Release from Mesoporous Silica Nanoparticles by PH-Sensitive Nanovalves. *J Am Chem Soc* 2010, 132 (36), 12690–12697. <https://doi.org/10.1021/ja104501a>.
- (17) Kundu, M.; Chatterjee, S.; Ghosh, N.; Manna, P.; Das, J.; Sil, P. C. Tumor Targeted Delivery of Umbelliferone via a Smart Mesoporous Silica Nanoparticles Controlled-Release Drug Delivery System for Increased Anticancer Efficiency. *Materials Science and Engineering C* 2020, 116. <https://doi.org/10.1016/j.msec.2020.111239>.
- (18) Sharma, A.; Sood, K.; Kaur, J.; Khatri, M. Agrochemical Loaded Biocompatible Chitosan Nanoparticles for Insect Pest Management. *Biocatal Agric Biotechnol* 2019, 18. <https://doi.org/10.1016/j.bcab.2019.101079>.
- (19) Lvov, Y. M.; Shchukin, D. G.; Möhwald, H.; Price, R. R. Halloysite Clay Nanotubes for Controlled Release of Protective Agents. *ACS Nano* 2008, 2 (5), 814–820. <https://doi.org/10.1021/nm800259q>.
- (20) Kolgesiz, S.; Tas, C. E.; Koken, D.; Genc, M. H.; Yalcin, I.; Kalender, K.; Unal, S.; Unal, H. Extending the Shelf Life of Bananas with Cinnamaldehyde-Impregnated Halloysite/Polypropylene Nanocomposite Films. *ACS Food Science and Technology* 2023, 3 (2), 340–349. <https://doi.org/10.1021/acsfoodscitech.2c00371>.
- (21) Kumar, L.; Deshmukh, R. K.; Hakim, L.; Gaikwad, K. K. Halloysite Nanotube as a Functional Material for Active Food Packaging Application: A Review. *Food and Bioprocess Technology*. Springer 2023. <https://doi.org/10.1007/s11947-023-03092-3>.
- (22) Gaikwad, K. K.; Singh, S.; Lee, Y. S. High Adsorption of Ethylene by Alkali-Treated Halloysite Nanotubes for Food-Packaging Applications. *Environ Chem Lett* 2018, 16 (3), 1055–1062. <https://doi.org/10.1007/s10311-018-0718-7>.
- (23) Karewicz, A.; Machowska, A.; Kasprzyk, M.; Ledwójcik, G. Application of Halloysite Nanotubes in Cancer Therapy—A Review. *Materials*. MDPI AG June 1, 2021. <https://doi.org/10.3390/ma14112943>.

- (24) Liao, J.; Wang, D.; Tang, A.; Fu, L.; Ouyang, J.; Yang, H. Surface Modified Halloysite Nanotubes with Different Lumen Diameters as Drug Carriers for Cancer Therapy. *Chemical Communications* 2021, 57 (74), 9470–9473. <https://doi.org/10.1039/d1cc01879e>.
- (25) Li, W.; Liu, D.; Zhang, H.; Correia, A.; Mäkilä, E.; Salonen, J.; Hirvonen, J.; Santos, H. A. Microfluidic Assembly of a Nano-in-Micro Dual Drug Delivery Platform Composed of Halloysite Nanotubes and a PH-Responsive Polymer for Colon Cancer Therapy. *Acta Biomater* 2017, 48, 238–246. <https://doi.org/10.1016/j.actbio.2016.10.042>.
- (26) Ammala, A. Biodegradable Polymers as Encapsulation Materials for Cosmetics and Personal Care Markets. *International Journal of Cosmetic Science*. April 2013, pp 113–124. <https://doi.org/10.1111/ics.12017>.
- (27) Bayer, I. S. Hyaluronic Acid and Controlled Release: A Review. *Molecules*. MDPI AG June 1, 2020. <https://doi.org/10.3390/molecules25112649>.
- (28) Budinčić, J. M.; Petrović, L.; Đekić, L.; Fraj, J.; Bučko, S.; Katona, J.; Spasojević, L. Study of Vitamin E Microencapsulation and Controlled Release from Chitosan/Sodium Lauryl Ether Sulfate Microcapsules. *Carbohydr Polym* 2021, 251. <https://doi.org/10.1016/j.carbpol.2020.116988>.
- (29) Yun, Y. H.; Lee, B. K.; Park, K. Controlled Drug Delivery: Historical Perspective for the next Generation. *Journal of Controlled Release* 2015, 219, 2–7. <https://doi.org/10.1016/j.jconrel.2015.10.005>.
- (30) Jin, Q.; Mitschang, F.; Agarwal, S. Biocompatible Drug Delivery System for Photo-Triggered Controlled Release of 5-Fluorouracil. *Biomacromolecules* 2011, 12 (10), 3684–3691. <https://doi.org/10.1021/bm2009125>.
- (31) Xiang, J.; Tong, X.; Shi, F.; Yan, Q.; Yu, B.; Zhao, Y. Near-Infrared Light-Triggered Drug Release from UV-Responsive Diblock Copolymer-Coated Upconversion Nanoparticles with High Monodispersity. *J Mater Chem B* 2018, 6 (21), 3531–3540. <https://doi.org/10.1039/c8tb00651b>.
- (32) Liu, J.; Bu, W.; Pan, L.; Shi, J. NIR-Triggered Anticancer Drug Delivery by Upconverting Nanoparticles with Integrated Azobenzene-Modified Mesoporous Silica.

- Angewandte Chemie - International Edition* 2013, 52 (16), 4375–4379.
<https://doi.org/10.1002/anie.201300183>.
- (33) Liu, Q.; Wang, H.; Li, G.; Liu, M.; Ding, J.; Huang, X.; Gao, W.; Huayue, W. A Photocleavable Low Molecular Weight Hydrogel for Light-Triggered Drug Delivery. *Chinese Chemical Letters* 2019, 30 (2), 485–488.
<https://doi.org/10.1016/j.ccllet.2018.06.009>.
- (34) Xu, J.; Zhou, X.; Gao, Z.; Song, Y. Y.; Schmuki, P. Visible-Light-Triggered Drug Release from TiO₂ Nanotube Arrays: A Controllable Antibacterial Platform. *Angewandte Chemie - International Edition* 2016, 55 (2), 593–597.
<https://doi.org/10.1002/anie.201508710>.
- (35) Almasi, H.; Jahanbakhsh Oskouie, M.; Saleh, A. A Review on Techniques Utilized for Design of Controlled Release Food Active Packaging. *Critical Reviews in Food Science and Nutrition*. Taylor and Francis Ltd. 2021, pp 2601–2621.
<https://doi.org/10.1080/10408398.2020.1783199>.
- (36) Mastromatteo, M.; Mastromatteo, M.; Conte, A.; Del Nobile, M. A. Advances in Controlled Release Devices for Food Packaging Applications. *Trends in Food Science and Technology*. December 2010, pp 591–598.
<https://doi.org/10.1016/j.tifs.2010.07.010>.
- (37) Promsorn, J.; Harnkarnsujarit, N. Oxygen Absorbing Food Packaging Made by Extrusion Compounding of Thermoplastic Cassava Starch with Gallic Acid. *Food Control* 2022, 142. <https://doi.org/10.1016/j.foodcont.2022.109273>.
- (38) Wu, L. T.; Tsai, I. L.; Ho, Y. C.; Hang, Y. H.; Lin, C.; Tsai, M. L.; Mi, F. L. Active and Intelligent Gellan Gum-Based Packaging Films for Controlling Anthocyanins Release and Monitoring Food Freshness. *Carbohydr Polym* 2021, 254.
<https://doi.org/10.1016/j.carbpol.2020.117410>.
- (39) Singh, A.; Dhiman, N.; Kar, A. K.; Singh, D.; Purohit, M. P.; Ghosh, D.; Patnaik, S. Advances in Controlled Release Pesticide Formulations: Prospects to Safer Integrated Pest Management and Sustainable Agriculture. *Journal of Hazardous Materials*. Elsevier B.V. March 5, 2020. <https://doi.org/10.1016/j.jhazmat.2019.121525>.

- (40) Xiang, Y.; Zhang, G.; Chen, C.; Liu, B.; Cai, D.; Wu, Z. Fabrication of a PH-Responsively Controlled-Release Pesticide Using an Attapulgitite-Based Hydrogel. *ACS Sustain Chem Eng* 2018, 6 (1), 1192–1201. <https://doi.org/10.1021/acssuschemeng.7b03469>.
- (41) Xu, X.; Bai, B.; Wang, H.; Suo, Y. A Near-Infrared and Temperature-Responsive Pesticide Release Platform through Core-Shell Polydopamine@PNIPAm Nanocomposites. *ACS Appl Mater Interfaces* 2017, 9 (7), 6424–6432. <https://doi.org/10.1021/acsami.6b15393>.
- (42) Chi, Y.; Zhang, G.; Xiang, Y.; Cai, D.; Wu, Z. Fabrication of a Temperature-Controlled-Release Herbicide Using a Nanocomposite. *ACS Sustain Chem Eng* 2017, 5 (6), 4969–4975. <https://doi.org/10.1021/acssuschemeng.7b00348>.
- (43) Taş, C. E.; Gundogdu, S. O.; Ünal, H. Polydopamine-Coated Halloysite Nanotubes for Sunlight-Triggered Release of Active Substances. *ACS Appl Nano Mater* 2022, 5 (4), 5407–5415. <https://doi.org/10.1021/acsanm.2c00403>.
- (44) Alvarez-Lorenzo, C.; Concheiro, A.; Dubovik, A. S.; Grinberg, N. V.; Burova, T. V.; Grinberg, V. Y. Temperature-Sensitive Chitosan-Poly(N-Isopropylacrylamide) Interpenetrated Networks with Enhanced Loading Capacity and Controlled Release Properties. *Journal of Controlled Release* 2005, 102 (3), 629–641. <https://doi.org/10.1016/j.jconrel.2004.10.021>.
- (45) Lee, A. S.; Gast, A. P.; Bütün, V.; Armes, S. P. Characterizing the Structure of PH Dependent Polyelectrolyte Block Copolymer Micelles. *Macromolecules* 1999, 32 (13), 4302–4310. <https://doi.org/10.1021/ma981865o>.
- (46) Chen, L.; Di, J.; Cao, C.; Zhao, Y.; Ma, Y.; Luo, J.; Wen, Y.; Song, W.; Song, Y.; Jiang, L. A PH-Driven DNA Nanoswitch for Responsive Controlled Release. *Chemical Communications* 2011, 47 (10), 2850–2852. <https://doi.org/10.1039/c0cc04765a>.
- (47) Bernardos, A.; Aznar, E.; Marcos, M. D.; Martínez-Mañez, R.; Sancenón, F.; Soto, J.; Barat, J. M.; Amorós, P. Enzyme-Responsive Controlled Release Using Mesoporous Silica Supports Capped with Lactose. *Angewandte Chemie - International Edition* 2009, 48 (32), 5884–5887. <https://doi.org/10.1002/anie.200900880>.

- (48) Thornton, P. D.; Mart, R. J.; Webb, S. J.; Ulijn, R. V. Enzyme-Responsive Hydrogel Particles for the Controlled Release of Proteins: Designing Peptide Actuators to Match Payload. *Soft Matter* 2008, 4 (4), 821–827. <https://doi.org/10.1039/b714750c>.
- (49) Liu, J.; Huang, Y.; Kumar, A.; Tan, A.; Jin, S.; Mozhi, A.; Liang, X. J. PH-Sensitive Nano-Systems for Drug Delivery in Cancer Therapy. *Biotechnology Advances*. Elsevier Inc. 2014, pp 693–710. <https://doi.org/10.1016/j.biotechadv.2013.11.009>.
- (50) Zhao, X.; Qi, M.; Liang, S.; Tian, K.; Zhou, T.; Jia, X.; Li, J.; Liu, P. Synthesis of Photo- and PH Dual-Sensitive Amphiphilic Copolymer PEG43-b-P(AA76-Co-NBA35-Co-TBA9) and Its Micellization as Leakage-Free Drug Delivery System for UV-Triggered Intracellular Delivery of Doxorubicin. *ACS Appl Mater Interfaces* 2016, 8 (34), 22127–22134. <https://doi.org/10.1021/acsami.6b08935>.
- (51) Dispinar, T.; Colard, C. A. L.; Du Prez, F. E. Polyurea Microcapsules with a Photocleavable Shell: UV-Triggered Release. *Polym Chem* 2013, 4 (3), 763–772. <https://doi.org/10.1039/c2py20735d>.
- (52) Yao, Y.; Wang, Y.; Huang, F. Synthesis of Various Supramolecular Hybrid Nanostructures Based on Pillar[6]Arene Modified Gold Nanoparticles/Nanorods and Their Application in PH- and NIR-Triggered Controlled Release. *Chem Sci* 2014, 5 (11), 4312–4316. <https://doi.org/10.1039/c4sc01647e>.
- (53) Zheng, D.; Bai, B.; Xu, X.; He, Y.; Li, S.; Hu, N.; Wang, H. Fabrication of Detonation Nanodiamond@sodium Alginate Hydrogel Beads and Their Performance in Sunlight-Triggered Water Release. *RSC Adv* 2019, 9 (48), 27961–27972. <https://doi.org/10.1039/c9ra03914g>.
- (54) Liu, J.; Bu, W.; Pan, L.; Shi, J. NIR-Triggered Anticancer Drug Delivery by Upconverting Nanoparticles with Integrated Azobenzene-Modified Mesoporous Silica. *Angewandte Chemie - International Edition* 2013, 52 (16), 4375–4379. <https://doi.org/10.1002/anie.201300183>.
- (55) Ye, Z.; Guo, J.; Wu, D.; Tan, M.; Xiong, X.; Yin, Y.; He, G. Photo-Responsive Shell Cross-Linked Micelles Based on Carboxymethyl Chitosan and Their Application in Controlled Release of Pesticide. *Carbohydr Polym* 2015, 132, 520–528. <https://doi.org/10.1016/j.carbpol.2015.06.077>.

- (56) Liu, B.; Zhang, J.; Chen, C.; Wang, D.; Tian, G.; Zhang, G.; Cai, D.; Wu, Z. Infrared-Light-Responsive Controlled-Release Pesticide Using Hollow Carbon Microspheres@Polyethylene Glycol/ α -Cyclodextrin Gel. *J Agric Food Chem* 2021, 69 (25), 6981–6988. <https://doi.org/10.1021/acs.jafc.1c01265>.
- (57) Xu, J. W.; Yao, K.; Xu, Z. K. Nanomaterials with a Photothermal Effect for Antibacterial Activities: An Overview. *Nanoscale*. Royal Society of Chemistry May 14, 2019, pp 8680–8691. <https://doi.org/10.1039/c9nr01833f>.
- (58) Yu, H.; Peng, Y.; Yang, Y.; Li, Z. Y. Plasmon-Enhanced Light–Matter Interactions and Applications. *npj Computational Materials*. Nature Publishing Group December 1, 2019. <https://doi.org/10.1038/s41524-019-0184-1>.
- (59) Gartner, W. W. *PHYSICAL REVIEW Phototheruial Effect in Semiconductors* I. DEFINITION OF THE EFFECT HEN a Sample of Semiconducting Material (See.*
- (60) Han, B.; Zhang, Y. L.; Chen, Q. D.; Sun, H. B. Carbon-Based Photothermal Actuators. *Advanced Functional Materials*. Wiley-VCH Verlag October 4, 2018. <https://doi.org/10.1002/adfm.201802235>.
- (61) Zou, Q.; Abbas, M.; Zhao, L.; Li, S.; Shen, G.; Yan, X. Biological Photothermal Nanodots Based on Self-Assembly of Peptide-Porphyrin Conjugates for Antitumor Therapy. *J Am Chem Soc* 2017, 139 (5), 1921–1927. <https://doi.org/10.1021/jacs.6b11382>.
- (62) Tankiewicz, M.; Fenik, J.; Biziuk, M. Solventless and Solvent-Minimized Sample Preparation Techniques for Determining Currently Used Pesticides in Water Samples: A Review. *Talanta*. Elsevier B.V. October 30, 2011, pp 8–22. <https://doi.org/10.1016/j.talanta.2011.08.056>.
- (63) Huang, B.; Chen, F.; Shen, Y.; Qian, K.; Wang, Y.; Sun, C.; Zhao, X.; Cui, B.; Gao, F.; Zeng, Z.; Cui, H. Advances in Targeted Pesticides with Environmentally Responsive Controlled Release by Nanotechnology. *Nanomaterials* 2018, 8 (2). <https://doi.org/10.3390/nano8020102>.
- (64) Kumar, S.; Chauhan, N.; Gopal, M.; Kumar, R.; Dilbaghi, N. Development and Evaluation of Alginate-Chitosan Nanocapsules for Controlled Release of Acetamiprid.

- Int J Biol Macromol* 2015, *81*, 631–637.
<https://doi.org/10.1016/j.ijbiomac.2015.08.062>.
- (65) Xu, L.; Cao, L. D.; Li, F. M.; Wang, X. J.; Huang, Q. L. Utilization of Chitosan-Lactide Copolymer Nanoparticles as Controlled Release Pesticide Carrier for Pyraclostrobin Against *Colletotrichum Gossypii* Southw. *J Dispers Sci Technol* 2014, *35* (4), 544–550.
<https://doi.org/10.1080/01932691.2013.800455>.
- (66) Kaziem, A. E.; Gao, Y.; He, S.; Li, J. Synthesis and Insecticidal Activity of Enzyme-Triggered Functionalized Hollow Mesoporous Silica for Controlled Release. *J Agric Food Chem* 2017, *65* (36), 7854–7864. <https://doi.org/10.1021/acs.jafc.7b02560>.
- (67) Wu, W.; Wan, M.; Fei, Q.; Tian, Y.; Song, S.; Shen, H.; Shen, J. PDA@Ti3C2Tx as a Novel Carrier for Pesticide Delivery and Its Application in Plant Protection: NIR-Responsive Controlled Release and Sustained Antipest Activity. *Pest Manag Sci* 2021, *77* (11), 4960–4970. <https://doi.org/10.1002/ps.6538>.
- (68) Mossa, A. T. H. Green Pesticides: Essential Oils as Biopesticides in Insect-Pest Management. *Journal of Environmental Science and Technology*. Asian Network for Scientific Information 2016, pp 354–378. <https://doi.org/10.3923/jest.2016.354.378>.
- (69) Nikolić, M.; Jovanović, K. K.; Marković, T.; Marković, D.; Gligorijević, N.; Radulović, S.; Soković, M. Chemical Composition, Antimicrobial, and Cytotoxic Properties of Five Lamiaceae Essential Oils. *Ind Crops Prod* 2014, *61*, 225–232.
<https://doi.org/10.1016/j.indcrop.2014.07.011>.
- (70) Radaelli, M.; da Silva, B. P.; Weidlich, L.; Hoehne, L.; Flach, A.; da Costa, L. A. M. A.; Ethur, E. M. Antimicrobial Activities of Six Essential Oils Commonly Used as Condiments in Brazil against *Clostridium Perfringens*. *Brazilian Journal of Microbiology* 2016, *47* (2), 424–430. <https://doi.org/10.1016/j.bjm.2015.10.001>.
- (71) Martucci, J. F.; Gende, L. B.; Neira, L. M.; Ruseckaite, R. A. Oregano and Lavender Essential Oils as Antioxidant and Antimicrobial Additives of Biogenic Gelatin Films. *Ind Crops Prod* 2015, *71*, 205–213. <https://doi.org/10.1016/j.indcrop.2015.03.079>.
- (72) Eswara Reddy, S. G.; Kirti Dolma, S.; Koundal, R.; Singh, B. *Chemical Composition and Insecticidal Activities of Essential Oils against Diamondback Moth, Plutella 2 Xylostella (L.) (Lepidoptera: Yponomeutidae) 3*. www.sdfine.com.

- (73) Wang, Y.; Cen, C.; Chen, J.; Zhou, C.; Fu, L. Nano-Emulsification Improves Physical Properties and Bioactivities of Litsea Cubeba Essential Oil. *LWT* 2021, *137*.
<https://doi.org/10.1016/j.lwt.2020.110361>.
- (74) Atli, O.; Can Karaca, A.; Ozcelik, B. Encapsulation of Cumin (*Cuminum Cyminum* L.) Seed Essential Oil in the Chickpea Protein-Maltodextrin Matrix. *ACS Omega* 2022.
<https://doi.org/10.1021/acsomega.2c07184>.
- (75) Lisuzzo, L.; Cavallaro, G.; Milioto, S.; Lazzara, G. Halloysite Nanotubes Filled with Salicylic Acid and Sodium Diclofenac: Effects of Vacuum Pumping on Loading and Release Properties. *J Nanostructure Chem* 2021, *11* (4), 663–673.
<https://doi.org/10.1007/s40097-021-00391-z>.
- (76) Taş, C. E.; Gundogdu, S. O.; Ünal, H. Polydopamine-Coated Halloysite Nanotubes for Sunlight-Triggered Release of Active Substances. *ACS Appl Nano Mater* 2022, *5* (4), 5407–5415. <https://doi.org/10.1021/acsanm.2c00403>.
- (77) Yuce, S.; Demirel, O.; Alkan Tas, B.; Sungur, P.; Unal, H. Halloysite Nanotube/Polydopamine Nanohybrids as Clay-Based Photothermal Agents for Antibacterial Applications. *ACS Appl Nano Mater* 2021, *4* (12), 13432–13439.
<https://doi.org/10.1021/acsanm.1c02936>.
- (78) Kolgesiz, S.; Tas, C. E.; Koken, D.; Genc, M. H.; Yalcin, I.; Kalender, K.; Unal, S.; Unal, H. Extending the Shelf Life of Bananas with Cinnamaldehyde-Impregnated Halloysite/Polypropylene Nanocomposite Films. *ACS Food Science and Technology* 2023, *3* (2), 340–349. <https://doi.org/10.1021/acfoodscitech.2c00371>.
- (79) Hendessi, S.; Sevinis, E. B.; Unal, S.; Cebeci, F. C.; Menciloglu, Y. Z.; Unal, H. Antibacterial Sustained-Release Coatings from Halloysite Nanotubes/Waterborne Polyurethanes. *Prog Org Coat* 2016, *101*, 253–261.
<https://doi.org/10.1016/j.porgcoat.2016.09.005>.
- (80) Popp, J.; Pető, K.; Nagy, J. Pesticide Productivity and Food Security. A Review. *Agronomy for Sustainable Development*. Springer-Verlag France 2013, pp 243–255.
<https://doi.org/10.1007/s13593-012-0105-x>.
- (81) Tudi, M.; Ruan, H. D.; Wang, L.; Lyu, J.; Sadler, R.; Connell, D.; Chu, C.; Phung, D. T. Agriculture Development, Pesticide Application and Its Impact on the Environment.

International Journal of Environmental Research and Public Health. MDPI AG
February 1, 2021, pp 1–24. <https://doi.org/10.3390/ijerph18031112>.

- (82) Huang, B.; Chen, F.; Shen, Y.; Qian, K.; Wang, Y.; Sun, C.; Zhao, X.; Cui, B.; Gao, F.; Zeng, Z.; Cui, H. Advances in Targeted Pesticides with Environmentally Responsive Controlled Release by Nanotechnology. *Nanomaterials*. MDPI AG February 11, 2018. <https://doi.org/10.3390/nano8020102>.
- (83) Zhao, X.; Cui, H.; Wang, Y.; Sun, C.; Cui, B.; Zeng, Z. Development Strategies and Prospects of Nano-Based Smart Pesticide Formulation. *Journal of Agricultural and Food Chemistry*. American Chemical Society July 5, 2018, pp 6504–6512. <https://doi.org/10.1021/acs.jafc.7b02004>.
- (84) Massinon, M.; De Cock, N.; Forster, W. A.; Nairn, J. J.; McCue, S. W.; Zabkiewicz, J. A.; Lebeau, F. Spray Droplet Impaction Outcomes for Different Plant Species and Spray Formulations. *Crop Protection* 2017, 99, 65–75. <https://doi.org/10.1016/j.cropro.2017.05.003>.
- (85) He, Y.; Zhao, B.; Yu, Y. *Effect, Comparison and Analysis of Pesticide Electrostatic Spraying and Traditional Spraying*; 2016; Vol. 48.
- (86) Lian, L.; Jiang, B.; Xing, Y.; Zhang, N. Identification of Photodegradation Product of Organophosphorus Pesticides and Elucidation of Transformation Mechanism under Simulated Sunlight Irradiation. *Ecotoxicol Environ Saf* 2021, 224. <https://doi.org/10.1016/j.ecoenv.2021.112655>.
- (87) Xiang, Y.; Zhang, G.; Chen, C.; Liu, B.; Cai, D.; Wu, Z. Fabrication of a PH-Responsively Controlled-Release Pesticide Using an Attapulgate-Based Hydrogel. *ACS Sustain Chem Eng* 2018, 6 (1), 1192–1201. <https://doi.org/10.1021/acssuschemeng.7b03469>.
- (88) Kaziem, A. E.; Gao, Y.; He, S.; Li, J. Synthesis and Insecticidal Activity of Enzyme-Triggered Functionalized Hollow Mesoporous Silica for Controlled Release. *J Agric Food Chem* 2017, 65 (36), 7854–7864. <https://doi.org/10.1021/acs.jafc.7b02560>.
- (89) Xu, X.; Bai, B.; Wang, H.; Suo, Y. A Near-Infrared and Temperature-Responsive Pesticide Release Platform through Core-Shell Polydopamine@PNIPAm

- Nanocomposites. *ACS Appl Mater Interfaces* 2017, 9 (7), 6424–6432.
<https://doi.org/10.1021/acsami.6b15393>.
- (90) Zhang, L.; Ren, S.; Chen, C.; Wang, D.; Liu, B.; Cai, D.; Wu, Z. Near Infrared Light-Driven Release of Pesticide with Magnetic Collectability Using Gel-Based Nanocomposite. *Chemical Engineering Journal* 2021, 411.
<https://doi.org/10.1016/j.cej.2020.127881>.
- (91) Li, L. Y.; Zhou, Y. M.; Gao, R. Y.; Liu, X. C.; Du, H. H.; Zhang, J. L.; Ai, X. C.; Zhang, J. P.; Fu, L. M.; Skibsted, L. H. Naturally Occurring Nanotube with Surface Modification as Biocompatible, Target-Specific Nanocarrier for Cancer Phototherapy. *Biomaterials* 2019, 190–191, 86–96. <https://doi.org/10.1016/j.biomaterials.2018.10.046>.
- (92) Saucedo-Zuñiga, J. N.; Sánchez-Valdes, S.; Ramírez-Vargas, E.; Guillen, L.; Ramos-deValle, L. F.; Graciano-Verdugo, A.; Uribe-Calderón, J. A.; Valera-Zaragoza, M.; Lozano-Ramírez, T.; Rodríguez-González, J. A.; Borjas-Ramos, J. J.; Zuluaga-Parra, J. D. Controlled Release of Essential Oils Using Lamellar Nanoclay and Porous Halloysite / Essential Oil Composites in a Multilayer Film Reservoir. *Microporous and Mesoporous Materials* 2021, 316. <https://doi.org/10.1016/j.micromeso.2021.110882>.
- (93) Ganguly, S.; Das, T. K.; Mondal, S.; Das, N. C. Synthesis of Polydopamine-Coated Halloysite Nanotube-Based Hydrogel for Controlled Release of a Calcium Channel Blocker. *RSC Adv* 2016, 6 (107), 105350–105362. <https://doi.org/10.1039/c6ra24153k>.
- (94) García-Vázquez, R.; Rebitski, E. P.; Viejo, L.; de los Ríos, C.; Darder, M.; García-Frutos, E. M. Clay-Based Hybrids for Controlled Release of 7-Azaindole Derivatives as Neuroprotective Drugs in the Treatment of Alzheimer's Disease. *Appl Clay Sci* 2020, 189. <https://doi.org/10.1016/j.clay.2020.105541>.
- (95) Li, L. Y.; Zhou, Y. M.; Gao, R. Y.; Liu, X. C.; Du, H. H.; Zhang, J. L.; Ai, X. C.; Zhang, J. P.; Fu, L. M.; Skibsted, L. H. Naturally Occurring Nanotube with Surface Modification as Biocompatible, Target-Specific Nanocarrier for Cancer Phototherapy. *Biomaterials* 2019, 190–191, 86–96. <https://doi.org/10.1016/j.biomaterials.2018.10.046>.
- (96) Tas, C. E.; Hendessi, S.; Baysal, M.; Unal, S.; Cebeci, F. C.; Menciloglu, Y. Z.; Unal, H. Halloysite Nanotubes/Polyethylene Nanocomposites for Active Food Packaging

- Materials with Ethylene Scavenging and Gas Barrier Properties. *Food Bioproc Tech* 2017, 10 (4), 789–798. <https://doi.org/10.1007/s11947-017-1860-0>.
- (97) Grimes, W. R.; Luo, Y.; McFarland, A. W.; Mills, D. K. Bi-Functionalized Clay Nanotubes for Anti-Cancer Therapy. *Applied Sciences (Switzerland)* 2018, 8 (2). <https://doi.org/10.3390/app8020281>.
- (98) Surya, I.; Waesateh, K.; Masa, A.; Hayeemasae, N. Selectively Etched Halloysite Nanotubes as Performance Booster of Epoxidized Natural Rubber Composites. *Polymers (Basel)* 2021, 13 (20). <https://doi.org/10.3390/polym13203536>.
- (99) Oliyaei, N.; Moosavi-Nasab, M.; Tamaddon, A. M.; Fazaeli, M. Encapsulation of Fucoxanthin in Binary Matrices of Porous Starch and Halloysite. *Food Hydrocoll* 2020, 100. <https://doi.org/10.1016/j.foodhyd.2019.105458>.
- (100) Saadat, S.; Rawtani, D.; Rao, P. K. Antibacterial Activity of Chitosan Film Containing Syzygium Aromaticum (Clove) Oil Encapsulated Halloysite Nanotubes against Foodborne Pathogenic Bacterial Strains. *Mater Today Commun* 2022, 32. <https://doi.org/10.1016/j.mtcomm.2022.104132>.
- (101) Jang, S. H.; Jang, S. R.; Lee, G. M.; Ryu, J. H.; Park, S. Il; Park, N. H. Halloysite Nanocapsules Containing Thyme Essential Oil: Preparation, Characterization, and Application in Packaging Materials. *J Food Sci* 2017, 82 (9), 2113–2120. <https://doi.org/10.1111/1750-3841.13835>.
- (102) Lee, M. H.; Park, H. J. Preparation of Halloysite Nanotubes Coated with Eudragit for a Controlled Release of Thyme Essential Oil. *J Appl Polym Sci* 2015, 132 (46). <https://doi.org/10.1002/app.42771>.
- (103) Riela, S.; Barattucci, A.; Barreca, D.; Campagna, S.; Cavallaro, G.; Lazzara, G.; Massaro, M.; Pizzolanti, G.; Salerno, T. M. G.; Bonaccorsi, P.; Puntoriero, F. Boosting the Properties of a Fluorescent Dye by Encapsulation into Halloysite Nanotubes. *Dyes and Pigments* 2021, 187. <https://doi.org/10.1016/j.dyepig.2020.109094>.
- (104) Hamed, S.; Koosha, M. Designing a PH-Responsive Drug Delivery System for the Release of Black-Carrot Anthocyanins Loaded in Halloysite Nanotubes for Cancer Treatment. *Appl Clay Sci* 2020, 197. <https://doi.org/10.1016/j.clay.2020.105770>.

- (105) Hossieni-Aghdam, S. J.; Foroughi-Nia, B.; Zare-Akbari, Z.; Mojarad-Jabali, S.; motasadizadeh, H.; Farhadnejad, H. Facile Fabrication and Characterization of a Novel Oral PH-Sensitive Drug Delivery System Based on CMC Hydrogel and HNT-AT Nanohybrid. *Int J Biol Macromol* 2018, *107*, 2436–2449. <https://doi.org/10.1016/j.ijbiomac.2017.10.128>.
- (106) Tas, C. E.; Berksun, E.; Koken, D.; Unal, S.; Unal, H. Photothermal Waterborne Polydopamine/Polyurethanes with Light-to-Heat Conversion Properties. *ACS Appl Polym Mater* 2021, *3* (8), 3929–3940. <https://doi.org/10.1021/acsapm.1c00495>.
- (107) Fan, T.; Feng, J.; Ma, C.; Yu, C.; Li, J.; Wu, X. Preparation and Characterization of Porous Microspheres and Applications in Controlled-Release of Abamectin in Water and Soil. *Journal of Porous Materials* 2014, *21* (1), 113–119. <https://doi.org/10.1007/s10934-013-9754-7>.
- (108) Tas, C. E.; Ozbulut, E. B. S.; Ceven, O. F.; Tas, B. A.; Unal, S.; Unal, H. Purification and Sorting of Halloysite Nanotubes into Homogeneous, Agglomeration-Free Fractions by Polydopamine Functionalization. *ACS Omega* 2020, *5* (29), 17962–17972. <https://doi.org/10.1021/acsomega.0c01057>.
- (109) Lisuzzo, L.; Cavallaro, G.; Milioto, S.; Lazzara, G. Halloysite Nanotubes Filled with Salicylic Acid and Sodium Diclofenac: Effects of Vacuum Pumping on Loading and Release Properties. *J Nanostructure Chem* 2021, *11* (4), 663–673. <https://doi.org/10.1007/s40097-021-00391-z>.
- (110) Guan, W.; Zhang, W.; Tang, L.; Wang, Y.; Cui, H. Fabrication of Novel Avermectin Nanoemulsion Using a Polyurethane Emulsifier with Cleavable Disulfide Bonds. *J Agric Food Chem* 2018, *66* (26), 6569–6577. <https://doi.org/10.1021/acs.jafc.7b01427>.
- (111) Demirel, O.; Kolgesiz, S.; Yuce, S.; Hayat Soytaş, S.; Koseoglu-Imer, D. Y.; Unal, H. Photothermal Electrospun Nanofibers Containing Polydopamine-Coated Halloysite Nanotubes as Antibacterial Air Filters. *ACS Appl Nano Mater* 2022, *5* (12), 18127–18137. <https://doi.org/10.1021/acsanm.2c04026>.
- (112) Yu, M.; Yao, J.; Liang, J.; Zeng, Z.; Cui, B.; Zhao, X.; Sun, C.; Wang, Y.; Liu, G.; Cui, H. Development of Functionalized Abamectin Poly(Lactic Acid) Nanoparticles with

Regulatable Adhesion to Enhance Foliar Retention. *RSC Adv* 2017, 7 (19), 11271–11280. <https://doi.org/10.1039/c6ra27345a>.

- (113) Cao, J.; Guenther, R. H.; Sit, T. L.; Lommel, S. A.; Opperman, C. H.; Willoughby, J. A. Development of Abamectin Loaded Plant Virus Nanoparticles for Efficacious Plant Parasitic Nematode Control. *ACS Applied Materials and Interfaces*. American Chemical Society May 13, 2015, pp 9546–9553. <https://doi.org/10.1021/acsami.5b00940>.
- (114) Fu, Z.; Chen, K.; Li, L.; Zhao, F.; Wang, Y.; Wang, M.; Shen, Y.; Cui, H.; Liu, D.; Guo, X. Spherical and Spindle-like Abamectin-Loaded Nanoparticles by Flash Nanoprecipitation for Southern Root-Knot Nematode Control: Preparation and Characterization. *Nanomaterials* 2018, 8 (6). <https://doi.org/10.3390/nano8060449>.
- (115) Feng, J.; Chen, W.; Shen, Y.; Chen, Q.; Yang, J.; Zhang, M.; Yang, W.; Yuan, S. Fabrication of Abamectin-Loaded Mesoporous Silica Nanoparticles by Emulsion-Solvent Evaporation to Improve Photolysis Stability and Extend Insecticidal Activity. *Nanotechnology* 2020, 31 (34). <https://doi.org/10.1088/1361-6528/ab91f0>.